AWARD NUMBER: W81XWH-19-1-0572

TITLE: Novel Therapeutics for Bone Marrow Failure Disorders Due to Telomere Exhaustion

PRINCIPAL INVESTIGATOR: Suneet Agarwal, MD, PhD

CONTRACTING ORGANIZATION: Boston Children's Hospital

REPORT DATE: December 2020

TYPE OF REPORT: Final Report

PREPARED FOR: U.S. Army Medical Research and Development Command
Fort Detrick, Maryland 21702-5012

REPORT DOCUMENTATION PAGE

Form Approved
OMB No. 0704-0188

1. REPORT DATE	2. REPORT TYPE	3. DATES COVERED
DECEMBER 2020	Final	08/15/2019 – 08/14/2020

4. TITLE AND SUBTITLE

Novel Therapeutics for Bone Marrow Failure Disorders Due to Telomere Exhaustion

5a. CONTRACT NUMBER
W81XWH-19-1-0572

5b. GRANT NUMBER
BM180089

5c. PROGRAM ELEMENT NUMBER

6. AUTHOR(S)
Suneet Agarwal, MD, PhD

E-Mail: suneet.agarwal@childrens.harvard.edu

5d. PROJECT NUMBER

5e. TASK NUMBER

5f. WORK UNIT NUMBER

7. PERFORMING ORGANIZATION NAME(S) AND ADDRESS(ES)

Boston Children's Hospital
300 Longwood Avenue,
Boston MA 02115-5724

8. PERFORMING ORGANIZATION REPORT NUMBER

9. SPONSORING / MONITORING AGENCY NAME(S) AND ADDRESS(ES)

U.S. Army Medical Research and Development Command
Fort Detrick, Maryland 21702-5012

10. SPONSOR/MONITOR'S ACRONYM(S)

11. SPONSOR/MONITOR'S REPORT NUMBER(S)

12. DISTRIBUTION / AVAILABILITY STATEMENT

Approved for Public Release; Distribution Unlimited

13. SUPPLEMENTARY NOTES

14. ABSTRACT

The overall goal of this project is to understand molecular pathways leading to bone marrow failure (BMF) caused by impaired telomere maintenance, and exploit them for therapy. The proposal builds on our recently published work that for the first time defines non-coding RNA pathways and novel enzymatic targets regulating human telomerase. In preliminary work, we identified a hit molecule in a high-throughput screen that increases telomerase activity. Here, we propose to study how manipulation of these pathways using novel small molecule analogs of the hit compound impact telomere biology and hematopoiesis in stem cells, including those from patients with BMF disorders caused by telomere dysfunction such as dyskeratosis congenita (DC). We find that analogs of the hit molecule show enhanced ability to augment telomerase and telomere length in patient cells. Such molecules restore telomerase RNA processing and do not adversely impact hematopoietic stem cell function in vitro. Taken together, this work advances novel therapeutic strategies for BMF disorders associated with telomere exhaustion.

15. SUBJECT TERMS
Aplastic anemia, Bone marrow failure, Dyskeratosis congenita, Non-coding RNA, Rare disease. Small molecule, Stem cell, Telomerase, Telomere

16. SECURITY CLASSIFICATION OF:			17. LIMITATION OF ABSTRACT	18. NUMBER OF PAGES	19a. NAME OF RESPONSIBLE PERSON
a. REPORT	b. ABSTRACT	c. THIS PAGE			19b. TELEPHONE NUMBER *(include area code)*
Unclassified	Unclassified	Unclassified	Unclassified	49	USAMRMC

TABLE OF CONTENTS

INTRODUCTION

The overall goal of this project is to understand molecular pathways leading to bone marrow failure (BMF), severe aplastic anemia (SAA) and myelodysplastic syndrome (MDS) caused by impaired telomere maintenance, and exploit them for therapy. The proposal builds on our recently published work, independently validated by others, that for the first time defines non-coding RNA pathways and novel enzymatic targets regulating human telomerase. Here, we propose to study how manipulation of these pathways impacts telomere biology and hematopoiesis in stem cells, including those from patients with BMF disorders caused by telomere dysfunction such as dyskeratosis congenita (DC), SAA, and MDS. Successful execution of the work will open new disease-relevant areas of basic investigation at the nexus of non-coding RNA and telomere biology, and advance novel therapeutic strategies for BMF disorders associated with telomere exhaustion.

KEYWORDS

Aplastic anemia
Bone marrow failure
Dyskeratosis congenita
Non-coding RNA
Rare disease
Small molecule
Stem cell
Telomerase
Telomere

ACCOMPLISHMENTS

What were the major goals of the project?

The major goals of this project were to: (1) test the effects of PAPD5 inhibition using PAPD5 inhibitor in induced pluripotent stem cells (iPSCs) from patients with genetic mutations that cause dyskeratosis congenita (DC) / telomere diseases, and (2) determine the impact of PAPD5 inhibitor on molecular and hematologic phenotypes in vitro of telomere deficiency in primary human HSCs by short term culture and colony-forming unit (CFU) assays. These activities contribute to the long-term goal of understanding the role of telomere biology in human health and how it can be manipulated in BMF and other disease states (see *Appendix*, Nagpal and Agarwal, Stem Cells, 2020).

What was accomplished under these goals?

Major activities

1) We tested a novel PAPD5 inhibitor, an analog developed via medicinal chemistry in our prior work, for its effects on telomere biology in iPSCs from patients with DC. Specifically, we evaluated telomerase RNA (TERC) 3' end processing, steady-state TERC levels, telomerase activity levels, and telomere length dynamics.

2) We also tested the PAPD5 inhibitor on its effects in primary human hematopoietic stem cells (HSCs) that were engineered using CRISPR/Cas9 to carry mutations in genes that cause DC. The readouts included TERC 3' end processing and functional impacts in CFU assays.

Specific objectives

1) We sought to determine whether the PAPD5 inhibitor possessed improved properties such as potency in PAPD5 inhibition, compared to a screening hit called BCH001 (see relevant publication in Appendix, Nagpal, et al, *Cell Stem Cell* 2020). Improved function would be predicted based on higher inhibition and binding of the analog in *in vitro* enzymatic assays, but required proof in cell-based assays, which were performed here in patient iPSCs.

2) We sought to determine whether the novel PAPD5 inhibitor would function in a disease-relevant stem cell model of bone marrow failure, specifically human HSCs. Because DC mutation-carrying primary HSCs from patients are very difficult to obtain, we engineered loss-of-function mutations in DC-relevant genes in commercially-available primary HSCs from healthy donors, which recapitulated a molecular phenotype of the genetic mutation seen in patient cells. We assayed whether the PAPD5 inhibitor could reverse this phenotype. We then asked whether engineering of the mutation or reversal of the molecular phenotype correlated with functional impacts in HSC CFU assays.

Significant results

In the course of creating and testing several BCH001 analogs under prior and separate awards, we identified novel PAPD5 inhibitors with improved potency based on (1) recombinant PAPD5 (rPAPD5) enzyme inhibition in an RNA poly-adenylation assay, and (2) rPAPD5 binding, as measured by differential scanning fluorimetry (DSF) assay. Here we tested a BCH001 analog dubbed BCH470 for effects on telomere biology in patient iPSCs. For detailed methods of experiments described below, see *Appendix*, Nagpal, et al, *Cell Stem Cell* 2020. Briefly, iPSCs from patients with *PARN* mutations were cultured in the presence of 1 μM BCH470, and compared to other analogs and the parent molecule BCH001, versus dimethylsulfoxide (DMSO) vehicle control, for five days. For TERC 3' end-processing assays, RNA-ligation mediated rapid amplification of cDNA ends (RLM-RACE) was performed as follows. RNA was prepared, a universal linker ligated to the 3' end, first-strand cDNA produced, and reverse transcription - polymerase chain reaction (RT-PCR) performed to profile the size distribution of the TERC 3' end, which is abnormal in patients with *PARN* mutations (Moon, *et al*, Nature Genetics, 2015). We found that BCH470 showed improved TERC 3' end maturation compared

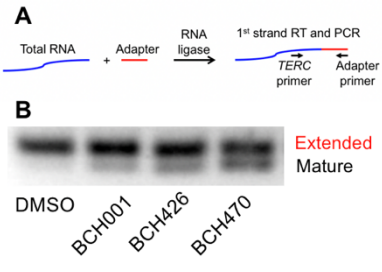

Figure 1. Activity of BCH001 analogs from medicinal chemistry in patient cell-based assays. A. Schema of RLM-RACE assay. **B.** BCH001 analogs BCH426 and BCH470 show increased 3' end maturation of TERC RNA compared to BCH001. Five days, 1 μM drug, in patient iPSCs. Representative image of n=3 replicates.

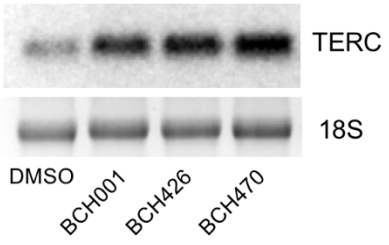

Figure 2. BCH470 increases TERC levels in patient iPSCs. Northern blot, showing increases of TERC steady-state levels in iPSCs treated with BCH0470 (1 μM) compared to parent molecule or vehicle.

to BCH001 (Figure 1). In correlation with this finding, TERC steady-state RNA levels were increased by northern blot (Figure 2). Next iPSCs were cultured in the presence of BCH470 versus controls for seven days, after which they were harvested and cell lysates produced. Telomerase repeat amplification protocol (TRAP) assay was performed in cells treated with BCH470. We found that patient iPSCs showed higher relative cellular telomerase activity with the PAPD5 inhibitor compared to vehicle control, consistent with the fact that TERC levels are limiting for overall telomerase levels in human cells. To determine the impact of TERC and telomerase restoration on telomere length, patient iPSCs were cultured for 21 days were BCH470, other BCH analogs and BCH001 versus vehicle control (Figure 3). We find that BCH001 analogs developed via medicinal chemistry and triaged using in vitro rPAPD5 enzymatic and binding assays showed enhanced telomere elongating capacity, which correlated with their relative effects on TERC 3' end processing. The data demonstrate superiority of BCH470 compared to BCH001 in the patient iPSC-based assays.

Next, we engineered commercially-available primary human CD34+ blood cells (NIDDK Cooperative Centers for Excellence in Hematology, University of Washington) to be PARN-deficient using high-efficiency CRISPR/Cas9 ribonucleoprotein transfection. For detailed methods see Nagpal, et al, Cell Stem Cell, 2020 (*Appendix*). By RLM-RACE, we were able to recapitulate defective TERC 3' processing five days after highly-efficient *PARN* disruption in primary HSCs. Co-culture with BCH470 resulted in reversal of the aberrant TERC 3' end maturation phenotype. These data demonstrate that small molecule PAPD5 inhibitors can reverse a molecular hallmark of telomerase insufficiency (TERC 3' end maturation defects) *in vitro*. We next assessed *in vitro* HSC function using methylcellulose CFU assays. Briefly, HSCs are plated in limiting number in semi-solid agar in the presence of several cytokines that direct hematopoietic differentiation. After culture for 10-14 days, colonies appear in the agar plate, and possess morphologic features that are used to classify lineage-specific characteristics. In this manner, quantitative and qualitative aspects of HSC function can be scored. However, we found that CRISPR-engineered PARN-deficient CD34+ cells did not display significant defects in CFU formation. Accordingly, because of this technical limitation, we could not assess a restorative effect of BCH470 on HSC function via the CFU assay. We speculate that this may be because telomere length is sufficiently long in normal HSCs which have been made PARN-deficient to support their function during the time course of this experiment. Future experiments will attempt to use patient-derived HSCs which would be expected not only to carry the pathogenic mutation but also short telomeres due to their replicative history in vivo. Nevertheless, BCH470 did not show adverse effects on HSCs in the CFU assay, neither in colony number nor in lineage distribution. These data indicate that PAPD5 inhibition is tolerated by HSCs without toxicity, further supporting the translational potential of this strategy for BMF.

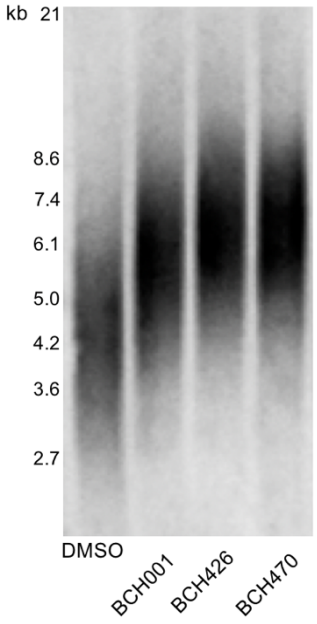

Figure 3. Telomere elongation in patient iPSCs is enhanced by BCH470. Telomere restriction fragment length assay (Southern blot) showing mean telomere length increased in BCH470 (1 μM) treated patient iPSCs versus BCH001 (1 μM) or vehicle, cultured for 21 days. Representative image of n=2 replicates.

Other achievements
Nothing to report.

What opportunities for training and professional development has the project provided?
Dr. Neha Nagpal is a post-doctoral fellow who performed the work under this award under the direct mentorship of Dr. Suneet Agarwal, including one-on-one meetings, technical development and

knowledge acquisition. Dr. Nagpal took advantage opportunities to present the work related to this project in publications (*see Appendix*) and participation in conferences (e.g. Boston Children's Hospital Stem Cell Program, Harvard Initiative in RNA Medicine), which enhanced professional career development.

How were the results disseminated to communities of interest?
Nothing to report.

What do you plan to do during the next reporting period to accomplish the goals?
Nothing to report.

IMPACT

What was the impact on the development of the principal discipline(s) of the project?
The work represents a significant advance in the principal disciplines of the project, namely bone marrow failure (BMF) and telomere biology. A commentary accompanying our publication on related work (see Appendix: Nagpal, *et al*, *Cell Stem Cell*, 2020) recognized it as a "spectacular demonstration" of potentially translating basic biology to clinical use (Reddel, *et al*, *Cell Stem Cell*, 2020). The work performed here represents advances towards the first small molecule human telomerase regulators for use in BMF and potentially other degenerative diseases. The results generated under this award reinforce PAPD5 as a potential therapeutic target, and provide proof-of-concept that a small molecule strategy can be advanced to enhance TERC and telomerase activity in human stem cells. Ultimately, if successful, we expect such molecules will be candidates to restore telomere maintenance and HSC regenerative capacity in patients with BMF.

What was the impact on other disciplines?
While the work is focused on BMF and telomere biology in human cells, there is potential impact in the field of RNA biology. The demonstration of PAPD5 inhibitor using small molecules provides tools and knowledge for others studying non-coding RNA biology in various systems. The experiments performed here add to the burgeoning data that factors such as PARN and PAPD5 play different roles in human biology versus those of their orthologs in other organisms.

What was the impact on technology transfer?
BCH001 analogs being tested are the subject of intellectual property (Boston Children's Hospital), pre-dating this award. It is possible that the work conducted in this award will positively impact the development and ultimately commercialization of PAPD5 inhibitors for BMF and telomere diseases.

What was the impact on society beyond science and technology?
Nothing to report

CHANGES/PROBLEMS

Changes in approach and reasons for change
Nothing to report

Actual or anticipated problems or delays and actions or plans to resolve them
Nothing to report

Changes that had a significant impact on expenditures
Nothing to report

Significant changes in use or care of human subjects, vertebrate animals, biohazards, and/or select agents
Nothing to report

Significant changes in use or care of human subjects
Nothing to report

Significant changes in use or care of vertebrate animals
Nothing to report

Significant changes in use of biohazards and/or select agents
Nothing to report

PRODUCTS

Publications, conference papers, and presentations

1. Nagpal N, Wang J, Zeng J, Lo E, Moon DH, Luk K, Braun RO, Burroughs LM, Keel SB, Reilly C, Lindsley RC, Wolfe SA, Tai AK, Cahan P, Bauer DE, Fong YW, Agarwal S. Small molecule PAPD5 inhibitors restore telomerase activity in patient stem cells. Cell Stem Cell. 2020; 26(6): 896-909. PMID: 32320679
2. Nagpal N, Agarwal S. Telomerase RNA processing: implications for human health and disease. Stem Cells. 2020; 38(12): 1532-1543. PubMed PMID: 32875693.

Books or other non-periodical, one-time publications

Nothing to report

Other publications, conference papers, and presentations

Nothing to report

Website(s) or other Internet site(s)

Nothing to report

Technologies or techniques

Nothing to report

Inventions, patent applications, and/or license

Nothing to report

Other Products

Nothing to report

PARTICIPANTS & OTHER COLLABORATING ORGANIZATIONS

What individuals have worked on the project?

Name:	Suneet Agarwal, MD, PhD
Project Role:	PI
Nearest person month worked:	1
Contribution to Project:	No change
Funding Support:	No change
Name:	Neha Nagpal, PhD
Project Role:	Post-doctoral fellow
Nearest person month worked:	4
Contribution to Project:	No change
Funding Support:	No change

Has there been a change in the active other support of the PD/PI(s) or senior/key personnel since the last reporting period?

No change

What other organizations were involved as partners?

Nothing to report

SPECIAL REPORTING REQUIREMENTS

Not applicable

APPENDICES

1. Nagpal N, Wang J, Zeng J, Lo E, Moon DH, Luk K, Braun RO, Burroughs LM, Keel SB, Reilly C, Lindsley RC, Wolfe SA, Tai AK, Cahan P, Bauer DE, Fong YW, Agarwal S. Small molecule PAPD5 inhibitors restore telomerase activity in patient stem cells. Cell Stem Cell. 2020; 26(6): 896-909. PMID: 32320679
2. Nagpal N, Agarwal S. Telomerase RNA processing: implications for human health and disease. Stem Cells. 2020; 38(12): 1532-1543. PubMed PMID: 32875693.

Cell Stem Cell

Article

Small-Molecule PAPD5 Inhibitors Restore Telomerase Activity in Patient Stem Cells

Graphical Abstract

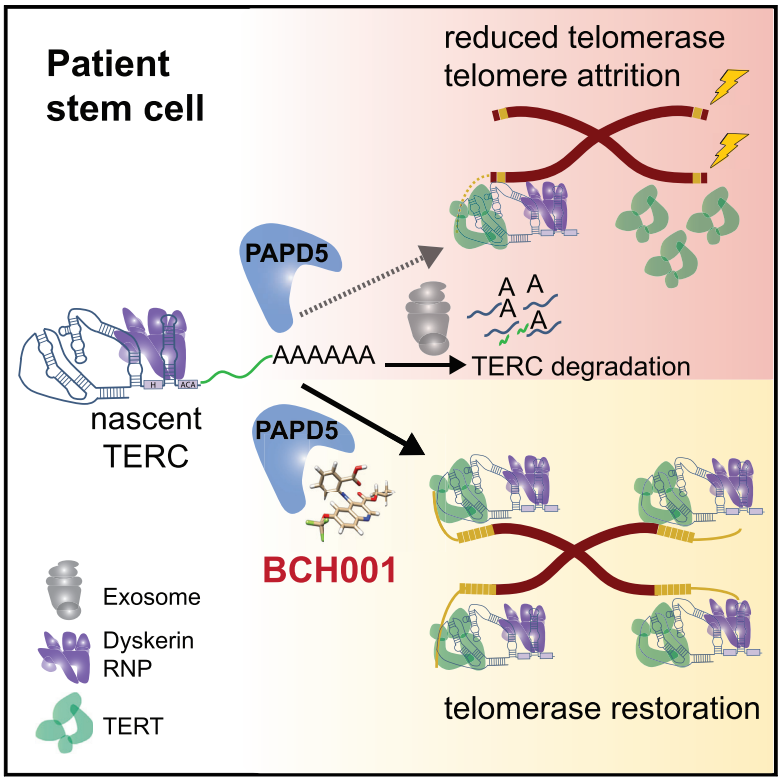

Authors

Neha Nagpal, Jianing Wang, Jing Zeng, ..., Daniel E. Bauer, Yick W. Fong, Suneet Agarwal

Correspondence

suneet.agarwal@childrens.harvard.edu

In Brief

Nagpal et al. identify small-molecule inhibitors of PAPD5, a non-canonical polymerase, as regulators of the telomerase RNA component TERC. PAPD5 inhibitors restore telomere length in cells from patients with genetic "telomeropathies" and human blood stem cells xenotransplanted into mice, providing a therapeutic strategy to manipulate telomerase systemically.

Highlights

- High-throughput screening identifies specific small-molecule PAPD5 inhibitor BCH001
- BCH001 restores telomere length in iPSCs from patients with dyskeratosis congenita
- Repurposed HBsAg suppressors, dihydroquinolizinones, increase TERC in stem cells
- Oral PAPD5 inhibitors restore TERC and telomeres in human HSPCs *in vivo*

Nagpal et al., 2020, Cell Stem Cell *26*, 896–909
June 4, 2020
https://doi.org/10.1016/j.stem.2020.03.016

CellPress

CellPress

Cell Stem Cell

Article

Small-Molecule PAPD5 Inhibitors Restore Telomerase Activity in Patient Stem Cells

Neha Nagpal,[1,2,3,4,5,6,7] Jianing Wang,[3,8,9] Jing Zeng,[1,2,3,4,10] Emily Lo,[11] Diane H. Moon,[1,2,3,4,5,6,7] Kevin Luk,[12] Roman O. Braun,[1,2,3,4,5,6,7] Lauri M. Burroughs,[13,14,15] Sioban B. Keel,[16] Christopher Reilly,[17] R. Coleman Lindsley,[17] Scot A. Wolfe,[12] Albert K. Tai,[18] Patrick Cahan,[11] Daniel E. Bauer,[1,2,3,4,10] Yick W. Fong,[3,8,9] and Suneet Agarwal[1,2,3,4,5,6,7,19,*]

[1]Division of Hematology/Oncology, Boston Children's Hospital, Boston, MA, USA
[2]Department of Pediatric Oncology, Dana-Farber Cancer Institute, Boston, MA, USA
[3]Harvard Stem Cell Institute, Boston, MA, USA
[4]Department of Pediatrics, Harvard Medical School, Boston, MA, USA
[5]Stem Cell Program, Boston Children's Hospital, Boston, MA, USA
[6]Manton Center for Orphan Disease Research, Boston Children's Hospital, Boston, MA, USA
[7]Harvard Initiative in RNA Medicine, Boston, MA, USA
[8]Brigham Regenerative Medicine Center, Cardiovascular Division, Brigham and Women's Hospital, Boston, MA, USA
[9]Department of Medicine, Harvard Medical School, Boston, MA, USA
[10]Broad Institute, Boston, MA, USA
[11]Department of Biomedical Engineering and Institute for Cell Engineering, Johns Hopkins University School of Medicine, Baltimore, MD, USA
[12]Department of Molecular, Cell and Cancer Biology, Li Weibo Institute for Rare Diseases Research, University of Massachusetts Medical School, Worcester, MA, USA
[13]Fred Hutchinson Cancer Research Center, Seattle, WA, USA
[14]Seattle Children's Hospital, Seattle, WA, USA
[15]Department of Pediatrics, University of Washington, Seattle, WA, USA
[16]Division of Hematology, Department of Medicine, University of Washington, Seattle, WA, USA
[17]Department of Medical Oncology, Division of Hematological Malignancies, Dana-Farber Cancer Institute, Boston, MA, USA
[18]Department of Immunology, Tufts University School of Medicine, Boston, MA, USA
[19]Lead Contact
*Correspondence: suneet.agarwal@childrens.harvard.edu
https://doi.org/10.1016/j.stem.2020.03.016

SUMMARY

Genetic lesions that reduce telomerase activity inhibit stem cell replication and cause a range of incurable diseases, including dyskeratosis congenita (DC) and pulmonary fibrosis (PF). Modalities to restore telomerase in stem cells throughout the body remain unclear. Here, we describe small-molecule PAPD5 inhibitors that demonstrate telomere restoration *in vitro*, in stem cell models, and *in vivo*. PAPD5 is a non-canonical polymerase that oligoadenylates and destabilizes telomerase RNA component (TERC). We identified BCH001, a specific PAPD5 inhibitor that restored telomerase activity and telomere length in DC patient induced pluripotent stem cells. When human blood stem cells engineered to carry DC-causing *PARN* mutations were xenotransplanted into immunodeficient mice, oral treatment with a repurposed PAPD5 inhibitor, the dihydroquinolizinone RG7834, rescued TERC 3′ end maturation and telomere length. These findings pave the way for developing systemic telomere therapeutics to counteract stem cell exhaustion in DC, PF, and possibly other aging-related diseases.

INTRODUCTION

Telomeres, the repetitive DNA sequences capping chromosome ends, regulate cellular aging (López-Otin et al., 2013). Telomeres undergo attrition with each cell division due to the inability of DNA polymerases to completely replicate linear chromosome ends (Olovnikov, 1973; Watson, 1972). When telomeres become critically short, cellular senescence is triggered to prevent DNA double-stranded break repair, resulting in chromosomal fusions (d'Adda di Fagagna et al., 2003; Harley et al., 1990; Takai et al., 2003). To maintain replicative capacity, human stem cells express telomerase reverse transcriptase (TERT), which together with the non-coding RNA (ncRNA) template telomerase RNA component (TERC) comprise a functional telomerase ribonucleoprotein (RNP) to replenish telomere repeats (Feng et al., 1995; Meyerson et al., 1997; Nakamura et al., 1997). TERC is a 451-nt-long box H/ACA small Cajal body RNA (scaRNA) bound by several additional factors (dyskerin, NOP10, NHP2, GAR1, and TCAB1) that stabilize and traffic telomerase RNP to Cajal bodies (Jády et al., 2004; Mitchell et al., 1999a; Venteicher et al., 2009). TERC and its associated factors are ubiquitously expressed in human somatic cells but are insufficient to elongate telomeres (Feng et al., 1995). The ectopic expression of TERT completes the telomerase RNP and confers

immortality to somatic cells (Bodnar et al., 1998; Vaziri and Benchimol, 1998).

Mendelian disorders associated with compromised telomere maintenance cause a spectrum of telomere biology diseases (TBDs), ranging from severe, early-onset syndromes such as dyskeratosis congenita (DC) to more common midlife presentations of seemingly isolated aplastic anemia, liver cirrhosis, or pulmonary fibrosis (PF) (Armanios and Blackburn, 2012; Bertuch, 2016; Calado and Young, 2009). Mutations impacting TERT and TERC most often underlie TBDs, alongside other genes regulating telomere structure and replication (Bertuch, 2016). Across the range of TBDs there are no curative therapies, only bone marrow or organ transplantation that are associated with poor outcomes due to impaired tissue function and regenerative capacity throughout the body (Agarwal, 2018; Dietz et al., 2011; Stuart et al., 2014; Swaminathan et al., 2019).

Although TERT is the "on/off" switch for telomerase activity, human genetic data indicate that TERC is limiting and determines telomerase activity in human stem cells once TERT is expressed (Greider, 2006). Heterozygous *TERC* loss of function impairs telomerase activity in stem cells to an extent sufficient to cause TBDs (Aubert et al., 2012; Marrone et al., 2004; Vulliamy et al., 2001). Mutations in genes encoding factors that stabilize TERC (e.g., dyskerin, NOP10, and NHP2) are associated with more profound telomerase deficiency and severe TBD phenotypes (Heiss et al., 1998; Mitchell et al., 1999b; Vulliamy et al., 2008; Walne et al., 2007). Overexpression of TERC in TERT-expressing cells carrying such TBD-causing mutations restores telomerase levels and telomere elongating capacity (Kirwan et al., 2009; Westin et al., 2007; Wong and Collins, 2006). However, a genetic approach to overexpress TERC in stem cells throughout the body is not tractable, and how to systemically modulate levels of a specific ncRNA by other means is unknown.

Recent genetic discoveries of poly(A)-specific ribonuclease (*PARN*) mutations in TBD patients (Dhanraj et al., 2015; Moon et al., 2015; Stuart et al., 2015; Tummala et al., 2015) have revealed enzymatic components of the post-transcriptional machinery that regulate TERC. PARN is an exoribonuclease that removes post-transcriptionally added 3′ extensions on nascent TERC RNA transcripts, promoting maturation and stability of TERC (Moon et al., 2015; Nguyen et al., 2015; Tseng et al., 2015). Conversely, the non-canonical poly(A) polymerase PAPD5 recognizes and oligo-adenylates nascent TERC RNA 3′ends, thereby targeting transcripts for destruction by the RNA exosome (Boyraz et al., 2016; Nguyen et al., 2015; Tseng et al., 2015). PAPD5 knockdown increases TERC (Boyraz et al., 2016; Nguyen et al., 2015; Roake et al., 2019; Shukla et al., 2016; Son et al., 2018; Tseng et al., 2015) and restores telomere length in *PARN*-deficient patient cells (Boyraz et al., 2016). Whether PAPD5, a polymerase predicted to function generally in ncRNA quality control and mRNA stability (Lim et al., 2018; Lubas et al., 2011), can be targeted with sufficient specificity to control TERC and telomere maintenance at a systemic level is unclear.

Here, we identify the PAPD5 inhibitors BCH001 and RG7834, one from a high-throughput screen and the other repurposed, as small-molecule enhancers of TERC. We show that pharmacologic PAPD5 inhibition reverses TERC oligoadenylation and increases TERC in human cell lines, primary cells and induced pluripotent stem cells (iPSCs) from DC patients, and CRISPR/Cas9-engineered *PARN*-deficient primary human hematopoietic stem and progenitor cells (HSPCs). While TERC levels are restored across all of the different cell types tested, we find an increase in telomerase activity and telomere length only in *TERT*-expressing cells. At PAPD5 inhibitor levels sufficient to increase telomere length in patient iPSCs, few changes are observed in other mRNAs and ncRNAs across the transcriptome, revealing unexpected specificity and supporting a potential therapeutic window. In mice xenotransplanted with human *PARN*-deficient HSPCs, oral administration of PAPD5 inhibitors is tolerated for months and restores TERC maturation and telomere elongation. Our findings validate PAPD5 as a target to control TERC levels and telomere elongation in human stem cells and identify BCH001 and RG7834 as promising leads in a new class of telomere therapeutics.

RESULTS

High-Throughput Screening Identifies BCH001, a Novel PAPD5 Inhibitor

To discover PAPD5 inhibitors, we designed and executed a high-throughput luciferase-based screen, measuring ATP consumption by recombinant PAPD5 (rPAPD5) during RNA poly-adenylation *in vitro* (Figures 1A and S1A–S1D). We screened 100,055 chemically diverse small molecules and identified several that reduced rPAPD5-mediated RNA 3′- polyadenylation (Figures 1B and S1E). 480 compounds were selected for their ability to inhibit PAPD5 in a dose-dependent manner, and 72 of these showed specificity for PAPD5 versus the canonical yeast poly(A) polymerase. We further triaged the compounds using four assays: (1) direct visualization of dose-dependent inhibition of RNA oligoadenylation on a polyacrylamide gel; (2) specificity versus other canonical and non-canonical poly-nucleotide polymerases; (3) specificity versus PARN, which like PAPD5 is a member of the superfamily of β-nucleotidyltransferases (Aravind and Koonin, 1999) and whose inhibition would be expected to be counterproductive; and (4) cell-based assays using *PARN* mutant DC patient iPSCs (Figure 1B).

Through this process, we identified a single compound, a quinoline derivative dubbed BCH001 (Figure 1B). BCH001 inhibited rPAPD5 in the low micromolar range *in vitro* and showed no inhibition of PARN or several other canonical and non-canonical polynucleotide polymerases (Figures 1C–1E). By differential scanning fluorimetry (DSF), BCH001 exhibited ATP- and dose-dependent binding to rPAPD5 (Figure 1F). In multiple clones of *PARN* mutant iPSCs from three patients, treatment with 1 μM BCH001 for 7 days reversed TERC 3′ end processing defects, including a decrease in overall 3′ end adenylation of TERC species (Figures 2A, 2B, S2A, and S2B). Concordant with this result, northern blot analysis showed that TERC steady-state levels increased across all replicates and were accompanied by increases in telomerase activity levels without affecting *TERT* expression (Figures 2C–2E). Remarkably, with continued exposure, we observed elongation of telomere ends by thousands of nucleotides in BCH001-treated patient iPSCs compared to DMSO-treated controls (Figure 2F). Telomeres were elongated in a dose-dependent manner at 0.1–1 μM BCH001 in patient iPSCs (Figure S2C). These results

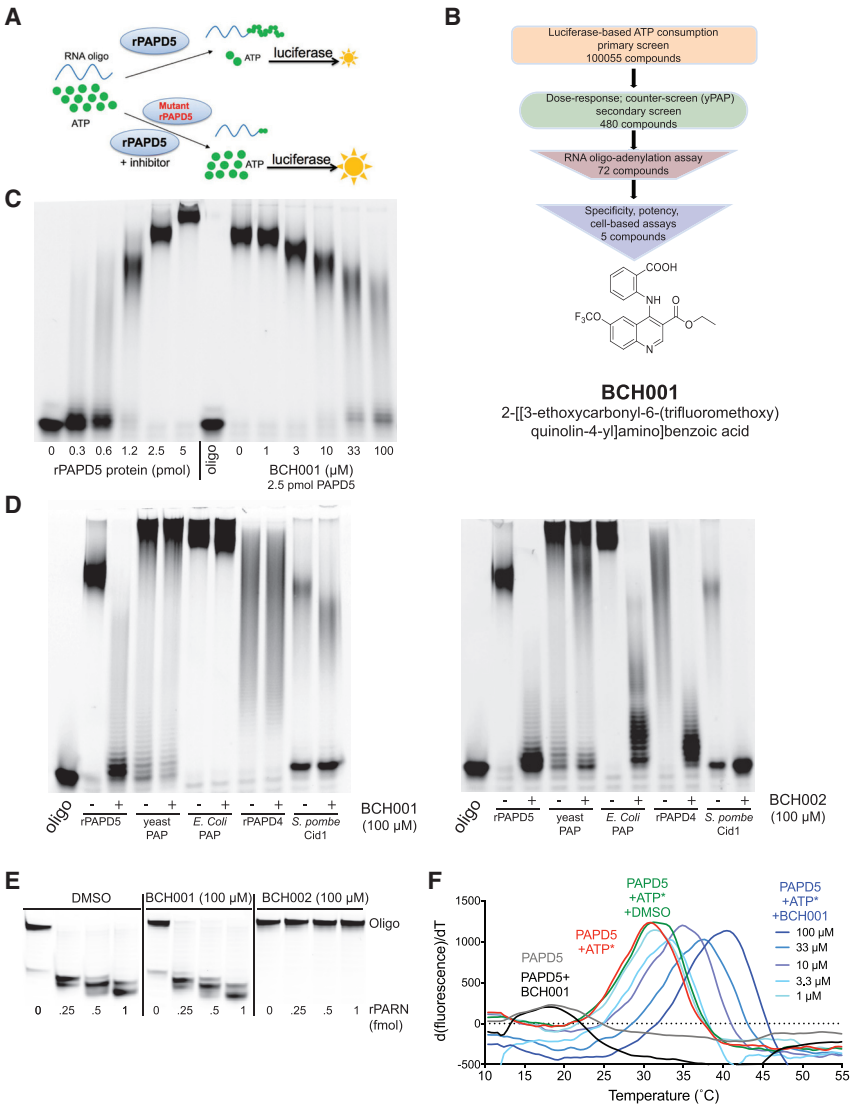

Figure 1. BCH001, a Novel, Specific PAPD5 Inhibitor

(A) Luciferase-based high-throughput screening strategy of reading out ATP consumption based on rPAPD5-mediated RNA poly-adenylation.

(B) Screening triage resulting in identification of BCH001.

(C) Adenylation of an RNA oligonucleotide (oligo) using 2-fold increments of rPAPD5 (left), demonstrating 50% inhibition of rPAPD5 with low micromolar concentrations of BCH001 (right) (n = 3).

(D) Specificity of polymerase inhibition by BCH001 (left) compared to BCH002, 1-(1,3-benzodioxol-5-ylmethyl)-5-oxopyrrolidine-3-carboxylic acid (right). Shown is RNA oligo-adenylation using rPAPD5, yeast poly(A) polymerase (PAP), *E. coli* PAP, rPAPD4, and *S. pombe* Cid1 ± BCH001 or BCH002 (100 μM) (n = 3).

(E) RNA substrate degradation assay using recombinant PARN (rPARN) ± BCH001 or BCH002 (100 μM) (n = 3).

(F) Direct binding of BCH001 to rPAPD5 by differential scanning fluorimetry (n = 5 in triplicates). ATP*, 3′-azidomethyl-ATP, non-extendable ATP analog.

were similar to those seen when we used CRISPR/Cas9 to delete *PAPD5* in *PARN* mutant patient iPSCs, which showed "dose-dependent" rescue of TERC processing, TERC levels, and telomere length (Figures S2D–S2G). When we tested BCH001 in a *PARN*-deficient HEK293 heterologous cell context, we also found restored TERC 3′ end maturation and steady-state levels and increased telomere length (Figures S3A–S3C). Taken together, these results comprise a novel demonstration of TERC modulation using small molecules to increase telomere length in human cells.

PAPD5 Inhibition Reversibly Normalizes Telomere Length in *PARN* Mutant iPSCs

We found that patient iPSCs could be cultured continuously in 1 μM BCH001 for months, establishing a normalized telomere length setpoint (Figure 3A). Importantly, telomere length did not continue to extend beyond that of wild-type (WT) iPSCs (Figure 3A), as we observed in *PAPD5*-null CRISPR/Cas9-engineered clones (Figure S2G), consistent with the notion that counterregulatory mechanisms limiting excessive telomere elongation remain intact (Greider, 2016; Smogorzewska et al., 2000; Teixeira et al., 2004). We found there was no adverse impact on cell growth, cell cycle, or apoptosis when cells were cultured with BCH001 at concentrations sufficient to increase telomere length (Figures S3D–S3F). When BCH001 was removed, TERC maturation and TERC levels reverted to pathological levels, and telomere length decreased gradually over the course of weeks (Figures 3A–3C). Collectively, these results indicate that ongoing PAPD5 inhibition is required for telomere maintenance and argue against selection of cells with higher TERC levels, longer telomeres, or activation of alternative mechanisms of telomere maintenance by BCH001.

Small-Molecule PAPD5 Inhibitors Cause Few Transcriptome-wide Changes and Rescue Other ncRNAs Disrupted by *PARN* Mutations

To identify transcriptome-wide changes caused by PAPD5 inhibitors in *PARN* mutant patient iPSCs, we performed RNA sequencing (RNA-seq) on total RNA. We found that only the non-coding small Cajal body RNA13 (scaRNA13), which is known to be dependent on PARN for stability (Moon et al., 2015; Son et al., 2018), was significantly differentially expressed across BCH001-treated versus untreated *PARN* mutant patient iPSCs from three patients (Figure S3G). When we examined scaRNA13 transcripts by rapid amplification of cDNA ends (RACE) and northern blot, we found 3′ extended forms and decreased steady-state levels, both of which were rescued by treatment with BCH001, as seen with TERC (Figures 3D and 3E). We found similar results upon analysis of scaRNA8 (Figures 3D and 3E), another ncRNA recently

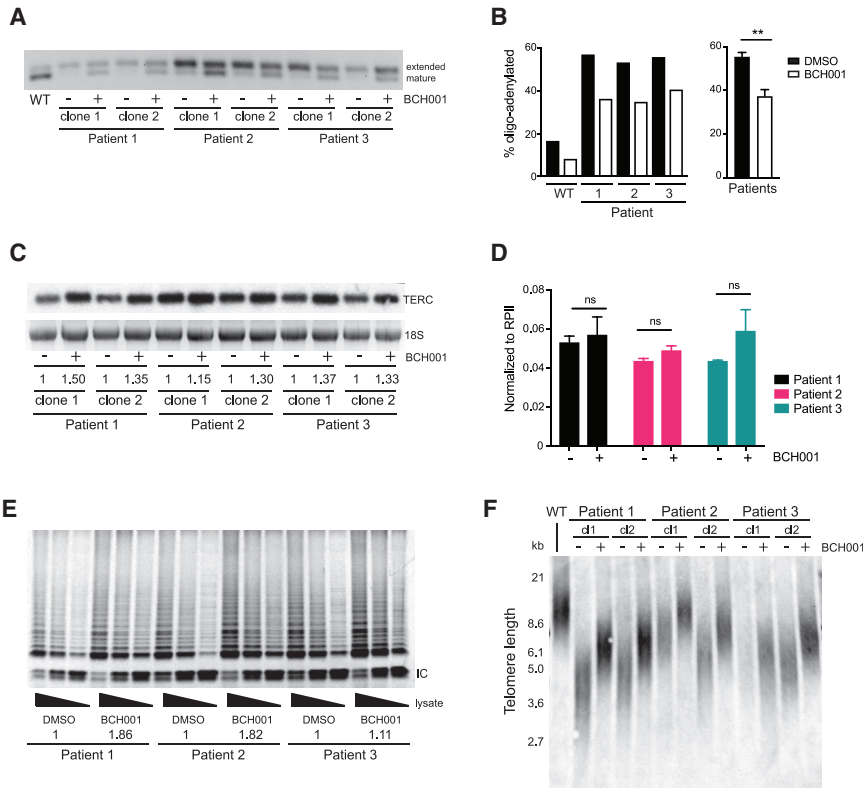

Figure 2. A Small Molecule Restores TERC and Telomere Length in DC Patient iPSCs

(A) TERC 3′ end profiles in independent iPSC clones from three DC patients with biallelic *PARN* mutations after 7 days ± BCH001 (1 μM) (n = 3).

(B) Quantitation of cumulative TERC oligo-adenylated species. Data are presented as mean ± SD of three biological replicates (right). **p < 0.001, two-tailed t test.

(C) TERC RNA levels by northern blot in iPSC clones from three DC patients as in (A) after 7 days ± BCH001 (1 μM). 18S rRNA was used as a loading control. Relative normalized TERC levels are indicated (n = 3).

(D) TERT RNA levels by quantitative RT-PCR of *PARN* mutant iPSCs treated with BCH001 (1μM) for 7 days versus DMSO, with RPII for normalization (n = 2 biological replicates). Data are presented as mean ± SD. ns, not significant, two-tailed t test.

(E) Telomeric repeat amplification protocol (TRAP) assay for telomerase activity in iPSCs using 5-fold extract dilutions. Internal control (IC) is indicated. Relative telomerase activity (TA) was quantified (n = 2).

(F) Terminal restriction fragment (TRF) telomere length analysis in patient iPSC clones (cl) after 4 weeks ± BCH001 (1μM) compared to normal (WT) iPSCs (n = 3).

shown to be regulated by PARN and PAPD5 (Son et al., 2018). These data lend further evidence that mRNAs are not a major target of the PARN/PAPD5 axis and are consistent with findings that other RNAs impacted by PARN loss of function are restored by RNA interference of PAPD5 (Shukla et al., 2019; Shukla and Parker, 2017; Son et al., 2018). Taken together, the results indicate minimal changes in the ncRNA transcriptome after PAPD5 inhibition, and demonstrate that ncRNAs dysregulated by *PARN* deficiency beyond TERC can be restored by small-molecule PAPD5 inhibitors.

PAPD5 Inhibition Restores Telomere Maintenance in Normal and *DKC1* Mutant Cells

Mutations not only in *PARN* but also in *DKC1*, *NAF1*, *NHP2*, *NOP10*, *ZCCHC8*, and *TERC* itself cause telomere disease by decreasing TERC levels (Gable et al., 2019; Mitchell et al., 1999b; Moon et al., 2015; Stanley et al., 2016; Vulliamy et al., 2008; Vulliamy et al., 2001; Walne et al., 2007). To evaluate if PAPD5 inhibition could be more broadly applicable than the *PARN* mutant setting, we inactivated *PAPD5* by CRISPR/Cas9 in patient iPSCs carrying pathogenic *DKC1* mutations (p.del37L and p.A386T) (Agarwal et al., 2010). We observed increased telomere length with genetic deletion of *PAPD5* (Figures S4A and S4B), consistent with RNA interference experiments (Fok et al., 2019; Shukla et al., 2016), and without adverse effects on cell viability or growth. In keeping with this, we found that small-molecule PAPD5 inhibitor treatment enhanced TERC maturation, TERC levels, telomerase activity, and telomere length in *DKC1* mutant patient iPSCs (Figures 4A–4C, S4C, and S4D). In normal iPSCs, *PAPD5* deletion led to increased TERC maturation and telomere length, with a similar trend but decreased effect of BCH001 than in *PARN*-deficient cells (Figures 4D–4F and S4E). Collectively, these results indicate that small-molecule PAPD5 inhibition could be a strategy for telomeropathies beyond PARN-deficient states.

PAPD5 Inhibitors Upregulate TERC without Immortalizing TERT-Negative Cells

We next asked whether telomere elongation by PAPD5 inhibition is dependent on TERT expression. Most human somatic cells do not express TERT (Kim et al., 1994), and because of the end-replication problem, telomere length decreases with each cell division (Harley et al., 1990). The replicative capacity of somatic cells, reflected in the Hayflick limit (Hayflick, 1965), is determined by telomere length reserve, which once depleted triggers cellular senescence. When we treated fibroblasts from patients with *PARN* mutations with BCH001, we found reversal of aberrant TERC 3′ end processing and increases in steady-state TERC levels as expected (Figures 4G and S4F). However, fibroblasts did not show telomere elongation and underwent senescence regardless of BCH001 treatment, consistent with their lack of *TERT* expression (Figures S4G and S4H). When primary fibroblasts were transduced with a retrovirus encoding *TERT*, both BCH001-treated and untreated cells were immortalized, but only cells treated with BCH001 showed telomere lengthening (Figure 4H). Collectively, these data demonstrate that despite augmenting TERC levels, BCH001 treatment does not confer immortality or irreversible telomere lengthening capacity on cells. Rather, the impact of pharmacological PAPD5 inhibition

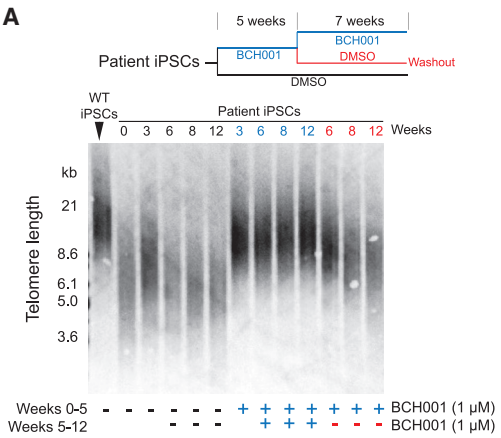

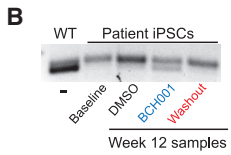

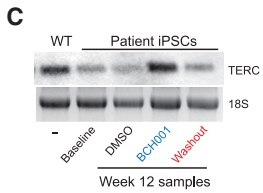

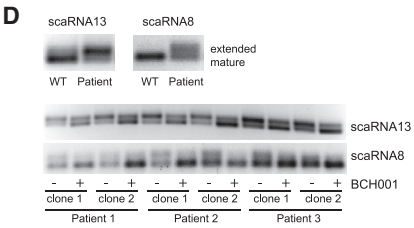

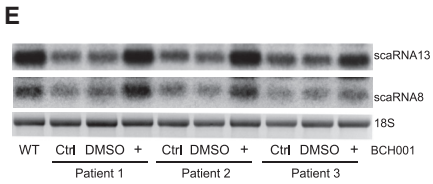

Figure 3. BCH001 Reversibly Normalizes Telomere Length and Non-coding RNA Biogenesis

(A) TRF analysis in *PARN* mutant patient iPSCs treated ± BCH001 (1μM). After 5 weeks, BCH001 treatment continued (blue) or was removed ("washout"; red).

(B) TERC 3′ end profiles in BCH001-treated/washout samples from (A) after 12 weeks (normal [WT] control).

(C) TERC RNA levels in the samples shown in (B) by northern blot (18S rRNA loading control).

(D) scaRNA13 and scaRNA8 RLM-RACE 3′ end profiles in *PARN* mutant patient iPSCs ± BCH001 (1μM) (normal [WT] control) (n = 3).

(E) scaRNA13 and scaRNA8 RNA levels as in (D) by northern blot (18S rRNA loading control) (n = 3).

on telomere length depends on normal physiologic regulation of *TERT* in target cells.

Repurposing Hepatitis B Surface Antigen Suppressors to Restore Telomeres

PAPD5 has recently been implicated in the pathogenesis of chronic hepatitis B virus (cHBV) infection (Mueller et al., 2018). During the course of our studies, a class of dihydroquinolizinones was reported to suppress hepatitis B surface antigen (HBsAg) in a cell-based screen. A yeast three-hybrid screen to identify the cellular target unexpectedly revealed association of the dihydroquinolizinone probe with the catalytic domains of PAPD5 and the related polymerase PAPD7 (Mueller et al., 2019), but direct biochemical evidence was not provided. We hypothesized that dihydroquinolizinone analogs, as inhibitors of PAPD5, could modulate TERC processing and restore telomere elongation in DC patients' cells. To test this, we synthesized 14 different dihydroquinolizinone analogs known to inhibit cellular HBsAg production in the low nanomolar range (Figure 5A) and studied their effects on PAPD5 *in vitro* and on TERC and telomere biology in patient iPSCs. In DSF assays, all dihydroquinolizinones directly bound rPAPD5 in a dose-dependent manner (Figure S5A). Remarkably, we found that applying any of these molecules to *PARN* mutant DC patient iPSCs restored TERC 3′ end maturation and telomere length (Figures 5B and S5B). For more in-depth studies, we focused on the clinical candidate RG7834 (Mueller et al., 2018) (Figure 5A), and found that it bound to rPAPD5 by DSF in a dose-dependent manner, inhibited RNA polyadenylation *in vitro*, and showed selectivity for rPAPD5 compared to PARN and different polynucleotide polymerases, an exception being yeast poly(A) polymerase (Figures 5C, 5D, S5C, and S5D). In *PARN* mutant patient iPSCs, RG7834 restored TERC 3′ end processing and TERC steady-state levels and elongated telomeres at 10 nM, exhibiting greater potency than BCH001, consistent with *in vitro* data (Figures 5E, 5F, S5E, and S5F). Taken together, these data identify dihydroquinolizinones as telomere length regulators, revealing an unexpected convergence of the roles of PAPD5 in HBsAg production and TERC regulation and supporting pharmacologic PAPD5 inhibition as a means to modulate telomere length in human cells.

PAPD5 Inhibitors Augment TERC and Telomerase in CRISPR/Cas9-Engineered PARN-Deficient Primary Human HSPCs

We next asked whether PAPD5 inhibition could impact telomere biology in disease-relevant human stem cells. Bone marrow failure occurs at high frequency in DC (Dokal, 2000). This is driven by a cell-intrinsic telomere maintenance defect in HSPCs, as evidenced by the curative effects of allogeneic bone marrow transplantation, and the selection of somatically reverted *TERC* mutations in the blood *in vivo* (Jongmans et al., 2012). We therefore asked whether we could restore TERC defects in primary human $CD34^+$ cells, which are enriched for HSPCs, by treatment with PAPD5 inhibitors. Using an optimized CRISPR/Cas9 RNP gene-editing strategy (Wu et al., 2019), we obtained high (≥85%) indel frequencies of target genes in mobilized peripheral blood $CD34^+$ cells from healthy volunteers (Figure 6A). After 5 days of *in vitro* culture, we found extended TERC forms specifically in *PARN*-targeted $CD34^+$ cells, which were absent in cells targeted with both *PARN* and *PAPD5* guide RNAs (gRNAs) (Figures 6B, 6C, and S6A). When we treated *PARN*-deficient $CD34^+$ cells with BCH001 or RG7834, we found decreased TERC 3′ adenylation and increased TERC RNA levels after 7 days of culture, corresponding with an increase in telomerase activity in primary HSPCs (Figures 6C–6E and S6B). To further evaluate if telomere-lengthening effects of PAPD5 inhibitors are restricted to stem cells, we performed *in vitro* differentiation of primary HSPCs into myeloid cells in the presence of BCH001, RG7834, or vehicle. We found that despite exposure to PAPD5 inhibitors for three weeks which elongates telomeres in iPSCs (Figures 2F and S5F), telomeres did not lengthen in differentiated myeloid

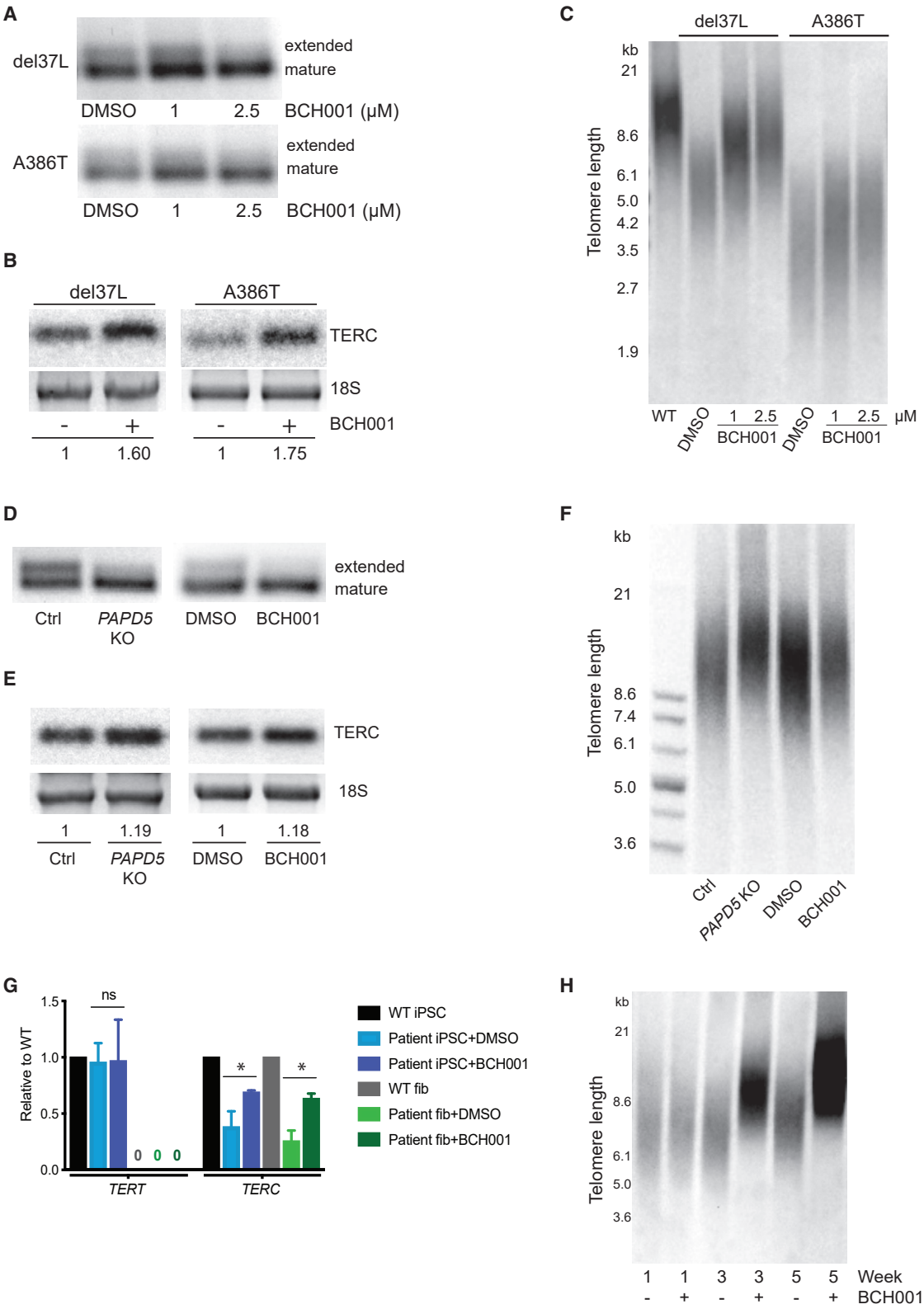

Figure 4. Telomere Elongation due to PAPD5 Inhibition Occurs in WT and *DKC1* Mutant iPSCs and Is TERT Dependent

(A) TERC 3′ end maturation in *DKC1* mutant DC patient iPSCs treated ± BCH001 for 10 days (n = 3 biological replicates for each patient).

(B) TERC RNA levels by northern blot as in (A) (18S rRNA loading control) (n = 3 biological replicates for each patient).

(legend continued on next page)

cells (Figure S6C), consistent with decreased or absent TERC and *TERT* expression in mature peripheral blood cells compared to HSPCs (Figures S6D). Notably, we found no defects in multilineage colony formation in methylcellulose assays performed in the presence or absence of PAPD5 inhibitors (Figure S6E). Taken together, these data demonstrate that PAPD5 inhibitors promote TERC maturation and telomerase in primary human HSPCs, without perturbing hematopoietic differentiation.

PAPD5 Inhibitors Augment TERC in Primary HSPCs from DC Patients

We directly evaluated the effects of PAPD5 inhibitors on hematopoietic cells from DC patients with biallelic *PARN* mutations. As expected, $CD34^+$ cell numbers were limited due the patients' bone marrow failure. To overcome this, we performed *in vitro* hematopoietic differentiation of patient-derived bone marrow $CD34^+$ cells in methylcellulose in the presence or absence of BCH001, RG7834, or vehicle (Figure 6F) and found restoration of TERC 3′ end processing specifically in the presence of PAPD5 inhibitors (Figures 6G). Similar effects on TERC maturation were seen in an independent sample of patient-derived bone marrow mononuclear cells (BMMCs) cultured with PAPD5 inhibitors *in vitro* (Figure 6H). These data demonstrate restoration of TERC processing using small-molecule PAPD5 inhibitors in primary DC patients' HSPCs without impeding hematopoietic differentiation while reversing a molecular phenotype of telomeropathy.

Effects of PAPD5 Inhibition on MDS and AML Cells

Bone marrow failure in telomeropathies is associated with an increased risk of hematology malignancy, including myelodysplastic syndrome (MDS) and acute myeloid leukemia (AML). AML cells have been shown to have shorter telomere length than normal peripheral blood cells (Aalbers et al., 2013), raising the question of whether AML cell growth would be fostered by PAPD5-inhibitor-mediated telomerase augmentation. To address this, we asked whether PAPD5 inhibitors increased proliferation and capacity for clonal outgrowth in human MDS/AML cells. With both short- and long- term exposure to RG7834, we found no significant change in growth rate, viability, or colony-forming potential of human AML cell lines (K562, MV4-11, and MOLM-13) carrying varying driver mutations (Figures S6F–S6H). Verifying the effects of PAPD5 inhibitors on AML cells, we found that TERC processing was altered by CRISPR/Cas9-mediated *PARN* disruption and restored by RG7834 (Figure 6I). Nevertheless, we found no augmentation of cell viability or colony-forming capacity in PARN-deficient AML cells (Figures 6J and S6I). Next, we examined primary samples from a DC patient with *PARN* mutations and MDS characterized by a clonal cytogenetic abnormality (unbalanced translocation of chromosomes 1 and 7 in 80% of bone marrow cells). In methylcellulose assays, there was no significant difference in colony-formation potential of BMMCs in the presence or absence of PAPD5 inhibitors over the course of 3 weeks (Figure S6J). We further tested the effects of PAPD5 inhibitors on primary AML cells from an adult patient with telomeropathy. The patient had telomere length $<1^{st}$ percentile, a germline heterozygous truncating *RTEL1* mutation, a history of PF, and AML with complex karyotype and somatic *TP53* mutations. In methylcellulose assays using primary peripheral blood mononuclear cells with 64% AML blasts, we found no differences in leukemic blast colony-forming potential in the presence or absence of PAPD5 inhibitors (Figure S6K). While further assessment requires developing robust human stem cell models of leukemogenesis in the setting of telomeropathy, together, these data indicate that PAPD5 inhibitors do not stimulate clonal outgrowth or proliferation of human MDS/AML cells.

Orally Administered PAPD5 Inhibitors Restore TERC Maturation and Telomere Length in Human HSPCs *In Vivo*

Next, we asked whether we could rescue telomere homeostasis in human cells *in vivo* by oral administration of PAPD5 inhibitors. We transplanted primary human $CD34^+$ cells in which *PARN* was disrupted by CRISPR/Cas9 into immunodeficient NOD,B6.SCID *Il2rγ*$^{-/-}$ *Kit*$^{W41/W41}$ (NBSGW) mice, which engraft human HSPCs without exposure to radiation or chemotherapy (McIntosh et al., 2015). Mice were treated with RG7834 supplied continuously in drinking water, which we confirmed to be stable and orally bioavailable by serum measurements (Mueller et al., 2018) (Figure 7A). BCH001 was not tested *in vivo* due to relatively lower solubility and potency. Six weeks after infusion, when we analyzed human $CD45^+$ cells engrafted in the bone marrow, we found evidence of increased TERC maturation and decreased 3′ oligoadenylation in RG7834-treated compared with DMSO-treated mice in both $CD34^+$+ HSPCs (Figures 7B and 7C) and $CD19^+$ B cells (Figures 7D, 7E, and S7A). We assessed telomere length in bone marrow cells of xenotransplanted mice by flow cytometry-fluorescence *in situ* hybridization (flow-FISH) (Baerlocher et al., 2006). We were able to distinguish human from mouse bone marrow cells based on human CD45 staining and also the significant difference in telomere length between humans and laboratory mice (Figure 7F). Remarkably, we found that oral administration of RG7834 reversed telomere shortening in *PARN*-deficient human $CD45^+$ cells compared to vehicle treated mice (Figures 7F and 7G). By analyzing chimerism and lineage distribution in xenotransplants, we found that RG7834 treatment also did not adversely affect overall human hematopoietic cell engraftment or result in lineage skewing *in vivo* (Figures 7H and 7I). To explore the impact of

(C) TRF length analysis in *DKC1* mutant DC patient iPSCs treated ± BCH001 for 4 weeks (n = 3 biological replicates for each patient).
(D) TERC 3′ end profiles by RLM-RACE in normal cells. Left: WT iPSC parental cells (Ctrl) compared to a CRISPR/Cas9 *PAPD5*-null clone (PAPD5-KO) (n = 2). Right: WT iPSCs treated ± BCH001 (1 μM) for 7 days (n = 4).
(E) TERC RNA levels by northern blot of samples in (D) (18S rRNA loading control) (n = 2).
(F) TRF length analysis in WT iPSCs (Ctrl), a *PAPD5*-null clone (*PAPD5*-KO), and WT iPSCs treated ± BCH001 (1 μM) for 3 weeks (n = 4).
(G) Quantitative RT-PCR (qPCR) of TERT and TERC RNA from normal (WT) and *PARN* mutant patient iPSCs and fibroblasts treated with BCH001 (1 μM for iPSCs and 100 μM for fibroblasts) for 7 days (n = 2; mean ± SD). Statistics: one-way ANOVA; ns, not significant; *$p < 0.05$.
(H) TRF analysis in *TERT*-immortalized *PARN* mutant fibroblasts treated ± BCH001 (100 μM) for 5 weeks (n = 3).

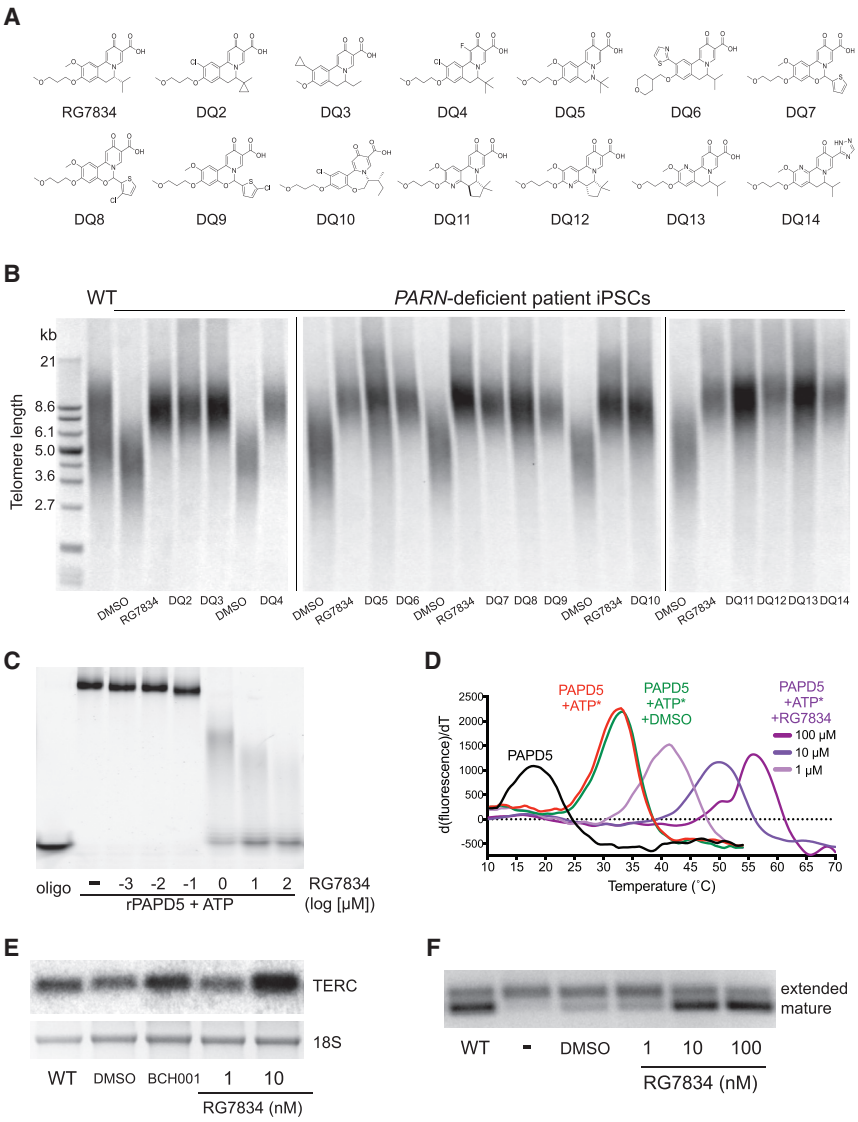

Figure 5. Dihydroquinolizinone Analogs Restore Telomere Maintenance in DC Patient iPSCs

(A) Structures of RG7834 and dihydroquinolizinones (DQ).

(B) TRF analysis in normal (WT) versus *PARN* mutant patient iPSCs cells ± DQ analogs (1 μM) for 3 weeks (n = 2).

(C) Inhibition of rPAPD5 by RG7834 in an RNA oligonucleotide (oligo) adenylation assay (n = 3).

(D) Direct binding of RG7834 to rPAPD5 by differential scanning fluorimetry (n = 5, in triplicates). ATP*, 3-azidomethyl-ATP, non-extendable ATP analog.

(E) TERC levels by northern blot in normal (WT) and *PARN* mutant iPSCs treated with BCH001, RG7834, or DMSO for 2 weeks (18S rRNA loading control) (n = 2).

(F) TERC 3′ end profiles by RLM-RACE in normal (WT) and *PARN* mutant DC patient iPSCs ± RG7834 for 1 week (n = 2).

telomere attrition in the xenotransplant model, when we ablated *TERC*, we found no functional defects in engraftment or lineage specification in long-term primary transplants and secondary transplants (Figures S7B–S7H). Based on comparison to bone-marrow-derived primary CD34$^+$ cells from patient 1, this is likely due to insufficient telomere attrition in the xenotransplant model when starting with normal HSPCs (Figure S7F). Importantly, mice tolerated continuous administration of RG7834 in drinking water for months without adverse effects, indicating that drug levels sufficient to restore TERC and telomere length were not toxic. Taken together, these data indicate that orally administered PAPD5 inhibitors can safely restore TERC maturation and telomere length in a disease-relevant human primary stem cell compartment and set the stage for clinical studies in patients.

DISCUSSION

Telomere length maintenance is important in human health and disease, from rare TBDs to aging, but methods to safely manipulate telomerase have been elusive. Challenges drugging TERT and using genetic approaches to inhibit or upregulate telomerase have yielded limited if any therapeutic applications. Regarding gene therapy, recent studies employed transient ectopic expression of *TERT* via AAV vectors or modified mRNA to avoid cellular immortalization (Povedano et al., 2018; Ramunas et al., 2015). These approaches cannot achieve reliable widespread tissue exposure and do not specifically target stem cells, the physiologic reservoir of regenerative capacity. TBDs and aging are systemic diseases. No strategy put forth to date modulates telomerase specifically in stem cells throughout the body.

We focused on TERC rather than TERT for several reasons. An abundance of genetic evidence implicates TERC in regulating telomere length and tissue regenerative capacity in humans. Across TBDs, several genetic mutations (*TERC*, *DKC1*, *NOP10*, *NHP2*, *TCAB1*, *NAF1*, *PARN*, *ZCCHC8*) cause disease by impairing the processing, folding, stability, RNP assembly, and/or trafficking of TERC (Dhanraj et al., 2015; Gable et al., 2019; Mitchell et al., 1999b; Moon et al., 2015; Stanley et al., 2016; Vulliamy et al., 2001, 2008; Walne et al., 2007; Zhong et al., 2011). While it is clear that TERT is the on-off switch for telomerase activity, TERC levels limit telomerase activity and thus telomere maintenance and self-renewal capacity in human stem cells (Greider, 2006; Westin et al., 2007; Wong and Collins, 2006). Further support comes from population genetic studies showing that variants in the *TERC* locus reproducibly associate with telomere length and longevity (Codd et al., 2010; Shen et al., 2011; Soerensen et al., 2012) and contribute to polygenic risk in common cardiovascular and lung diseases (Haycock et al., 2017). Despite this preponderance of data, TERC has not been a focus of therapeutic efforts, because methods to manipulate TERC specifically have been unknown.

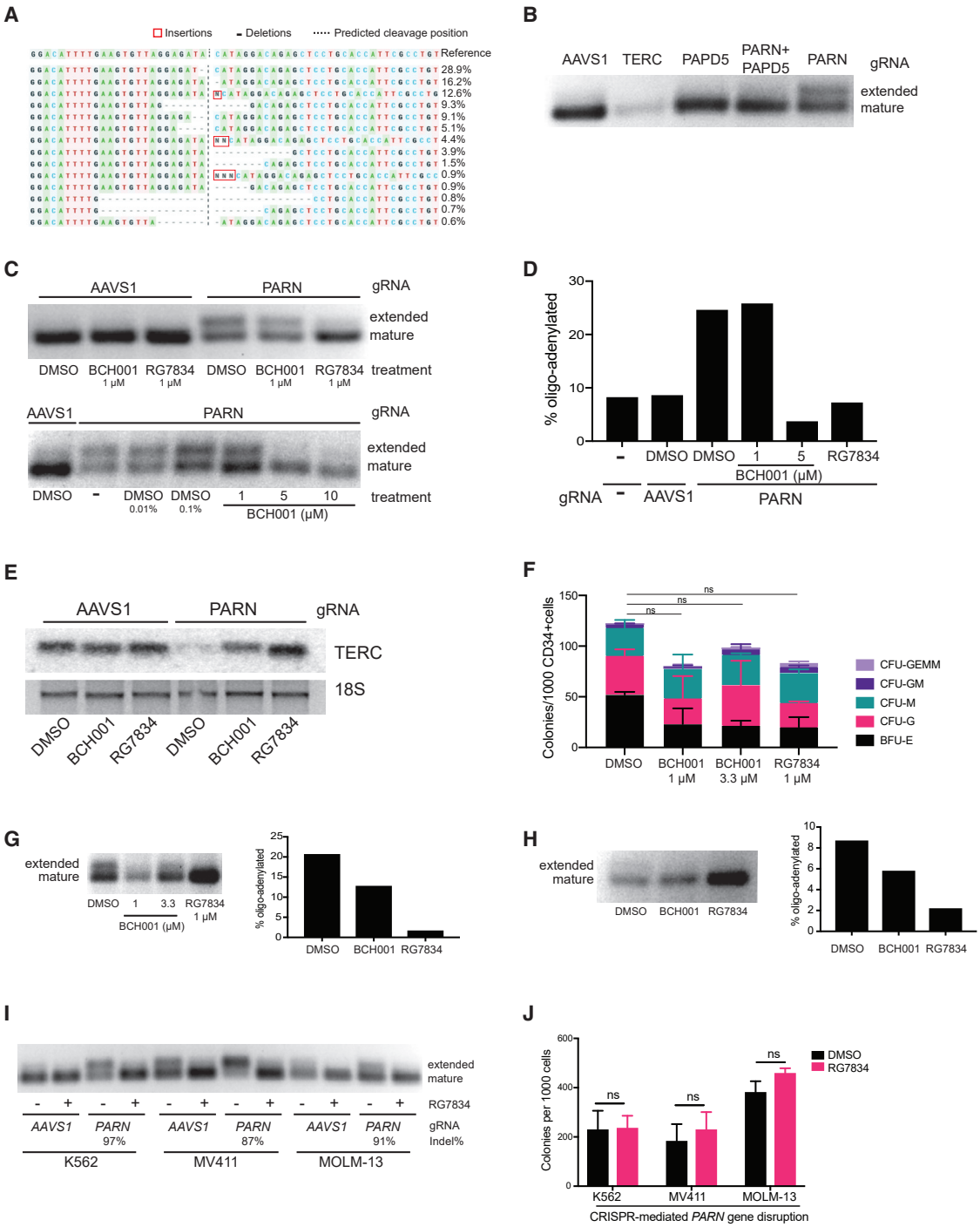

Figure 6. Small-Molecule PAPD5 Inhibitors Restore TERC Maturation in PARN-Deficient Primary Human HSPCs and Leukemia Cell Lines

(A) Inference of CRISPR edits (ICE) analysis in human HSPCs 5 days after CRISPR/Cas9 targeting *PARN* (n = 5).

(B) TERC 3′ end profiling in primary human HSPCs after CRISPR/Cas9 targeting genes indicated (n = 3).

(C) TERC 3′ end profiles in primary human HSPCs following CRISPR/Cas9, cultured 5 days with DMSO, BCH001, or RG7834 (n = 5).

(D) Quantitation of oligo-adenylated TERC by deep sequencing amplicons shown in (C).

(E) TERC RNA levels in primary human HSPCs following CRISPR/Cas9, cultured 5 days with DMSO, BCH001 (5 μM), or RG7834 (1 μM) (n = 3).

(F) Methylcellulose differentiation assay using patient 2 bone marrow (BM) CD34$^+$ cells treated with BCH001, RG7834, or DMSO (n = 2; mean ± SD). Statistics: one-way ANOVA; ns, not significant.

(G) Left: TERC 3′ end profiles in patient 2 BM CD34$^+$ cells as in (F). Right: Cumulative TERC 3′ oligoadenylation by deep sequencing. n = 1 patient sample.

(legend continued on next page)

Here, we leveraged recent insights from ncRNA biology and TBD genetics to develop a small-molecule strategy targeting TERC. The discovery of *PARN* mutations in DC and PF and the elucidation of PARN's role in ncRNA 3′ end maturation uncovered the post-transcriptional machinery responsible for tightly controlling TERC steady-state levels. Nascent TERC transcripts emerge in extended forms consisting of genomically encoded as well as non-templated bases (Goldfarb and Cech, 2013; Moon et al., 2015; Roake et al., 2019). Mechanisms of TERC transcriptional termination are unknown, but it is clear that once extended forms undergo initial trimming, PARN is required for terminal 3′ end maturation and stability (Moon et al., 2015; Nguyen et al., 2015; Roake et al., 2019; Shukla et al., 2016; Son et al., 2018; Tseng et al., 2015, 2018). PAPD5 counteracts TERC maturation by adding non-genomically encoded adenosine residues, which destabilize TERC and target them for degradation by the RNA exosome (Boyraz et al., 2016; Fok et al., 2019; Roake et al., 2019; Shukla et al., 2016; Tseng et al., 2015). Collectively these data point to two enzymes, one a deadenylase and the other a polymerase, with opposing effects that could be modulated to impact TERC levels (Boyraz et al., 2016). The "natural genetic experiment" of TBDs indicates a surprising sensitivity of TERC to *PARN* loss of function in humans, with phenotypes ranging from isolated PF with heterozygous *PARN* mutations to DC with biallelic mutations (Dhanraj et al., 2015; Moon et al., 2015; Stuart et al., 2015; Tummala et al., 2015). Whether PAPD5 downregulation to restore TERC could be tolerated was less clear, given PAPD5's presumed general roles in ncRNA quality control via the TRAMP complex (PAPD5, ZCCHC7, and MTR4) based on studies in yeast (Lubas et al., 2011; Vanácová et al., 2005). Using CRISPR/Cas9 in several cell types and iPSCs, we show that complete PAPD5 loss of function is tolerated in human cells. More importantly, we found that pharmacologic disruption of PAPD5 function sufficient to yield TERC maturation and telomere lengthening showed few transcriptome-wide effects and no obvious toxicity *in vivo* for months. These findings provide a first example of small-molecule modulation of a long ncRNA with sufficient specificity for a therapeutic effect, in this case restoration of telomere maintenance.

Unexpectedly, PAPD5 plays a role in cHBV infection (Mueller et al., 2019). The identification of dihydroquinolizinones as HBsAg suppressors in cell-based screens preceded identification of their cellular target (Mueller et al., 2018). HBsAg is a hallmark of cHBV, wherein continuous expression of HBsAg protein from latent HBV episomal genomes in hepatocytes plays a role in host immune escape, and eradication of HBsAg expression is associated with functional cure. Recent studies indicate that PAPD5 is recruited via the RNA-binding protein ZCCHC14 to poly-adenylate and stabilize nascent HBsAg-encoding transcripts, which is interrupted by treatment with RG7834 (Hyrina et al., 2019). In our hands, RG7834 and dihydroquinolizinones optimized through medicinal chemistry to suppress HBsAg expression showed potent PAPD5 binding, TERC maturation, and telomere elongation in *PARN* mutant DC patient iPSCs. Beyond a role in ncRNA and telomere biology, PAPD5 thus appears to have been co-opted as an essential host factor for viral mRNA production, a discovery from small-molecule screens yielding potential therapeutics for both cHBV and TBDs.

To enable translation, we developed a novel *in vivo* model to read out the effects of pharmacological PAPD5 inhibition on TERC processing and telomere length in human cells. Telomere length is longer and telomerase differentially expressed in somatic cells of laboratory mice compared to wild-derived mice and humans (Kipling and Cooke, 1990; Starling et al., 1990; Zijlmans et al., 1997). The xenotransplant model we developed here utilizes high-efficiency CRISPR/Cas9 RNP-mediated disruption of target genes in primary HSPCs (Wu et al., 2019), which in the case of *PARN* recapitulates TERC processing defects and accelerated telomere attrition *in vivo*. We were thus able to simultaneously evaluate the effects of small molecules on human molecular biomarkers of telomerase, hematopoietic function, and toxicology in an *in vivo* model. We found that mice treated orally for months achieved serum levels of RG7834 sufficient to alter TERC processing and telomere length, without altering human hematopoietic cell engraftment or lineage distribution and without adverse systemic effects in mice. This model overcomes differences in TERC regulation and telomere biology between mice and humans and sets the stage for the clinical development of human telomerase modulators.

In summary, we demonstrate that pharmacological manipulation of a ncRNA biogenesis pathway restores telomere maintenance in TBDs. By targeting TERC, PAPD5 inhibition presents a new opportunity to upregulate telomerase specifically in stem cells based on their physiological expression of TERT, which addresses safety concerns about conferring excessive or aberrant self-renewal capacity on cells throughout the body. BCH001, RG7834, and other dihydroquinolizinones comprise a suite of exciting first-in-class therapeutic leads for a spectrum of TBDs without curative treatments. Further studies will determine the potential of TERC modulation across a range of human degenerative conditions caused by genetic or acquired defects in telomere maintenance.

STAR★METHODS

Detailed methods are provided in the online version of this paper and include the following:

- KEY RESOURCES TABLE
- LEAD CONTACT AND MATERIALS AVAILABILITY
- EXPERIMENTAL MODEL AND SUBJECT DETAILS
  - Human subjects
  - CD34+ HSPCs
  - Fibroblasts

(H) Left: TERC 3′ end profiles of patient 3 BM mononuclear cells following 5 days culture with BCH001 (10 μM), RG7834 (1 μM), or DMSO. Right: Cumulative TERC 3′ oligoadenylation. n = 1 patient sample.
(I) TERC 3′ end profiles in AML cell lines following CRISPR/Cas9, cultured 6 days with DMSO or RG7834 (1 μM) (n = 2).
(J) Methylcellulose colony formation assay in *PARN*-disrupted AML cell lines from (I) treated with RG7834 (1 μM) versus DMSO 8–10 days after plating (n = 2; mean ± SD).

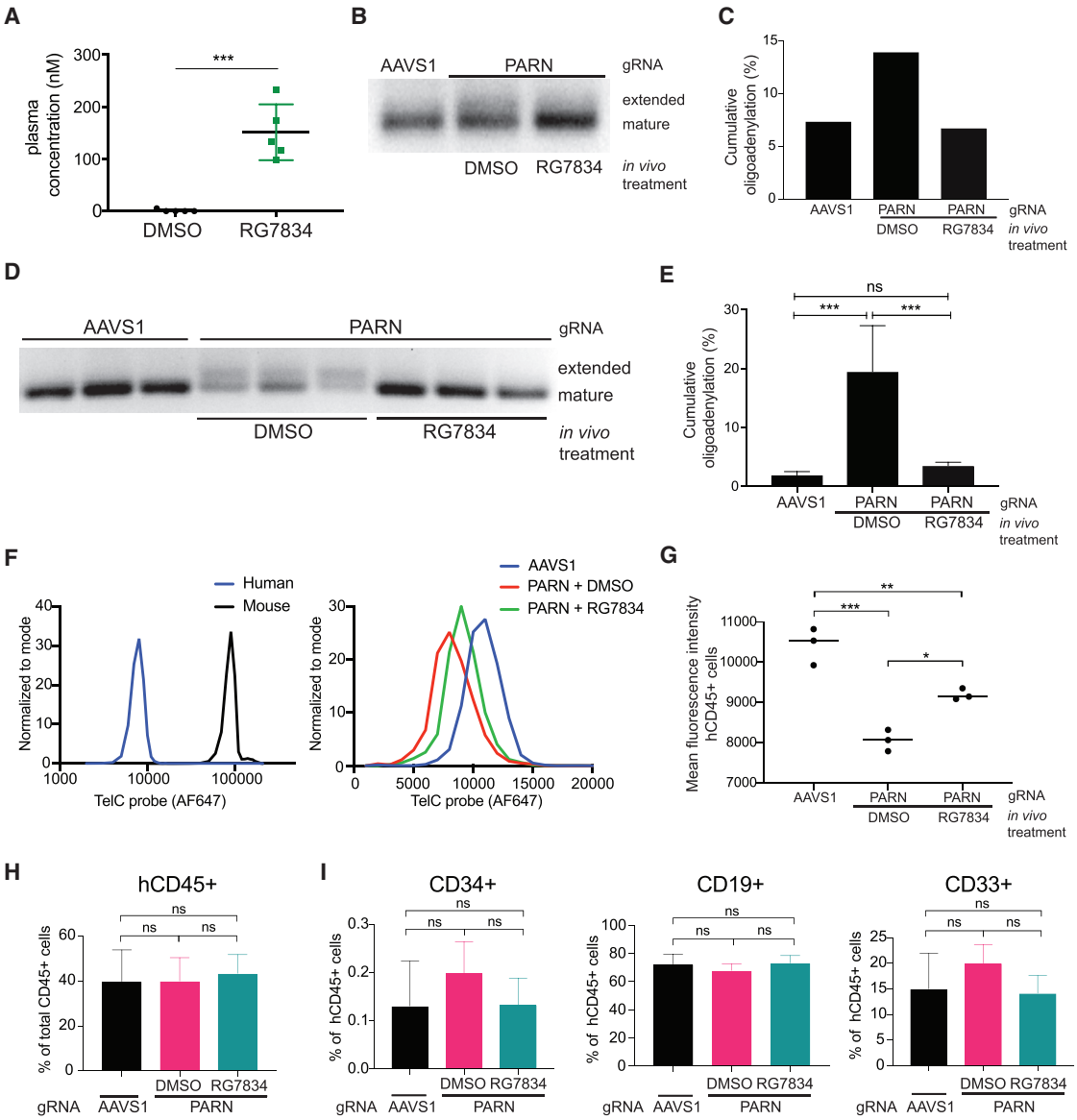

Figure 7. PAPD5 Inhibitor Treatment Restores TERC Maturation and Telomere Length in *PARN* Mutant Primary HSPCs *In Vivo*

(A) Random plasma concentration of RG7834 in mice xenotransplanted with human HSPCs (n = 5 mice) Statistics: ***$p < 0.0005$, two-tailed t test.

(B) TERC 3′ end profiles of HSPCs recovered and sorted from whole bone marrow (BM), 6 weeks after xenotransplantation, treated ± RG7834. Data reflect pooled human $CD34^+$ cells for each condition (n = 4 mice).

(C) Quantitation of oligo-adenylated TERC by deep sequencing amplicons shown in (B).

(D) TERC 3′ end profiles in human $CD19^+$ cells recovered as in (B). Data reflect individual mice.

(E) Quantitation of amplicons shown in (D) by deep sequencing, with n = 5 mice per category (mean ± SD). Statistics: one-way ANOVA; ns, not significant; ***$p < 0.0005$.

(F) Flow-FISH analysis of total BM cells recovered from xenotransplanted mice. Left: Human cells ($hCD45^+$) cells distinguished from mouse cells ($hCD45^-$). Right: Flow-FISH of $hCD45^+$ cells recovered from xenotransplants with *AAVS1* versus *PARN*-targeted HSPCs ± RG7834. One representative trace out of three for each category is shown.

(G) Quantitation of telomere length measured in human $CD45^+$ cells from whole bone marrow 6 weeks after xenotransplantation (n = 3 mice per category) as in (F). Statistics: one-way ANOVA, Tukey's multiple comparison test (*$p < 0.05$, **$p < 0.01$, and ***$p < 0.0005$).

(H) Human hematopoietic cell engraftment ($hCD45^+$) as a percentage of total mouse plus human $CD45^+$ cells in bone marrow 6 weeks after xenotransplantation of *AAVS1* or *PARN*-targeted HSPCs ± RG7834 (n = 5 mice per group), mean +SD. Statistics: one-way ANOVA.

(I) Comparison of human HSPCs ($CD34^+$), B cell ($CD19^+$), and myeloid cell ($CD33^+$) compartments as a percentage of $hCD45^+$ cells 6 weeks after xenotransplantation ± RG7834 (n = 5 mice per group), mean + SD. Statistics: one-way ANOVA.

SUPPLEMENTAL INFORMATION

Supplemental Information can be found online at https://doi.org/10.1016/j.stem.2020.03.016.

ACKNOWLEDGMENTS

We thank patients and families for participation in research; ICCB-Longwood for HTS support; Ronald Mathieu and BCH Flow Cytometry; Myriam Armant and BCH TransLab; Akiko Shimamura and BCH BMF/MDS registry (NIH grant R24DK099808); David Yadock and Cooperative Centers of Excellence in Hematology, University of Washington (NIH grant U54DK106829); and Thomas Hohman, John Piwinski, Pat Weber, Diana Wetmore, and Michael Hallen (Harrington Discovery Institute). We thank Leonard Zon, David Weinstock, and Scott Armstrong for critical input. We acknowledge the following funding sources: BCH Manton Center for Orphan Disease Research (to N.N.); MWC ARCS Scholar Award (to E.L.); NIH grant 1F31HL147482 (to K.L.); NIH grants R01AI117839, R01GM115911, and UG3TR002668 (to S.A.W.); NIH grants R01HL105669 and R01HL150553 (to S.A.W. and D.E.B.); NIH grant R35GM124725 (to P.C.); the Burroughs Wellcome Fund and NIH grants DP2HL137300 and P01HL032262 (to D.E.B.); NIH grant R01HL125527 (to Y.W.F); Harvard Stem Cell Institute (to Y.W.F. and S.A.); Charles H. Hood Foundation (to Y.W.F. and S.A); and NIH grant R01DK107716, U.S. Department of Defense grant W81XWH-19-1-0572, the Harrington Discovery Institute, Team Telomere, the Penn Orphan Disease Center, the BCH Translational Research Program and Technology Development Fund, and philanthropic gifts from the Agudelo, Brizio, Martin, and Theander-Adam families (to S.A.).

AUTHOR CONTRIBUTIONS

S.A. conceived and supervised this study. S.A. and N.N. designed the experiments. N.N. performed high-throughput screening, optimization, and execution; small-molecule testing *in vitro*; cell-based and xenotransplantation studies; CRISPR/Cas9 RNP genome editing of cell lines and primary cells; and molecular and cellular analyses. D.H.M. generated and characterized genome-edited iPSCs. D.E.B. and J.Z. advised on and performed CRISPR/Cas9 RNP editing and xenotransplant of $CD34^+$ HSPC cells. R.O.B. performed xenotransplant and flow-FISH analysis. J.W. and Y.W.F. purified recombinant proteins and participated in assay development. K.L. and S.A.W. designed and purified 3xNLS-SpCas9 protein. L.M.B., S.B.K., C.R., and R.C.L. provided patient samples. A.K.T., E.L., and P.C. performed computational analyses. S.A. and N.N. wrote the manuscript. All authors edited the manuscript.

DECLARATION OF INTERESTS

S.A., N.N., Y.W.F., and D.H.M. are named as inventors on patent applications relating to targeting PAPD5 in telomere diseases.

Received: November 1, 2019
Revised: January 21, 2020
Accepted: March 27, 2020
Published: April 21, 2020

REFERENCES

Aalbers, A.M., Calado, R.T., Young, N.S., Zwaan, C.M., Wu, C., Kajigaya, S., Coenen, E.A., Baruchel, A., Geleijns, K., de Haas, V., et al. (2013). Telomere length and telomerase complex mutations in pediatric acute myeloid leukemia. Leukemia *27*, 1786–1789.

Agarwal, S. (2018). Evaluation and management of hematopoietic failure in dyskeratosis congenita. Hematol. Oncol. Clin. North Am. *32*, 669–685.

Agarwal, S., Loh, Y.H., McLoughlin, E.M., Huang, J., Park, I.H., Miller, J.D., Huo, H., Okuka, M., Dos Reis, R.M., Loewer, S., et al. (2010). Telomere elongation in induced pluripotent stem cells from dyskeratosis congenita patients. Nature *464*, 292–296.

Aravind, L., and Koonin, E.V. (1999). DNA polymerase beta-like nucleotidyltransferase superfamily: identification of three new families, classification and evolutionary history. Nucleic Acids Res. *27*, 1609–1618.

Armanios, M., and Blackburn, E.H. (2012). The telomere syndromes. Nat. Rev. Genet. *13*, 693–704.

Aubert, G., Baerlocher, G.M., Vulto, I., Poon, S.S., and Lansdorp, P.M. (2012). Collapse of telomere homeostasis in hematopoietic cells caused by heterozygous mutations in telomerase genes. PLoS Genet. *8*, e1002696.

Baerlocher, G.M., Vulto, I., de Jong, G., and Lansdorp, P.M. (2006). Flow cytometry and FISH to measure the average length of telomeres (flow FISH). Nat. Protoc. *1*, 2365–2376.

Bertuch, A.A. (2016). The molecular genetics of the telomere biology disorders. RNA Biol. *13*, 696–706.

Bodnar, A.G., Ouellette, M., Frolkis, M., Holt, S.E., Chiu, C.P., Morin, G.B., Harley, C.B., Shay, J.W., Lichtsteiner, S., and Wright, W.E. (1998). Extension of life-span by introduction of telomerase into normal human cells. Science *279*, 349–352.

Boyraz, B., Moon, D.H., Segal, M., Muosieyiri, M.Z., Aykanat, A., Tai, A.K., Cahan, P., and Agarwal, S. (2016). Posttranscriptional manipulation of TERC reverses molecular hallmarks of telomere disease. J. Clin. Invest. *126*, 3377–3382.

Calado, R.T., and Young, N.S. (2009). Telomere diseases. N. Engl. J. Med. *361*, 2353–2365.

Codd, V., Mangino, M., van der Harst, P., Braund, P.S., Kaiser, M., Beveridge, A.J., Rafelt, S., Moore, J., Nelson, C., Soranzo, N., et al.; Wellcome Trust Case Control Consortium (2010). Common variants near TERC are associated with mean telomere length. Nat. Genet. *42*, 197–199.

Counter, C.M., Hahn, W.C., Wei, W., Caddle, S.D., Beijersbergen, R.L., Lansdorp, P.M., Sedivy, J.M., and Weinberg, R.A. (1998). Dissociation among in vitro telomerase activity, telomere maintenance, and cellular immortalization. Proc. Natl. Acad. Sci. USA *95*, 14723–14728.

d'Adda di Fagagna, F., Reaper, P.M., Clay-Farrace, L., Fiegler, H., Carr, P., Von Zglinicki, T., Saretzki, G., Carter, N.P., and Jackson, S.P. (2003). A DNA

damage checkpoint response in telomere-initiated senescence. Nature *426*, 194–198.

Dhanraj, S., Gunja, S.M., Deveau, A.P., Nissbeck, M., Boonyawat, B., Coombs, A.J., Renieri, A., Mucciolo, M., Marozza, A., Buoni, S., et al. (2015). Bone marrow failure and developmental delay caused by mutations in poly(A)-specific ribonuclease (PARN). J. Med. Genet. *52*, 738–748.

Dietz, A.C., Orchard, P.J., Baker, K.S., Giller, R.H., Savage, S.A., Alter, B.P., and Tolar, J. (2011). Disease-specific hematopoietic cell transplantation: nonmyeloablative conditioning regimen for dyskeratosis congenita. Bone Marrow Transplant. *46*, 98–104.

Dokal, I. (2000). Dyskeratosis congenita in all its forms. Br. J. Haematol. *110*, 768–779.

Feng, J., Funk, W.D., Wang, S.S., Weinrich, S.L., Avilion, A.A., Chiu, C.P., Adams, R.R., Chang, E., Allsopp, R.C., Yu, J., et al. (1995). The RNA component of human telomerase. Science *269*, 1236–1241.

Fok, W.C., Shukla, S., Vessoni, A.T., Brenner, K.A., Parker, R., Sturgeon, C.M., and Batista, L.F.Z. (2019). Posttranscriptional modulation of TERC by PAPD5 inhibition rescues hematopoietic development in dyskeratosis congenita. Blood *133*, 1308–1312.

Gable, D.L., Gaysinskaya, V., Atik, C.C., Talbot, C.C., Jr., Kang, B., Stanley, S.E., Pugh, E.W., Amat-Codina, N., Schenk, K.M., Arcasoy, M.O., et al. (2019). *ZCCHC8*, the nuclear exosome targeting component, is mutated in familial pulmonary fibrosis and is required for telomerase RNA maturation. Genes Dev. *33*, 1381–1396.

Goldfarb, K.C., and Cech, T.R. (2013). 3′ terminal diversity of MRP RNA and other human noncoding RNAs revealed by deep sequencing. BMC Mol. Biol. *14*, 23.

Greider, C.W. (2006). Telomerase RNA levels limit the telomere length equilibrium. Cold Spring Harb. Symp. Quant. Biol. *71*, 225–229.

Greider, C.W. (2016). Regulating telomere length from the inside out: the replication fork model. Genes Dev. *30*, 1483–1491.

Harley, C.B., Futcher, A.B., and Greider, C.W. (1990). Telomeres shorten during ageing of human fibroblasts. Nature *345*, 458–460.

Haycock, P.C., Burgess, S., Nounu, A., Zheng, J., Okoli, G.N., Bowden, J., Wade, K.H., Timpson, N.J., Evans, D.M., Willeit, P., et al. (2017). Association Between Telomere Length and Risk of Cancer and Non-Neoplastic Diseases: A Mendelian Randomization Study. JAMA Oncol *3*, 636–651.

Hayflick, L. (1965). The limited in vitro lifetime of human diploid cell strains. Exp. Cell Res. *37*, 614–636.

Heiss, N.S., Knight, S.W., Vulliamy, T.J., Klauck, S.M., Wiemann, S., Mason, P.J., Poustka, A., and Dokal, I. (1998). X-linked dyskeratosis congenita is caused by mutations in a highly conserved gene with putative nucleolar functions. Nat. Genet. *19*, 32–38.

Huber, W., Carey, V.J., Gentleman, R., Anders, S., Carlson, M., Carvalho, B.S., Bravo, H.C., Davis, S., Gatto, L., Girke, T., et al. (2015). Orchestrating high-throughput genomic analysis with Bioconductor. Nat. Methods *12*, 115–121.

Hyrina, A., Jones, C., Chen, D., Clarkson, S., Cochran, N., Feucht, P., Hoffman, G., Lindeman, A., Russ, C., Sigoillot, F., et al. (2019). A genome-wide CRISPR screen identifies ZCCHC14 as a host factor required for hepatitis B surface antigen production. Cell Rep. *29*, 2970–2978.e2976.

Jády, B.E., Bertrand, E., and Kiss, T. (2004). Human telomerase RNA and box H/ACA scaRNAs share a common Cajal body-specific localization signal. J. Cell Biol. *164*, 647–652.

Jongmans, M.C., Verwiel, E.T., Heijdra, Y., Vulliamy, T., Kamping, E.J., Hehir-Kwa, J.Y., Bongers, E.M., Pfundt, R., van Emst, L., van Leeuwen, F.N., et al. (2012). Revertant somatic mosaicism by mitotic recombination in dyskeratosis congenita. Am. J. Hum. Genet. *90*, 426–433.

Kim, N.W., Piatyszek, M.A., Prowse, K.R., Harley, C.B., West, M.D., Ho, P.L., Coviello, G.M., Wright, W.E., Weinrich, S.L., and Shay, J.W. (1994). Specific association of human telomerase activity with immortal cells and cancer. Science *266*, 2011–2015.

Kim, D., Langmead, B., and Salzberg, S.L. (2015). HISAT: a fast spliced aligner with low memory requirements. Nat. Methods *12*, 357–360.

Kipling, D., and Cooke, H.J. (1990). Hypervariable ultra-long telomeres in mice. Nature *347*, 400–402.

Kirwan, M., Beswick, R., Vulliamy, T., Nathwani, A.C., Walne, A.J., Casimir, C., and Dokal, I. (2009). Exogenous TERC alone can enhance proliferative potential, telomerase activity and telomere length in lymphocytes from dyskeratosis congenita patients. Br. J. Haematol. *144*, 771–781.

Lim, J., Kim, D., Lee, Y.S., Ha, M., Lee, M., Yeo, J., Chang, H., Song, J., Ahn, K., and Kim, V.N. (2018). Mixed tailing by TENT4A and TENT4B shields mRNA from rapid deadenylation. Science *361*, 701–704.

López-Otín, C., Blasco, M.A., Partridge, L., Serrano, M., and Kroemer, G. (2013). The hallmarks of aging. Cell *153*, 1194–1217.

Love, M.I., Huber, W., and Anders, S. (2014). Moderated estimation of fold change and dispersion for RNA-seq data with DESeq2. Genome Biol. *15*, 550.

Lubas, M., Christensen, M.S., Kristiansen, M.S., Domanski, M., Falkenby, L.G., Lykke-Andersen, S., Andersen, J.S., Dziembowski, A., and Jensen, T.H. (2011). Interaction profiling identifies the human nuclear exosome targeting complex. Mol. Cell *43*, 624–637.

Marrone, A., Stevens, D., Vulliamy, T., Dokal, I., and Mason, P.J. (2004). Heterozygous telomerase RNA mutations found in dyskeratosis congenita and aplastic anemia reduce telomerase activity via haploinsufficiency. Blood *104*, 3936–3942.

Martin, M. (2011). Cutadapt removes adapter sequences from high-throughput sequencing reads. EMBnet. J. *17*, 10–12.

McIntosh, B.E., Brown, M.E., Duffin, B.M., Maufort, J.P., Vereide, D.T., Slukvin, I.I., and Thomson, J.A. (2015). Nonirradiated NOD,B6.SCID Il2rγ-/-Kit(W41/W41) (NBSGW) mice support multilineage engraftment of human hematopoietic cells. Stem Cell Reports *4*, 171–180.

Meyerson, M., Counter, C.M., Eaton, E.N., Ellisen, L.W., Steiner, P., Caddle, S.D., Ziaugra, L., Beijersbergen, R.L., Davidoff, M.J., Liu, Q., et al. (1997). hEST2, the putative human telomerase catalytic subunit gene, is up-regulated in tumor cells and during immortalization. Cell *90*, 785–795.

Mitchell, J.R., Cheng, J., and Collins, K. (1999a). A box H/ACA small nucleolar RNA-like domain at the human telomerase RNA 3′ end. Mol. Cell. Biol. *19*, 567–576.

Mitchell, J.R., Wood, E., and Collins, K. (1999b). A telomerase component is defective in the human disease dyskeratosis congenita. Nature *402*, 551–555.

Moon, D.H., Segal, M., Boyraz, B., Guinan, E., Hofmann, I., Cahan, P., Tai, A.K., and Agarwal, S. (2015). Poly(A)-specific ribonuclease (PARN) mediates 3′-end maturation of the telomerase RNA component. Nat. Genet. *47*, 1482–1488.

Mueller, H., Wildum, S., Luangsay, S., Walther, J., Lopez, A., Tropberger, P., Ottaviani, G., Lu, W., Parrott, N.J., Zhang, J.D., et al. (2018). A novel orally available small molecule that inhibits hepatitis B virus expression. J. Hepatol. *68*, 412–420.

Mueller, H., Lopez, A., Tropberger, P., Wildum, S., Schmaler, J., Pedersen, L., Han, X., Wang, Y., Ottosen, S., Yang, S., et al. (2019). PAPD5/7 are host factors that are required for hepatitis B virus RNA stabilization. Hepatology *69*, 1398–1411.

Nagpal, N., Ahmad, H.M., Molparia, B., and Kulshreshtha, R. (2013). MicroRNA-191, an estrogen-responsive microRNA, functions as an oncogenic regulator in human breast cancer. Carcinogenesis *34*, 1889–1899.

Nakamura, T.M., Morin, G.B., Chapman, K.B., Weinrich, S.L., Andrews, W.H., Lingner, J., Harley, C.B., and Cech, T.R. (1997). Telomerase catalytic subunit homologs from fission yeast and human. Science *277*, 955–959.

Nguyen, D., Grenier St-Sauveur, V., Bergeron, D., Dupuis-Sandoval, F., Scott, M.S., and Bachand, F. (2015). A polyadenylation-dependent 3′ end maturation pathway is required for the synthesis of the human telomerase RNA. Cell Rep. *13*, 2244–2257.

Olovnikov, A.M. (1973). A theory of marginotomy. The incomplete copying of template margin in enzymic synthesis of polynucleotides and biological significance of the phenomenon. J. Theor. Biol. *41*, 181–190.

Patro, R., Duggal, G., Love, M.I., Irizarry, R.A., and Kingsford, C. (2017). Salmon provides fast and bias-aware quantification of transcript expression. Nat. Methods *14*, 417–419.

Povedano, J.M., Martinez, P., Serrano, R., Tejera, Á., Gómez-López, G., Bobadilla, M., Flores, J.M., Bosch, F., and Blasco, M.A. (2018). Therapeutic effects of telomerase in mice with pulmonary fibrosis induced by damage to the lungs and short telomeres. eLife *7*, e31299.

Ramunas, J., Yakubov, E., Brady, J.J., Corbel, S.Y., Holbrook, C., Brandt, M., Stein, J., Santiago, J.G., Cooke, J.P., and Blau, H.M. (2015). Transient delivery of modified mRNA encoding TERT rapidly extends telomeres in human cells. FASEB J. *29*, 1930–1939.

Roake, C.M., Chen, L., Chakravarthy, A.L., Ferrell, J.E., Jr., Raffa, G.D., and Artandi, S.E. (2019). Disruption of telomerase RNA maturation kinetics precipitates disease. Mol. Cell *74*, 688–700.e683.

Sanjana, N.E., Shalem, O., and Zhang, F. (2014). Improved vectors and genome-wide libraries for CRISPR screening. Nat. Methods *11*, 783–784.

Shen, Q., Zhang, Z., Yu, L., Cao, L., Zhou, D., Kan, M., Li, B., Zhang, D., He, L., and Liu, Y. (2011). Common variants near TERC are associated with leukocyte telomere length in the Chinese Han population. Eur. J. Hum. Genet. *19*, 721–723.

Shukla, S., and Parker, R. (2017). PARN modulates Y RNA stability and its 3′-end formation. Mol. Cell. Biol. *37*, 37.

Shukla, S., Schmidt, J.C., Goldfarb, K.C., Cech, T.R., and Parker, R. (2016). Inhibition of telomerase RNA decay rescues telomerase deficiency caused by dyskerin or PARN defects. Nat. Struct. Mol. Biol. *23*, 286–292.

Shukla, S., Bjerke, G.A., Muhlrad, D., Yi, R., and Parker, R. (2019). The RNase PARN controls the levels of specific miRNAs that contribute to p53 regulation. Mol. Cell *73*, 1204–1216.e1204.

Smogorzewska, A., van Steensel, B., Bianchi, A., Oelmann, S., Schaefer, M.R., Schnapp, G., and de Lange, T. (2000). Control of human telomere length by TRF1 and TRF2. Mol. Cell. Biol. *20*, 1659–1668.

Soerensen, M., Thinggaard, M., Nygaard, M., Dato, S., Tan, Q., Hjelmborg, J., Andersen-Ranberg, K., Stevnsner, T., Bohr, V.A., Kimura, M., et al. (2012). Genetic variation in TERT and TERC and human leukocyte telomere length and longevity: a cross-sectional and longitudinal analysis. Aging Cell *11*, 223–227.

Son, A., Park, J.E., and Kim, V.N. (2018). PARN and TOE1 constitute a 3′ end maturation module for nuclear non-coding RNAs. Cell Rep. *23*, 888–898.

Stanley, S.E., Gable, D.L., Wagner, C.L., Carlile, T.M., Hanumanthu, V.S., Podlevsky, J.D., Khalil, S.E., DeZern, A.E., Rojas-Duran, M.F., Applegate, C.D., et al. (2016). Loss-of-function mutations in the RNA biogenesis factor NAF1 predispose to pulmonary fibrosis-emphysema. Sci. Transl. Med. *8*, 351ra107.

Starling, J.A., Maule, J., Hastie, N.D., and Allshire, R.C. (1990). Extensive telomere repeat arrays in mouse are hypervariable. Nucleic Acids Res. *18*, 6881–6888.

Stuart, B.D., Lee, J.S., Kozlitina, J., Noth, I., Devine, M.S., Glazer, C.S., Torres, F., Kaza, V., Girod, C.E., Jones, K.D., et al. (2014). Effect of telomere length on survival in patients with idiopathic pulmonary fibrosis: an observational cohort study with independent validation. Lancet Respir. Med. *2*, 557–565.

Stuart, B.D., Choi, J., Zaidi, S., Xing, C., Holohan, B., Chen, R., Choi, M., Dharwadkar, P., Torres, F., Girod, C.E., et al. (2015). Exome sequencing links mutations in PARN and RTEL1 with familial pulmonary fibrosis and telomere shortening. Nat. Genet. *47*, 512–517.

Swaminathan, A.C., Neely, M.L., Frankel, C.W., Kelly, F.L., Petrovski, S., Durheim, M.T., Bush, E., Snyder, L., Goldstein, D.B., Todd, J.L., and Palmer, S.M. (2019). Lung transplant outcomes in patients with pulmonary fibrosis with telomere-related gene variants. Chest *156*, 477–485.

Takai, H., Smogorzewska, A., and de Lange, T. (2003). DNA damage foci at dysfunctional telomeres. Curr. Biol. *13*, 1549–1556.

Teixeira, M.T., Arneric, M., Sperisen, P., and Lingner, J. (2004). Telomere length homeostasis is achieved via a switch between telomerase- extendible and -nonextendible states. Cell *117*, 323–335.

Tseng, C.K., Wang, H.F., Burns, A.M., Schroeder, M.R., Gaspari, M., and Baumann, P. (2015). Human telomerase RNA processing and quality control. Cell Rep. *13*, 2232–2243.

Tseng, C.K., Wang, H.F., Schroeder, M.R., and Baumann, P. (2018). The H/ACA complex disrupts triplex in hTR precursor to permit processing by RRP6 and PARN. Nat. Commun. *9*, 5430.

Tummala, H., Walne, A., Collopy, L., Cardoso, S., de la Fuente, J., Lawson, S., Powell, J., Cooper, N., Foster, A., Mohammed, S., et al. (2015). Poly(A)-specific ribonuclease deficiency impacts telomere biology and causes dyskeratosis congenita. J. Clin. Invest. *125*, 2151–2160.

Vanácová, S., Wolf, J., Martin, G., Blank, D., Dettwiler, S., Friedlein, A., Langen, H., Keith, G., and Keller, W. (2005). A new yeast poly(A) polymerase complex involved in RNA quality control. PLoS Biol. *3*, e189.

Vaziri, H., and Benchimol, S. (1998). Reconstitution of telomerase activity in normal human cells leads to elongation of telomeres and extended replicative life span. Curr. Biol. *8*, 279–282.

Venteicher, A.S., Abreu, E.B., Meng, Z., McCann, K.E., Terns, R.M., Veenstra, T.D., Terns, M.P., and Artandi, S.E. (2009). A human telomerase holoenzyme protein required for Cajal body localization and telomere synthesis. Science *323*, 644–648.

Vulliamy, T., Marrone, A., Goldman, F., Dearlove, A., Bessler, M., Mason, P.J., and Dokal, I. (2001). The RNA component of telomerase is mutated in autosomal dominant dyskeratosis congenita. Nature *413*, 432–435.

Vulliamy, T., Beswick, R., Kirwan, M., Marrone, A., Digweed, M., Walne, A., and Dokal, I. (2008). Mutations in the telomerase component NHP2 cause the premature ageing syndrome dyskeratosis congenita. Proc. Natl. Acad. Sci. USA *105*, 8073–8078.

Walne, A.J., Vulliamy, T., Marrone, A., Beswick, R., Kirwan, M., Masunari, Y., Al-Qurashi, F.H., Aljurf, M., and Dokal, I. (2007). Genetic heterogeneity in autosomal recessive dyskeratosis congenita with one subtype due to mutations in the telomerase-associated protein NOP10. Hum. Mol. Genet. *16*, 1619–1629.

Warlich, E., Kuehle, J., Cantz, T., Brugman, M.H., Maetzig, T., Galla, M., Filipczyk, A.A., Halle, S., Klump, H., Schöler, H.R., et al. (2011). Lentiviral vector design and imaging approaches to visualize the early stages of cellular reprogramming. Mol. Ther. *19*, 782–789.

Watson, J.D. (1972). Origin of concatemeric T7 DNA. Nat. New Biol. *239*, 197–201.

Westin, E.R., Chavez, E., Lee, K.M., Gourronc, F.A., Riley, S., Lansdorp, P.M., Goldman, F.D., and Klingelhutz, A.J. (2007). Telomere restoration and extension of proliferative lifespan in dyskeratosis congenita fibroblasts. Aging Cell *6*, 383–394.

Wong, J.M., and Collins, K. (2006). Telomerase RNA level limits telomere maintenance in X-linked dyskeratosis congenita. Genes Dev. *20*, 2848–2858.

Wu, Y., Zeng, J., Roscoe, B.P., Liu, P., Yao, Q., Lazzarotto, C.R., Clement, K., Cole, M.A., Luk, K., Baricordi, C., et al. (2019). Highly efficient therapeutic gene editing of human hematopoietic stem cells. Nat. Med. *25*, 776–783.

Zerbino, D.R., Achuthan, P., Akanni, W., Amode, M.R., Barrell, D., Bhai, J., Billis, K., Cummins, C., Gall, A., Girón, C.G., et al. (2018). Ensembl 2018. Nucleic Acids Res. *46* (D1), D754–D761.

Zhong, F., Savage, S.A., Shkreli, M., Giri, N., Jessop, L., Myers, T., Chen, R., Alter, B.P., and Artandi, S.E. (2011). Disruption of telomerase trafficking by TCAB1 mutation causes dyskeratosis congenita. Genes Dev. *25*, 11–16.

Zijlmans, J.M., Martens, U.M., Poon, S.S., Raap, A.K., Tanke, H.J., Ward, R.K., and Lansdorp, P.M. (1997). Telomeres in the mouse have large inter-chromosomal variations in the number of T2AG3 repeats. Proc. Natl. Acad. Sci. USA *94*, 7423–7428.

STAR★METHODS

KEY RESOURCES TABLE

REAGENT OR RESOURCE	SOURCE	IDENTIFIER
Antibodies		
Human TruStain FcX	BioLegend	Cat. No. 422302
Mouse TruStain fcX anti-mouse CD16/32	BioLegend	Cat. No. 101320
V450 Mouse Anti-Human CD45 Clone HI30	BD Biosciences	Cat. No. 560367; RRID: AB_1645574
PE-eFluor 610 mCD45 Monoclonal Antibody (30-F11)	ThermoFisher Scientific	Cat. No. 61–0451–82
FITC anti-human CD235a Antibody	BioLegend	Cat. No. 349104; RRID: AB_10613463
FITC anti-human CD34 antibody	BioLegend	Cat. No. 343504; RRID: AB_1731852
PE/Cy7 anti-human CD3 antibody	BioLegend	Cat. No. 300420; RRID: AB_439781
APC anti-human CD19 Antibody	BioLegend	Cat. No. 302212; RRID: AB_314242
PE anti-human CD33 Antibody	BioLegend	Cat. No. 366608; RRID: AB_2566107
BV421 Anti-Human CD45 antibody	BioLegend	Cat. No. 368522; RRID: AB_2687375
BUV395 Mouse Anti-Human CD19 antibody	BD Biosciences	Cat. No. 563549
Brilliant Violet 421 anti-human CD34 Antibody	BioLegend	Cat. No. 343610
Alexa Fluor® 488 anti-human CD45 Antibody	BioLegend	Cat. No. 368536; RRID: AB_2721364
PAPD5 rabbit polyclonal antibody	Atlas antibodies	Cat. No. HPA042968; RRID: AB_2678244
HRP-conjugated goat polyclonal actin antibody	Santa Cruz Biotechnology	Cat. No. sc-1615
Bacterial and viral strains		
pBABE-TERT-puro	Counter et al., 1998	Addgene 1771
pRRL.PPT.SF.hOKSMco.idTomato.preFRT	Warlich et al., 2011	Under MTA, Hannover Medical School
pLentiCRISPRv2	Sanjana et al., 2014	Addgene 52961
Biological Samples		
CD34+ HSPCs	Fred Hutchinson Cancer Research Center, Seattle, Washington	https://sharedresources.fredhutch.org/products/cd34-cells
PARN-mutant patient 3 bone marrow fibroblasts	University of Washington BMF registry	N/A
PARN-mutant patient MDS cells	Dana-Farber Cancer Institute protocol 01-206	N/A
RTEL1-mutant AML cells	Dana-Farber Cancer Institute protocol 01-206	N/A
Chemicals, Peptides, and Recombinant Proteins		
BS3 (bis(sulfosuccinimidyl)suberate)	ThermoFisher Scientific	Cat. No. A39266
TelC-Alexa647 telomere length probe	PNA Bio	Cat. No. F1013
SYPRO orange	ThermoFisher Scientific	Cat. No. S6651
GelRed Nucleic acid gel stain	Biotium	Cat. No. 41003
DAPI (4',6-Diamidino-2-Phenylindole, Dilactate)	BioLegend	Cat. No. 422801
Propidium iodide	BioLegend	Cat. No. 421301
3-(4,5-dimethylthiazole-2-yl)-2,5-diphenyl tetrazolium bromide (MTT)	Sigma	Cat. No. M5655
Azido-ATP, ATP analog (3′-O-azidomethyl-adenosine 5′-O-triphosphate)	Jena Biosciences	NA
BCH001, 2-[[3-ethoxycarbonyl-6-(trifluoromethoxy) quinolin-4-yl]amino]benzoic acid	ChemDiv	Cat. No. 8011-6852
RG7834, (6S)-6-Isopropyl-10-methoxy-9-(3-methoxypropoxy)-2-oxo-6,7-dihydrobenzo[a]quinolizine-3-carboxylic acid	MedKoo Biosciences	Cat. No. 563793
pMtac-His6-PAPD5	This study	N/A

(*Continued on next page*)

Continued

REAGENT OR RESOURCE	SOURCE	IDENTIFIER
pMtac-His6-PAPD4	This study	N/A
pMtac-His6-PARN	This study	N/A
3xNLS-SpCas9	Wu et al., 2019	N/A
E. coli poly (A) polymerase I	ThermoFisher Scientific	Cat. No. AM2030
S. pombe Cid1	New England BioLabs	Cat. No. M0337S
Yeast poly-A-polymerase	ThermoFisher Scientific	Cat. No. 74225Z25KU
Critical Commercial Assays		
TeloTAGGG telomere length assay kit	Roche Life Science	Cat. No. 12209136001
TRAPeze Telomerase Detection kit	EMD Millipore	Cat. No. S7700
Kinase-Glo® Max	Promega	Cat. No. V6074
eBioscience Annexin V Apoptosis Detection Kit APC	ThermoFisher Scientific	Cat. No. 88-8007-72; RRID: AB_2575165
CellTiter-Blue Cell Viability Assay	Promega	Cat. No. G8080
Lonza 4D Nucleofactor nucleocuvette strips	Lonza	Cat. No. V4XP-3032
Lonza 4D Nucleofactor nucleocuvettes	Lonza	Cat. No. V4XP-3024
TruSeq Nano DNA LT Library Prep Kit	Illumina	Cat. No. 20015965
TruSeq Stranded Total RNA with RiboZero Gold kit	Illumina	Cat. No. 20020599
Deposited Data		
RNA-Seq	NCBI	Accession number GEO: GSE144986
Experimental Models: Cell Lines		
Human: *PARN*-mutant patient 1 iPSCs	Moon et al., 2015	N/A
Human: *PARN*-mutant patient 2 iPSCs	Moon et al., 2015	N/A
Human: *PARN*-mutant patient 3 iPSCs	This study	N/A
Human: *DKC1*-mutant del37L iPSCs	Agarwal et al., 2010	N/A
Human: *DKC1*-mutant A386T iPSCs	Agarwal et al., 2010	N/A
Human: NHSF2 (normal) iPSCs	Agarwal et al., 2010	N/A
Human: HEK293	ATCC	Cat. No. CRL-1573; RRID:CVCL_0045
Human: K562	a kind gift from Dr. Stuart Orkin	Cat. No. CCL-243; RRID:CVCL_0004
Human: MOLM-13	a kind gift from Dr. Stuart Orkin	RRID: CVCL_2119
Human: MV411	a kind gift from Dr. Stuart Orkin	Cat. No. CRL-9591; RRID:CVCL_0064
Experimental Models: Organisms/Strains		
Mouse: NOD.Cg-Kit < W-41J-Tyr+Prkdc-scid-Il2rg-tm1Wjl/ThomJ	Jackson Laboratory	Cat. No. 026622; RRID:IMSR_JAX:026622
Oligonucleotides		
Please refer Table S1		N/A
Software and Algorithms		
Thermal Shift software	ThermoFisher Scientific	Cat. No. 4466038
ImageJ		https://imagej.nih.gov/ij/
Graphpad Prism 8		https://www.graphpad.com/scientific-software/prism/
Flowjo		https://www.flowjo.com/solutions/flowjo

LEAD CONTACT AND MATERIALS AVAILABILITY

Further information and requests for resources and reagents should be directed to and will be fulfilled by the Lead Contact, Suneet Agarwal (suneet.agarwal@childrens.harvard.edu). All unique/stable reagents generated in this study are available from the Lead Contact with a completed Materials Transfer Agreement.

EXPERIMENTAL MODEL AND SUBJECT DETAILS

Human subjects

Biological samples were procured under protocols approved by the Institutional Review Boards at Boston Children's Hospital, the University of Washington, and Dana-Farber Cancer Institute, after written informed consent in accordance with the Declaration of Helsinki. *PARN* mutant patients 1 and 2 are as described (Moon et al., 2015). *PARN* mutant patient 3 presented with BMF in early childhood, lymphocyte telomere length less than 1st percentile by flow-FISH, biallelic *PARN* mutations (p.K58X, p.K59R), and clinical features consistent with dyskeratosis congenita.

CD34+ HSPCs

Peripheral blood mobilized, cryopreserved CD34^{+} HSPCs from anonymous healthy donors were obtained from Fred Hutchinson Cancer Research Center, Seattle, Washington (NIDDK Cooperative Centers of Excellence in Hematology). CD34+ HSPCs were maintained in X-VIVO 15 (Lonza, 04-418Q) supplemented with 100ng/ml SCF (recombinant human stem cell factor, R & D Systems; 255-SC-200), 100ng/ml TPO (human thrombopoietin, Peprotech; 300-18) and 100ng/ml of Flt3-L (recombinant human Flt-3 ligand, Peprotech; 300-19). Patient bone marrow samples were obtained under approved protocols (Boston Children's Hospital Institutional Review Board). CD34+ cells were isolated using the human CD34+ cells isolation kit (Stem Cell Technologies) and maintained in the above media.

Fibroblasts

Fibroblasts were cultured from bone marrow obtained from patients and healthy volunteer subjects under IRB approved protocols. Briefly, 0.5-1.0 mL liquid bone marrow in heparin was cultured in DMEM media with 15% fetal calf serum (FCS) until fibroblast outgrowths were apparent. Fibroblasts were maintained in DMEM 15% FCS and expanded using trypsin 0.05%. Normal skin fibroblasts NHSF2 are as previously described (Moon et al., 2015).

iPSCs

Derivation, characterization, and culture conditions of iPSCs from fibroblasts for patients 1 and 2 were performed as described (Moon et al., 2015). Patient 3 fibroblasts were reprogrammed using the 4-in-1-dTomato lentiviral reprogramming vector (gift of Dr. A. Schambach) (Warlich et al., 2011). *DKC1* mutant iPSCs were as described (Agarwal et al., 2010). For feeder-free culture, iPSCs were maintained in Essential 8 medium (Life Technologies) on hES-qualified Matrigel matrix (BD Biosciences) and subcultured using Accutase (Stem Cell Technologies).

Cell lines

HEK293 (293) cells were obtained from ATCC, maintained in DMEM with 10% FCS, and subcultured using trypsin 0.05%. 293-sh*PARN* cells were as described (Moon et al., 2015). Leukemia cell lines (K562 (ATCC), MOLM-13 and MV411 (kind gifts from Dr. Stuart Orkin) were maintained in RPMI-1640 media with 10% FCS, and subcultured 1:5 in fresh media.

Mice

NOD.Cg-Kit < W-41J-Tyr+Prkdc-scid-Il2rg-tm1Wjl/ThomJ (NBSGW; strain number 026622) were purchased from Jackson Laboratories. All animal experiments were performed in accordance of protocols approved by the Boston Children's Hospital Institutional Animal Care and Use Committee (IACUC). Mice that were used for xenotransplant assays were 4-6 week old females, housed in autoclaved cages.

METHOD DETAILS

Purification of recombinant proteins

PAPD5 For purification of recombinant PAPD5, cDNA (GenBank: CCB84642.1) was cloned into a modified pMtac-His6 vector. The pMtac-His6-PAPD5 construct was transformed into BL21 RIPL competent cells. Cells were grown in LB medium supplemented with 1% dextrose and antibiotics (Kanamycin; 50μg/ml and chloramphenicol; 34 μg/ml) at 37°C until OD_{600} ~0.6. Expression of protein was induced overnight with IPTG (0.25mM final) at 16°C. Cells were lysed in resuspension buffer (50mM HEPES-KOH, pH 7.6, 0.6M NaCl, 0.05% NP-40, 0.6% Triton X-100, 10% glycerol) containing lysozyme (0.2 mg/ml), 10mM β-mercaptoethanol (β-ME), 0.25 mM PMSF and complete EDTA-free Protease Inhibitor Cocktail (Sigma 11873580001). Cell suspension was sonicated using Branson Sonifier SFX Cell Disruptor and Homogenizer. Lysate was cleared by ultracentifugation and supernatant was incubated with Ni-NTA agarose (QIAGEN) resins equilibrated with binding buffer (50mM HEPES-KOH, pH7.6, 0.6 M NaCl, 2mM MgCl2, 0.05% NP-40, 0.6% Triton X-100 and 10% glycerol) containing 10 mM β-ME, 1 mM benzamidine, 0.5 mM PMSF, 10 mM imidazole, and 100 μM ATP. Bound proteins were washed extensively with binding buffer as described except with 30 mM imidazole and eluted in elution buffer (50mM HEPES-KOH, pH7.6, 0.175 M NaCl, 2mM MgCl2, 0.05% NP-40 and 10% glycerol) containing 10 mM β-ME, 1 mM benzamidine, 0.5 mM PMSF, 250 mM imidazole, and 100 μM ATP. Peak fractions were pooled and applied to Heparin Sephar-

ose 6 Fast Flow (GE Healthcare, 17099801). Bound proteins were washed extensively with elution buffer containing 2 mM DTT, 1 mM benzamidine, 0.5 mM PMSF, and 2 mM MgCl2. Active PAPD5 proteins were eluted from Heparin Sepharose at 0.4 M NaCl. All steps were performed at 4°C.

PAPD4 Purification of recombinant PAPD4 (NCBI: NP_001107865.1) was performed essentially as described for PAPD5, except that proteins bound to Heparin Sepharose were washed extensively at 0.175 M NaCl, then again at 0.4 M NaCl before eluting the active PAPD4 with buffer containing 1M NaCl. Peak fractions were pooled and dialyzed against elution buffer containing 0.4 M NaCl.

PARN Purification of codon-optimized recombinant PARN (NCBI: NP_002573.1) in a modified pMtac-His6 vector in frame with a C-terminal FLAG tag was performed essentially as described for PAPD5 and PAPD4, except that ATP was omitted and Ni-NTA bound PARN proteins were eluted in elution buffer containing 0.4 M NaCl. Eluate was directly applied to anti-FLAG M2 agarose (Sigma). Bound proteins were washed extensively with high salt wash buffer (25 mM HEPES-KOH, pH 7.6, 0.7 M NaCl, 0.1 mM EDTA, 12.5 mM MgCl2, 0.2% NP-40, 10% glycerol) containing 0.5 mM DTT, 1 mM benzamidine and 0.5 mM PMSF, and then washed again extensively with the low salt wash buffer containing 0.25 M NaCl. Bound proteins were eluted in low salt wash buffer containing 0.4 mg/ml FLAG peptide.

High throughput screen

Primary screen was performed at ICCB-Longwood screening facility, Harvard Medical School, Boston, MA. Reactions were carried out in duplicate in 384-well plate (Corning, 3820) where each well contained 10μl of the reaction mixture (2.5 pmol of purified PAPD5 in a buffer containing 25mM Tris-HCl (pH7.4), 50mM KCl, 5mM MgCl2, 1mM ATP, 0.01 mM EDTA, 0.1 mg/ml BSA, 1mM DTT and 0.02% NP-40). 100nl of the library compound (10mM stock in DMSO) was transferred via stainless-steel pin array and plates were incubated for 2hr at room temperature. Wells on each plate with reaction mixture plus DMSO served as positive controls. The reactions were stopped via addition of 5μl of luciferase reagent (Kinase-Glo® Max, Promega; V6074) followed by centrifuge at 1000rpm for 1 min. Luciferase signal was read using Envision Plate Reader (PerkinElmer). Data obtained was analyzed manually and z-score was calculated for each well/replicate. The compounds with z-score > 3 for both the replicate wells were then considered for dose-titration analysis. Dose-response assays were performed in duplicate 10 μl reaction volume in the same reaction mixture as above, with compound added to final concentrations of 0.1 – 100 μM in 3-fold increments, dispensed using a small volume dispenser (Hewlett-Packard D300). Similar compound titrations/volumes were used for yeast poly-A-polymerase (ThermoFisher Scientific, 74225Z25KU) while reactions were carried out in enzyme-specific buffer with 1U of enzyme / 10μl reaction. All the reactions were incubated at room temperature for 2 hr followed by addition of luciferase reagent and reading as above. Data was analyzed manually and compounds with fold change > 1.5 compared to that of negative control were shortlisted. Further, PAPD5-specific compounds were then tested individually in a dose-dependent manner using oligoadenylation assay.

Oligoadenylation assay

For gel-based detection of substrate extension, the polyadenylation reactions were performed in a buffer containing 25mM Tris-HCl (pH7.4), 50mM KCl, 5mM $MgCl_2$, and 50μM ATP). 1 pmol of 5′-FAM-labeled RNA oligo $(CUGC)_5$ (Integrated DNA Technologies) and 2.5 pmol of purified PAPD5 or PAPD4 were added per 10μl of the reaction mix followed by incubation at room temperature for 1hr. For reactions with yeast poly-A-polymerase (ThermoFisher Scientific, 74225Z25KU), *E. coli* poly (A) polymerase I (ThermoFisher Scientific, AM2030) and *S. pombe* Cid1 (New England BioLabs, M0337S), reactions were performed in enzyme-specific buffers and 1U of enzyme was added per 10μl of the reaction mix containing 1 pmol of 5′-FAM-labeled RNA oligo $(CUGC)_5$ and 50μM ATP. Reactions were incubated at room temperature for 1hr and stopped using formamide loading buffer (10mM EDTA and 83.3% formamide) and resolved using denaturing polyacrylamide gels (15% Criterion TBE-Urea Polyacrylamide Gel, 26 well, 15 μl, Bio-Rad, 3450093). Gels were imaged using a FLA9000 imager (GE Healthcare).

PARN activity assay

To detect inhibitory activity of small molecules against recombinant PARN (rPARN), 1 pmol of 5′-FAM-labeled RNA oligo (5′-CCUUUCCAAAAAAAAA-3′, Integrated DNA Technologies) was incubated with indicated concentrations of rPARN in reaction buffer (25mM Tris-HCl (pH7.4), 50mM KCl, 5mM $MgCl_2$, 0.1mg/ml BSA, 0.02% NP-40, 0.01 mM EDTA and 1mM DTT) at room temperature for 20min. Reactions were stopped using formamide loading buffer (10mM EDTA and 83.3% formamide) and resolved using 20% TBE-urea polyacrylamide gels. Gels were imaged using an FLA9000 imager (GE Healthcare).

Differential scanning fluorimetry

Protein melting curve assays were performed using an indicator dye SYPRO orange (Thermo Fisher Scientific, S6651) diluted 1:5000 in 20μl of buffer containing 20 μM rPAPD5, 100 μM non-extendable ATP analog (3′-O-azidomethyl-adenosine 5′-O-triphosphate, custom synthesized by Jena Biosciences), 25 mM Tris-HCL, 5 mM MgCl2, 50 mM KCl. Inhibitors BCH001 and RG7834 were added to the dye-buffer mixture at indicated concentrations and heated from 10 to 95°C at a rate of 1°C/min and fluorescence signals were monitored by 7500 Fast Real-Time PCR Systems (Applied Biosystems). Each curve was an average of three measurements and Thermal Shift software (Thermo Fisher Scientific, 4466038) was used for analysis.

Quantitative RT-PCR

RNA isolation was done using TRIzol (Ambion, 15596-026) as per standard protocol followed by DNase treatment using Turbo DNA-free kit (Life Technologies AM1907). SuperScript III Reverse Transcriptase (ThermoFisher Scientific, 18080-093) was used for cDNA synthesis as described (Moon et al., 2015). qPCR was performed in CFX96 Real-Time PCR detection system (Bio-Rad) using SsoAdvanced Universal SYBR Green Supermix (Bio-Rad, 172-5274). POLR2A was used for the normalization and quantification. Graphing and statistical analysis of qPCR results were performed using GraphPad Prism. Primers used are given in Table S1.

Northern blot

Total RNA (5–7 μg) was electrophoresed on 1.5% agarose/formaldehyde gel followed by capillary transfer to Hybond N+ membranes (Amersham, GE Healthcare; RPN303B) in 10X SSC. Blot was hybridized for 12hrs with α-^{32}P-dCTP-labeled full-length *TERC* probe in ULTRAhyb buffer (Life Technologies, AM8669M). 18S rRNA signal obtained from ethidium bromide staining was used for normalization and signal quantification was performed using ImageJ software. Primers used for probe generation are given in Table S1.

RLM-RACE

The RNA ligation-mediated rapid amplification of cDNA ends (RLM-RACE) protocol was performed as described (Moon et al., 2015). Briefly, total RNA was extracted and equal amounts (100-600 ng) were ligated to 5′-adenylated, 3′-blocked adapters (Universal miRNA cloning linker, New England Biolabs; S1315S) using T4 RNA ligase truncated KQ (New England Biolabs, M0373S) and PEG 8000. Ligated RNA was then purified, followed by cDNA synthesis and RNA specific PCR amplification. PCR amplicons were resolved on high percentage (2.5%) agarose gels to visualize mature and extended amplicons. Primers used are given in Table S1.

RLM-RACE amplicon deep sequencing

Linker ligated cDNAs obtained using above described RACE protocol were used for the generation of TERC amplicons. After purification using Qiaquick PCR purification kit (QIAGEN, 28106), amplicons were prepated for deep sequencing using the TruSeq Nano DNA LT Library Prep Kit (Illumina, 20015965) per the kit protocol. Briefly, linkers carrying unique barcodes were ligated to individual RACE amplicons using DNA ligase followed by amplification with Illumina adapters, and size selection was performed using sample purification beads. The completed libraries were submitted to the Tufts University Genomics Core for paired-end 250 bp sequencing on a MiSeq instrument using the Illumina TruSeq V2 500 cycle kit. Sequencing and analysis was performed as described (Moon et al., 2015). Perl scripts used for *TERC* RNA 3′ analysis are available upon request. Cumulative percent oligo-adenylated TERC species were calculated as the fraction of all oligo-adenylated TERC RNA species divided by total TERC RNA species within eight genomically-encoded nucleotides of the mature TERC 3′ end.

Transcriptome / RNA-Seq analysis

Total RNA was isolated and RNA quality was checked by both fragment analyzer (Agilent Fragment Analyzer) and electrophoresis on a 1.5% agarose/formaldehyde gel. 0.1-1 μg of total RNA was used for library preparation using the TruSeq Stranded Total RNA with RiboZero Gold kit (Illumina- 20020599). Briefly, total RNA was subjected to rRNA depletion and fragmentation followed by first and second strand cDNA synthesis. Further, second strand was removed after end repair and A-tailing. Finally, libraries were amplified for size selection and pooled at equimolar concentrations based on quantification using Fragment Analyzer. The pooled libraries were sequenced on a HiSeq 2500 instrument using a High Output V4 kit / single-end 50 bp reads. Sequence reads were trimmed to a final length of 40 bases using Trimming software Cutadapt (Martin, 2011). Salmon (Patro et al., 2017) was used to quasi-map trimmed reads to the reference transcriptome (ENSEMBL (Zerbino et al., 2018) GRCh38.80), including 6511 non-coding RNAs (scaRNAs, lincRNAs, snRNAs, and snoRNAs), to estimate transcript abundances. The number of reads mapping to the transcriptome ranged from 7.7 to 12.0 million. Read counts per gene were derived by summing the counts per transcript across all transcripts associated with the gene. For quality control measures, 0.1% of reads were randomly sampled from each FASTQ and directly aligned to ENSEMBL GRC Release 80 (ftp://ftp.ensembl.org/pub/release-80/gtf/) reference genomes using HISAT2 (Kim et al., 2015) to determine percentage alignment to *H. sapiens*, *M. Musculus*, *S. cerevisiae*, *E. Coli*, and *D. Rerio* genomes, as well as overlaps with genomic features (including rRNA, mtRNA, protein-coding regions), ambiguous and non-unique alignments, and unaligned reads. Bioconductor (Huber et al., 2015) package DESeq2 (Love et al., 2014) was used for differential expression analysis. The raw counts matrix was first coerced to integer format as a requirement for DESeq2 input. Expression profiles of *PARN* mutant iPSCs treated with BCH001 were compared to those of untreated *PARN* mutants. DESeq2 uses the Wald test to generate a two-tailed p value for each gene by calculating the Wald statistic ($\log_2$ fold change (LFC) divided by the standard error of the LFC) for the gene and comparing it to a standard Normal distribution. False discovery rate (FDR)-adjusted p values were computed using the Benjamini-Hochberg correction method. Significant differentially expressed genes were determined with a threshold of $\alpha = 0.1$.

Telomerase activity assay

DC patient iPS cells were cultured and maintained in the presence of BCH001 versus DMSO for 10 days. Cells were harvested and lysed with CHAPS lysis buffer and protein concentration measured using DC Protein assay kit II (Bio-Rad, 5000112). 5-fold dilutions of equivalent total protein lysate were subjected to TRAP (telomere repeat amplification protocol) assay per the TRAPeze Telomerase Detection kit (EMD Millipore, S7700). Products were resolved on 10% TBE polyacrylamide gels and visualized by staining with

GelRed Nucleic acid gel stain (Biotium, 41003). Relative telomerase activity was quantified using ImageJ software, by pairwise comparison of the intensity of the first six amplicons in corresponding lanes with and without PAPD5 inhibitors, and averaging across the three dilutions for each sample.

Telomere length measurement

Southern blot-

For cell cultures, terminal restriction fragment (TRF) length analysis was performed per protocol using the TeloTAGGG telomere length assay kit (Roche Life Science; 12209136001). Briefly, 1-5μg of purified genomic DNA was digested with HinfI/RsaI restriction enzymes and followed by electrophoresis using 0.7% agarose gels. The gel was blotted and probed using kit reagents. Images were taken using Chemidoc Touch Imaging System (Bio-Rad).

Flow-FISH-

For telomere length analysis in iPSCs, cells were washed twice in PBS followed by denaturation in formamide at 82°C and hybridization with TelC-Alexa647 telomere length probe (PNA Bio, F1013). Hybridized cells were stained with DAPI (4',6-Diamidino-2-Phenylindole, Dilactate, BioLegend; 422801) and analyzed using a BD LSRII FACS machine (BD Biosciences). The cells were gated based on 2N DNA content and mean fluorescence intensity of the TelC probe was measured. To analyze blood cell telomere length in xenotransplanted mice, flow-FISH was performed as described (Baerlocher et al., 2006). Briefly, the total marrow cells isolated from 6-week xenotransplanted mice were incubated with blocking antibodies for human and mice ((Human TruStain FcX, BioLegend; 422302 and Mouse TruStain fcX anti-mouse CD16/32, BioLegend; 101320) for 10 min. Blocked cells were then stained with BV421 Anti-Human CD45 antibody (Brilliant Violet 421 anti-human CD45 Antibody, BioLegend; 368522) followed by crosslinking (with BS3 (bis(sulfosuccinimidyl)suberate); ThermoFisher Scientific; A39266), denaturation in formamide (at 82°C) and hybridization with or without TelC-Alexa647 telomere length probe (PNA Bio, F1013). For lineage specific telomere length analysis, blocked cells were stained with Alexa Fluor® 488 anti-human CD45 Antibody (BioLegend; 368536), Brilliant Violet 421 anti-human CD34 Antibody (BioLegend; 343610) and BUV395 Mouse Anti-Human CD19 antibody (BD Biosciences; 563549). Cells were then subject to the flow-FISH protocol described above using the TelC-Alexa647 telomere length probe, and telomere length and immunophenotype were determined using a BD LSRII FACS instrument (BD Biosciences). Cells were gated on hCD45+ population and mean fluorescence intensity was measured.

Fibroblast immortalization with TERT

Retroviral vectors encoding *TERT* were produced by co-transfection of HEK293 cells with pBABE-hTERT-puro (Addgene #1171; gift of Dr. R. Weinberg, MIT), VSV-G and Gag-Pol packaging plasmids as described (Agarwal et al., 2010). Retroviral vectors were transduced into patient fibroblasts in the presence of protamine sulfate (10 μg/ml) for 16 hr. For selection, media was supplemented with puromycin (0.2μg/ml) for 10 days.

CRISPR/Cas9 knockout generation

Lentiviral vectors-

A lentiviral vector containing Cas9 and gRNA (pLentiCRISPR v2; gift of Feng Zhang; Addgene #52961) targeting human *PAPD5* was co-transfected with pCMV_DR8.91 and pCMV_VSV-G in 293 cells using branched polyethylenimine (Sigma, 408727) to generate lentivirus. Supernatants were harvested after 24 and 48hrs of transfection and subjected to filtration followed by storage at −80°C in aliquots.

DC patient iPSCs were transduced with viral vectors in the presence of protamine sulfate (10 μg/ml) for 12 hours. Knockout efficiency was determined by amplification of the targeted locus followed by Sanger sequencing. Single cell clones were generated by serial dilution and culture in 96 well plates. Clones were screened for *PAPD5* knockout by western blotting. Sequences of gRNAs are given in Table S1.

RNP electroporation-

3xNLS-SpCas9 was prepared as described (Wu et al., 2019). sgRNAs were obtained from Synthego Corporation and gRNA sequences are given in Table S1. Electroporation was done using Lonza 4D Nucleofactor nucleocuvette strips (V4XP-3032, for *in vitro* culture; 20μl) or nucleocuvettes (V4XP-3024, for transplantation and knockout generation; 100μl) as described (Wu et al., 2019). Modified synthetic gRNAs (with first and last three nucleotides having 2′-O-methyl-3′-phosphorothrioate modification) and 3xNLS-SpCas9 were mixed in equimolar concentrations and incubated for 15 min at RT. CD34+ HSPCs were thawed in X-VIVO media supplemented with cytokines one day prior to electroporation, and resuspended in P3 solution immediately before electroporation. 50 μM RNPs were mixed with HSPCs and electroporation was done with program EO-100. Cells were maintained in X-VIVO media supplemented with cytokines for *in vitro* culture as well as for mice transplantation experiments.

CRISPR gene-targeting validation

Sanger sequencing-

Genomic DNA was isolated from primary cells and cell lines using GenJET genomic DNA purification kit (Thermo Fisher Scientific). Primers used for *AAVS1*, *TERC*, *PAPD5* and *PARN* gene amplification and sequencing are provided in Table S1. Sanger sequencing was performed by Genewiz and the efficiency of editing was analyzed by ICE software (Synthego Corporation). Western blotting-DC patient iPSCs were lysed in 2X Laemmli sample buffer (Bio-Rad, 1610737) and total cellular lysates were then subjected to

SDS–PAGE followed by transfer to PVDF membranes. Detection of detection of PAPD5 was done using anti-PAPD5 antibodies (Atlas antibodies, HPA042968, 1:1000) and HRP-conjugated goat anti-rabbit secondary antibody (Bio-Rad 170-5046, 1:10000) followed by chemiluminescent detection using Clarity Western ECL substrate (Bio-Rad, 1705060). The same membrane was probed with HRP-conjugated anti-actin antibodies (Santa Cruz sc-1615, dilution 1:1000) to estimate the protein loading. Imaging and quantification were performed using the Biorad ChemiDoc Touch imaging system.

Methylcellulose assay

For CD34+ HSPCs, 1000 cells were plated in methylcellulose medium containing human cytokines (Methocult h4434 classic, Stem Cell Technologies; 4434) and inhibitors BCH001, RG7834 or vehicle (DMSO). After 14 days of culture at 37°C, 5% CO_2, the progenitor colonies were counted manually under the microscope, with categories defined by colony morphology. CD34+ cells were isolated from patient 2 bone marrow cells by antibody-magnetic bead based methods and cultured as above to obtain progenitor colonies after 14 days. Leukemia cell lines were plated at a density of 1000 cells plate and colonies were scored after 8-10 days. For AML blast patient sample, 120,000 cells/plate were plated and colonies were scored after 10 days.

MTT assay

Cell toxicity in response to inhibitor was measured as described (Nagpal et al., 2013). 2×10^4 DC patient iPSCs were plated and 24hrs later treated with 1 μM BCH001 versus DMSO as vehicle control. Cell viability was monitored daily for 72 hr using 3-(4,5-dimethylthiazole-2-yl)-2,5-diphenyl tetrazolium bromide (MTT, Sigma; M5655) followed by quantification at 590 nm.

Cell viability assay

Cell viability in leukemia cell lines in response to inhibitor was measured using CellTiter-Blue Cell Viability Assay (Promega, G8080). 5×10^3 cells/well were seeded in triplicates in 96-well plates and PAPD5 inhibitor RG7834 (1 μM) versus DMSO control was added in media. 72 hr post-treatment, cell viability was assessed by using CellTiter-Blue reagent, as per the manufacturer's protocol. Fluorescence intensity of resorufin (at 590nm) was read using CLARIOstar BMG Labtech microplate reader.

Cell cycle analysis

Cell cycle stage distribution in response to inhibitor was measured as described (Nagpal et al., 2013). Equal numbers (1×10^5) of DC patient iPSCs were plated and 24 hr later treated with 1μM BCH001 versus DMSO as vehicle control. 72 hr post-treatment cells were harvested and fixed using 70% ethanol (in Dulbecco's phosphate-buffered saline, Corning; 21031CVR) at 4°C overnight. For analysis, fixed cells were washed twice with 1X PBS (phosphate-buffered saline) followed by treatment with 1% RNase A solution (Sigma, R6148) and staining with propidium iodide solution (0.5 mg/ml, BioLegend, 421301) and flow cytometry using BD LSR Fortessa (BD Biosciences). Cell cycle analysis was done using Watson (Pragmatic) model with FlowJo software.

Annexin V staining

For apoptosis analysis, eBioscience Annexin V Apoptosis Detection Kit APC (ThermoFisher Scientific, 88-8007-72) was used. Equal number (1×10^5) of DC patient iPSCs were plated and 24hrs later treated with 1μM BCH001 versus DMSO (as vehicle control). 72 hr post-treatment cells were harvested and washed twice with cold PBS and gently resuspended in 100μl 1X binding buffer. Further, incubation for 15 min at room temperature was done following addition of 5 μl each of annexin V-fluorescein isothiocyanate (FITC) and propidium iodide. The cells were washed once with 1X binding buffer and resuspended in 200μl 1X binding buffer and analyzed immediately using BD LSR Fortessa (BD Biosciences). The percentage of apoptotic cells was calculated using the FACSDiva 8.0 software (BD Biosciences), with early apoptotic cells defined as Annexin V+ / PI-, and late apoptotic cells being Annexin V+ / PI+.

Xenotransplantation

NBSGW were used for retro-orbital injection of $0.8 – 1 \times 10^6$ CD34+ HSPCs after electroporation and editing the gene of interest. 48 hr post-injection, oral treatment of RG7834 (125 μM) or DMSO (1% v/v) in sterile drinking water was initiated, with replacement every 4 days. Six weeks post-engraftment, bone marrow was harvested and cells obtained from bone marrow were analyzed and sorted by flow cytometry.

Xenotransplant engraftment analysis

For analysis of cells harvested from bone marrow, cells were first incubated with blocking antibodies (Human TruStain FcX, BioLegend; 422302 and Mouse TruStain fcX anti-mouse CD16/32, BioLegend; 101320) for 15 min, followed by incubation with V450 Mouse Anti-Human CD45 Clone HI30 (BD Biosciences, 560367), PE-eFluor 610 mCD45 Monoclonal Antibody (30-F11) (Thermo Fisher, 61–0451–82), FITC anti-human CD235a Antibody (BioLegend, 349104), PE anti-human CD33 Antibody (366608, BioLegend), APC anti-human CD19 Antibody (BioLegend, 302212), PE/Cy7 anti-human CD3 antibody (BioLegend, 300420), FITC anti-human CD34 antibody (BioLegend, 343504) and Fixable Viability Dye eFluor 780 for live/dead staining (Thermo Fisher, 65-0865-14). Percentage human engraftment was calculated as hCD45+ cells/(hCD45+ cells + mCD45+ cells). B cells (CD19+) and myeloid (CD33+) lineages were gated on the hCD45+ population. HSPCs (CD34+) and T cells (CD3+) were gated on the hCD45+CD19-CD33- population. hCD45+CD19-CD33-CD34-CD3- population was referred as lineage-. FACS analysis and sorting of CD34+ / CD19+ cells were done using the FACSAria II machine (BD Biosciences).

Plasma RG7834 levels

Blood samples were obtained via retro-orbital bleeding in heparinized tubes followed by plasma separation by centrifugation. An aliquot of 20μl plasma sample was extracted with 100μl of methanol:acetonitrile (5:95 v/v), with verapamil as an internal standard. The mixture was vortexed for 15min followed by spinning at 4000 rpm for 15min. A portion of supernatant was diluted 1:1 in water and used for injection in LC-MS/MS (Shimadzu Nexera UPLC (LC30AD pumps) with column (Waters Acquity UPLC BEH C18, 50X2.1mm, 1.7μ) temperature at 40°C. Water with 0.1% formic acid was used as mobile phase A while acetonitrile with 0.1% formic acid was used for mobile phase B. Standard curves were prepared by spiking RG7834 into blank plasma and processed similar to test plasma samples. The assay was developed in collaboration with Quintara Discovery, Hayward, CA

QUANTIFICATION AND STATISTICAL ANALYSIS

All the statistical analysis was done using GraphPad Prism 8 software. Unless otherwise indicated, error bars presented mean with standard error. P values were calculated based on two tailed Student's t test or ANOVA as indicated, and $p < 0.05$ was defined as significant. Statistical and replicate details can be found in the figure legends.

DATA AND CODE AVAILABILITY

The RNA-seq data have been deposited in NCBI's Gene Expression Omnibus and can be accessed through GEO series accession number GEO: GSE144986. Datasets and code used in this study will be made available upon request to the Lead Contact.

Received: 16 June 2020 | Accepted: 11 August 2020

DOI: 10.1002/stem.3270

CONCISE REVIEW

STEM CELLS

Telomerase RNA processing: Implications for human health and disease

Neha Nagpal[1,2,3,4] | Suneet Agarwal[1,2,3,4]

[1]Division of Hematology/Oncology and Stem Cell Program, Boston Children's Hospital, Boston, Massachusetts

[2]Pediatric Oncology, Dana-Farber Cancer Institute, Boston, Massachusetts

[3]Harvard Initiative for RNA Medicine and Department of Pediatrics, Harvard Medical School, Boston, Massachusetts

[4]Harvard Stem Cell Institute, Boston, Massachusetts

Correspondence
Suneet Agarwal, MD, PhD, Boston Children's Hospital, 1 Blackfan Circle, Karp 07214, Boston, MA 02115.
Email: suneet.agarwal@childrens.harvard.edu

Funding information
Harvard Stem Cell Institute; Harrington Discovery Institute; U.S. Department of Defense, Grant/Award Number: W81XWH-19-1-0572; NIH, Grant/Award Number: R01 DK107716

Abstract

Telomeres are composed of repetitive DNA sequences that are replenished by the enzyme telomerase to maintain the self-renewal capacity of stem cells. The RNA component of human telomerase (TERC) is the essential template for repeat addition by the telomerase reverse transcriptase (TERT), and also serves as a scaffold for several factors comprising the telomerase ribonucleoprotein (RNP). Unique features of TERC regulation and function have been informed not only through biochemical studies but also through human genetics. Disease-causing mutations impact TERC biogenesis at several levels including RNA transcription, post-transcriptional processing, folding, RNP assembly, and trafficking. Defects in TERC reduce telomerase activity and impair telomere maintenance, thereby causing a spectrum of degenerative diseases called telomere biology disorders (TBDs). Deciphering mechanisms of TERC dysregulation have led to a broader understanding of noncoding RNA biology, and more recently points to new therapeutic strategies for TBDs. In this review, we summarize over two decades of work revealing mechanisms of human telomerase RNA biogenesis, and how its disruption causes human diseases.

KEYWORDS

dyskeratosis congenita, dyskerin, noncoding RNA, stem cells, telomere, TERC, TERT

1 | INTRODUCTION

Telomeres are the repetitive DNA sequences that together with protein complexes called shelterin comprise the ends of mammalian chromosomes. Telomeres shorten with each cell division, in part due to incomplete replication of linear chromosome ends by DNA polymerases. Cellular senescence is triggered to protect genome integrity when telomeres reach a critically short length.[1,2] To address the need for replicative capacity in stem cells, the tightly regulated enzyme telomerase is activated to elongate telomeres. Telomerase is a ribonucleoprotein (RNP) that at its core is composed of the reverse transcriptase TERT and the long noncoding RNA (lncRNA) TERC, which serves as the template for telomere repeat addition by TERT. It has long been appreciated that *TERT* expression is the "on/off switch" that determines whether or not a human cell has telomerase activity. However, genetic studies in rare diseases have revealed the critical importance of TERC RNA levels in governing the amount of telomerase activity in the cell, once TERT is expressed. In other words, TERC levels are limiting for replicative capacity in stem cells.[3] Here, we summarize 25 years of molecular, biochemical, and genetic studies that have collectively revealed key mechanisms of TERC transcription and post-transcriptional processing, as well as a spectrum of diseases when these go awry. Most recently, these discoveries suggest strategies to manipulate telomerase via TERC for therapeutic benefit. This review focuses on human TERC. Readers are referred to excellent recent reviews on telomerase RNA structure and function in other eukaryotes.[4-8]

2 | HUMAN TELOMERASE RNA

Preceding the explosion of ncRNA discovery in the genomics era, telomerase RNA was one of the relatively few lncRNAs of established importance in eukaryotic biology and human diseases. Elegant biochemical studies implicated an RNA component in telomerase, whose in vitro enzymatic activity is capable of synthesizing telomere repeats from an oligonucleotide primer.[9] Isolation of the ciliate telomerase RNA demonstrated its template sequence and function.[10] The subsequent cloning of various telomerase RNAs from ciliates and yeast demonstrated a large diversity of sizes and sequences, hindering identification of mammalian telomerase RNAs by homology alone. To address this, PCR-based cyclic selection of RNAs carrying the predicted human telomeric template sequence ultimately led to cloning and functional characterization of the 451-nucleotide lncRNA encoding human TERC.[11] When TERC was inhibited by anti-sense oligonucleotides or mutated to alter the template, telomerase activity was reduced and telomere attrition ensued in cell lines, confirming its role in telomere biology. Notably, TERC expression alone did not correlate with telomerase activity in human cells,[11] consistent with findings that *TERT* expression is the gatekeeper of cellular immortality.[12]

In terms of transcriptional regulation, early studies showed that TERC was alpha-amanitin sensitive and thus transcribed by RNA polymerase (pol) II,[11] similarly to fungal telomerase RNAs but unlike those in ciliates that use RNA pol III.[10] Neither a transcriptional termination site nor a poly-adenylated precursor transcript was identified. Rather, the finding of a predominant 3′ end without poly-adenylation[13] suggested that nascent TERC transcripts were processed by other mechanisms, which remained largely undefined for almost two decades.

In early telomerase RNP biogenesis studies, Collins and colleagues noted that TERC had features of another class of ncRNAs. Mature TERC transcripts contained a consensus box H motif (5′-ANANNA-3′), terminated three nucleotides (nt) downstream of an ACA trinucleotide, and were predicted to fold into a hairpin-hinge-hairpin-tail structure,[14] all of which are characteristics of box H/ACA small nucleolar RNAs (snoRNAs)[15,16] (Figure 1). Although murine telomerase RNA differs substantially from human TERC in size (451 nt vs 397 nt) and sequence (65% identity),[11,19] the box H/ACA sequence motifs and predicted secondary structure were found to be conserved,[14] as was seen in other vertebrate telomerase RNAs.[20] The box H/ACA structure was shown to be required for TERC accumulation in cells and sufficient for transcriptional termination and 3′ end formation, albeit by unknown mechanisms.[14,21] Unlike snoRNAs, but as in small nuclear RNAs (snRNAs), TERC 5′ ends are modified with a trimethylguanosine cap,[22] which localizes nascent transcripts to subnuclear structures and protects the template sequence from exonucleolytic degradation. These studies demonstrated that TERC, unlike telomerase RNA in ciliates and yeast, was a bona fide snoRNA, but has distinct biogenesis characteristics.[21] These observations were also critical for linking TERC and telomere maintenance defects to human diseases.

Significance statement

Telomerase is critical for stem cell homeostasis. It is now clear that in humans, mutations in telomerase cause a range of life-threatening diseases driven at least in part by premature stem cell failure. Over the past 20 years, genetic discoveries have revealed that the long noncoding RNA component of telomerase (TERC) is a critical, limiting factor for telomerase activity in stem cells. Remarkably, recent work on TERC biogenesis and processing has illuminated potential targets for manipulation of telomerase. This article reviews molecular and genetic discoveries in human TERC biogenesis and telomere biology disorders, which have led to a better understanding and potential treatments for stem cell diseases.

3 | DYSKERATOSIS CONGENITA AND TELOMERE BIOLOGY DISORDERS: A SPECTRUM OF DISEASES UNIFIED BY HUMAN GENETICS

Dyskeratosis congenita (DC) is a rare disease described over 100 years ago, with onset usually occurring in childhood.[23] In its classic form, DC is characterized by a diagnostic triad of skin pigmentation abnormalities, oral mucosal lesions, and degenerative changes in the nails. Beyond these features, case reports over the years noted that DC patients frequently had other problems including low blood counts (anemia, thrombocytopenia, and/or leukopenia), microcephaly, learning/developmental disorders, short stature, failure to thrive, difficulty swallowing, dental abnormalities, premature graying of hair, osteopenia, and pathology of the lungs, liver, and other vital organs.[24] DC was thus recognized as a multisystem syndrome early on, but for decades the molecular basis and pathophysiology was unknown. A high male to female ratio and pedigree studies indicated X-linked inheritance in some forms of DC.[25] Through linkage studies of the UK DC patient registry established in the early 1990s, Dokal and Vulliamy discovered hemizygous mutations in males in a gene they named *DKC1*, which encoded a protein (dyskerin) of unknown function.[26] Dyskerin showed homology to yeast Cbf5p[27] and rat NAP57,[28] highly conserved pseudouridine synthases known to bind snoRNAs as guides for rRNA modification.[16] These findings led to speculation that DC might be driven by defects in ribosome biogenesis.[26]

The observation of a box H/ACA motif in human TERC led the Collins group to alternate hypotheses, that dyskerin might also bind TERC, and that telomerase might be compromised by *DKC1* mutations to result in the degenerative clinical features of DC. Indeed, dyskerin was found to associate directly with telomerase via TERC, and *DKC1*-mutant patients' cells had decreased TERC levels and short telomeres.[29] Soon thereafter, mutations in *TERC* itself were identified in autosomal dominant DC.[30] Together these findings firmly established DC as a disorder of telomere maintenance, and demonstrated the

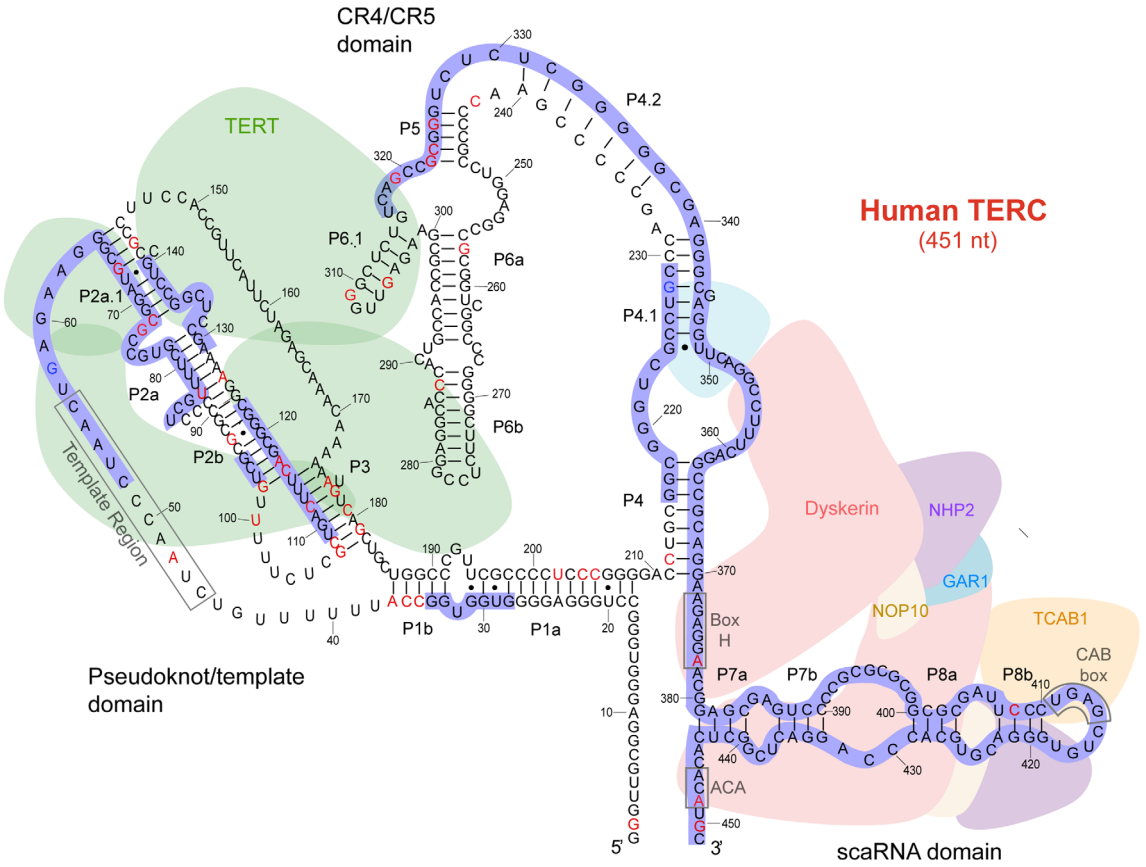

FIGURE 1 Model of telomerase RNA component (TERC) structure, function, and human dyskeratosis congenita/telomere biology disorder (DC/TBD) mutations. Adapted from References 17 and 18. The primary sequence of the 451 nucleotide TERC is depicted. Secondary structure and functional interactions are based on data from phylogenetic, biochemical, human genetic, and structural studies including cryo-electron microscopy. Conserved regions are indicated as P1a through P8b. The TERT-binding pseudoknot/template and CR4/CR5 domains, and the dyskerin/TCAB1-associated scaRNA domain are shown. Critical sequence motifs are defined: telomere repeat-encoding template region, Box H, ACA motif, and CAB box. Human genetic lesions reported in the literature include point mutations (red nucleotides) and regions where deletions have been described (blue outline). Known polymorphisms are shown as blue nucleotides. Point mutations, deletions, and the resulting DC/TBD phenotypes are detailed in Table 1

importance of TERC and telomerase in human health. These studies represent an important early example of the impact of genetics studies on understanding the composition and biogenesis of human telomerase.

The discoveries of *DKC1* and *TERC* mutations in DC patients ultimately revealed a spectrum of telomere biology disorders (TBDs).[31,32] Clinical features of patients in the DC registry suggested that another severe disorder of infancy, Hoyeraal-Hreidarsson syndrome (HHS), might also be caused by mutations in *DKC1*.[33] HHS is characterized by prenatal growth retardation, microcephaly, cerebellar hypoplasia, aplastic anemia, and immunodeficiency in infants, early clinical features that can precede the classic DC triad.[34] The same *DKC1* mutations that cause DC were found in children with HHS, demonstrating that HHS is an early onset, more severe form of DC.[33]

On the other end of the spectrum, independent genetic discoveries and detailed analyses of pedigrees revealed cryptic presentations of DC in previously healthy adults with seemingly isolated clinical problems. Heterozygous *TERC* mutations were found in adult patients with a variety of hematologic presentations including aplastic anemia, myelodysplastic syndrome (MDS), and paroxysmal nocturnal hemoglobinuria, in the absence of classic DC manifestations.[35-44] In some families, the same *TERC* mutation presented with hematologic disease in one individual but pulmonary fibrosis (PF) or liver disease in others. In keeping with this, germline *TERC* mutations were found in families afflicted by PF, as well as cohorts of liver disease patients presenting in late adulthood.[45-47] Some patients with acute myeloid leukemia (AML) or squamous cell cancers of the oral and anogenital regions were also found to carry DC-associated mutations,[38] reinforcing DC as a cancer predisposition syndrome.[48] Taken together, these findings indicated that genetic mutations in *TERC* present across a spectrum of disease (Table 1), with diverse TBD-associated manifestations presenting anywhere from childhood to mid-life and later.

Studies in DC/TBD pedigrees with *TERC* mutations have revealed several interesting genetic features beyond simple Mendelian inheritance, complicating genotype-phenotype correlations. First, in some families, transmission of heterozygous *TERC* mutations results in

TABLE 1 *TERC* gene mutations implicated in various telomere biology disorders (based on Podlevsky et al, *Nucleic Acids Research*, 2007, and references therein. http://telomerase.asu.edu)

Phenotype	*TERC* gene mutation
Myelodysplastic syndrome/ acute myeloid leukemia	*C35U*, *del52_55*, U83G, *del110_113*, *C212G*, *C287G*, C309U, *G319A*, *G322A*, *C323U*, *A377G*, *del389_390*
Dyskeratosis congenita/ hoyeraal hreidarsson syndrome	A37G, *A48G*, *del52_55*, del54_57, G73U, G93C, *del95_96*, *del96_97*, *U100A*, *GC107_108AG*, delins129_140GU, *G143A*, U202G, *C205U*, *C212U*, *del216_229*, *C242U*, del316_451, *del378_451*, *C408G*, *A448G*
Aplastic anemia	G2C, *del28_34*, *C36U*, A37G, *G67A*, *C72G*, *del79*, U83G, *G107U*, *del109_123*, *del110_113*, *C116U*, *A117C*, *A126G*, *G143A*, *A176C*, *G178A*, *C180U*, *G182A*, *C204G*, *C212G*, G257A, *G305A*, *del341_360*, *A377G*
Pulmonary fibrosis/lung disease	del52_86, U80A, G98A, C108U, G182C, *G325U*, del375_377
Liver fibrosis	A37G, *del28_34*, *G319A*, *del341_360*

Notes: Nucleotide position based Genbank accession number NR_001566 for the RNA sequence. Mutations in italics denote those verified by in vitro functional testing in the published literature. Literature references can be found at http://telomerase.asu.edu.

earlier onset and more severe disease in subsequent generations.[43] This *disease anticipation* is thought to result from inheritance of not only the genetic mutation compromising telomere maintenance, but also short telomeres from the carrier parent. A similar phenomenon is observed in autosomal dominant DC/TBD due to heterozygous germline loss-of-function mutations in *TERT*.[49,50] A second unusual genetic feature has been revealed in some *TERC* pedigrees wherein obligate carriers showed underrepresentation or absence of the mutation when genotyping blood DNA. To explain this, single nucleotide polymorphism (SNP) array analysis of non-blood tissue revealed somatic reversion of the *TERC* mutation in the hematopoietic system.[51] The reversion event was evident in both myeloid and lymphoid blood cells, indicating positive selection for restored TERC levels and telomere maintenance at the hematopoietic stem cell (HSC) level. Remarkably, in one patient, multiple independent events of somatic reversion could be documented by SNP arrays, indicating a significant advantage of eliminating the mutant *TERC* locus in HSCs. A third confounder of genotype-phenotype correlations is illustrated by a patient found to have a heterozygous *TERC* mutation but more pronounced disease manifestations compared to family members. Here, it was shown that the patient had also inherited a pathogenic *TERT* mutation, resulting in oligogenic phenotypic contributions from multiple partial loss-of-function alleles.[52] Taken together, these studies illustrate complexities in diagnosis and establishing genotypic-phenotype relationships in patients with germline *TERC* mutations.

From a clinical standpoint, the detection of *TERC* mutations and their associated disease burden are likely to be underestimated for several reasons. These include lack of familiarity with DC/TBD amongst clinicians, low suspicion of germline mutations in adult patients with MDS, cirrhosis or PF, and overlooking TERC (as a ncRNA) in clinical and research whole exome sequencing pipelines. Functional telomere length testing is a valuable diagnostic test, useful for increasing suspicion of underlying TBD, but with limitations in sensitivity and specificity in older age groups.[53] In summary, germline *TERC* mutations present across a spectrum of clinical severity and onset, but are likely underdiagnosed in patients without obvious syndromic features or family histories.

4 | *TERC* MUTATIONS AND MOLECULAR MECHANISMS OF DISEASE

In addition to *DKC1*, it is now clear that several other gene mutations result in decreased TERC levels to cause TBDs. These are discussed in detail below. However, it is first instructive to consider the various molecular mechanisms by which mutations in *TERC* itself have been found to result in loss of function.

4.1 | *TERC* mutations

More than 60 disease-associated mutations in *TERC* have been identified to date[17] (Table 1). TERC is 451 nt, and in aggregated databases of whole genome sequencing only two positions show polymorphism (n.58G>A, n.228G>A) at greater than 0.1% frequency (Figure 1). Different impairments caused by *TERC* mutations have been described, including defects in transcription, template function, secondary structure, assembly into H/ACA-RNPs, and interactions with TERT. With regard to primary transcriptional defects, mutations in the -99 Sp1 site and -58 CCATT box of the *TERC* promoter have been described in three different families with BMF or MDS.[37,42,54] However, there was limited data in these reports showing a direct effect on transcription. In terms of requirements for RNP assembly, point mutations and deletions in the box H/ACA motifs would be expected to impact dyskerin binding in cells (Figure 1). Consistent with this, the accumulation of variants with mutations in the box H or ACA domains is abrogated in cells, despite retaining template function in in vitro reconstitution assays.[55] A box H/ACA deletion truncating the last 74 nt of TERC as well as 747 nt downstream was shown to impact not only accumulation of the RNA transcript,[21] but chromatin configuration of the allele in *cis* as well, suggesting transcriptional regulatory function of the sequences immediately 3′ of the gene.[56] An extensive examination of multiple pseudoknot/template domain mutations indicated that most of these diminish holoenzyme catalytic activity[55] (Figure 1). Not only the template but also the conserved region (CR) CR4/CR5 domains of

TERC are required for telomerase assembly and activity in vitro and in vivo.[57] Mutations in the CR4/CR5 region have been found which do not affect accumulation or assembly with H/ACA-RNP, but rather impair interactions with TERT and prevent formation of active telomerase holoenzyme.[55,57,58] Interestingly, the secondary structure of the CR4/CR5 region has also been shown to be responsive to binding by TCAB1 (telomerase Cajal body protein 1), which is required for subsequent interactions with TERT.[59] These studies indicate that certain CR4/CR5 residues mutated in DC may serve as an "activity switch," which relays TCAB1 binding of the box H/ACA regions and licenses TERT assembly into the holoenzyme. In summary, human disease-associated mutations in TERC disrupt its biogenesis and function, leading to impaired telomerase function. Importantly, until now *TERC* mutations in patients have been found in heterozygous form, and biallelic or null mutations have not been reported, indicating that complete loss-of-function is unlikely to be tolerated in humans.

5 | MUTATIONS IN SEVERAL FACTORS IMPACT TERC TO CAUSE DISEASE

To date, mutations in 15 genes have been implicated in DC/TBDs, accounting for ~70% of cases.[60,61] Of these, besides *TERC* itself, loss or alteration of function in seven other genes—*DKC1*, *NOP10*, *NHP2*, *NAF1* (nuclear assembly factor 1), *TCAB1*, *PARN* (poly[A]-specific ribonuclease), and *ZCCHC8* (zinc finger CCHC-type containing 8)—impairs telomere maintenance by compromising TERC processing and biogenesis at different steps.

5.1 | Mutations impacting the H/ACA-RNP

The nascent H/ACA-RNP complex consists of four proteins: dyskerin, NAF1, NHP2, and NOP10.[62] Mutations in the genes encoding any of these four proteins cause DC.[26,63-65] NAF1 is exchanged for GAR1 after H/ACA-RNP maturation (Figure 1). Of note, *GAR1* mutations have not been reported in DC/TBDs.

Each H/ACA-RNP complex associates with one of hundreds of ncRNAs via the box H/ACA motif,[66] and the associated RNA directs the RNP to different substrates and subcellular locations. Dyskerin is a highly conserved enzyme that catalyzes the conversion of uridine to pseudouridine in cellular RNAs.[67] Box H/ACA snoRNAs serve as antisense guides for the pseudouridylation of ribosomal RNAs (rRNAs) in the nucleolus, and also play a role in rRNA processing.[68,69] Small Cajal body (sca)RNAs, including TERC, are a subset of snoRNAs with a binding motif for TCAB1, which re-routes H/ACA-RNPs to the Cajal body instead of nucleolus. There, certain scaRNAs act as guides to target snRNAs involved in RNA splicing for pseudouridylation, although many substrates are unknown.[70-72] There is no evidence that TERC serves to target dyskerin to other RNAs for pseudouridylation. However, TERC itself may contain pseudouridine modifications including two residues in the loop of hairpin P6.1 (Figure 1), a domain critical for telomerase catalytic activity.[73] Although it is not entirely clear why TERC co-opted a box H/ACA architecture for association with the H/ACA-RNP, possible reasons include exploitation of snoRNA 3′ end processing mechanisms, post-transcriptional fine-tuning of steady state RNA levels, subnuclear compartmentation for efficient telomere elongation.

Despite the fact that dyskerin, NOP10, NHP2, and NAF1 are found in numerous different snoRNPs, mutations in the genes encoding these factors phenocopy DC/TBDs. Although the spectrum of diseases associated with these mutations ranges from classic DC to PF, hemizygous mutations in *DKC1* and biallelic mutations in *NOP10* and *NHP2* tend to associate with earlier onset, multisystem disease. Heterozygous truncation mutations in *NAF1* have been found in adult patients with DC, MDS, liver disease, and PF.[63] In all cases, steady state levels of TERC are reduced. TERC is limiting for telomerase activity and telomere elongation in *DKC1*-mutant patient cells.[74] Importantly, some of these mutations cause a greater deficiency in TERC than heterozygous loss-of-function *TERC* mutations. As with *TERC* itself, mutations in *DKC1*, *NOP10*, *NHP2*, and *NAF1* have not been found in null states, which are unlikely to be tolerated. It remains unclear whether other sno/scaRNAs or pseudouridylation are meaningfully impacted by these mutations, with evidence for and against relevant effects in various studies.[29,75-82] However, it is clear that TERC is affected by these mutations. Importantly, the range and make-up of disease phenotypes overlap whether caused by mutations in H/ACA-RNP components or in genes regulating telomere maintenance by other mechanisms, such as *RTEL1* (regulator of telomere elongation helicase 1) and *TINF2* (TERF1 interacting nuclear factor 2). These observations suggest that defects in TERC alone may be sufficient to explain pathophysiology in DC/TBDs driven by mutations in *DKC1*, *NOP10*, *NHP2*, or *NAF1*.

How does one explain the apparent preferential impact of these mutations on TERC, compared to hundreds of other sno/scaRNAs? TERC is unique amongst this class of RNAs in being encoded by an autonomous RNA pol II-transcribed gene, unlike other sno/scaRNAs that are intron-embedded and processed from host gene transcripts. It has been suggested that nascent TERC RNA is more sensitive to efficient recruitment of pre-assembled dyskerin/NOP10/NHP2/NAF1 complexes due to its lack of 3′ end protection, unlike sno/scaRNAs that are initially contained within a lariat structure during their biogenesis.[83] Impairments of dyskerin/NOP10/NHP2/NAF1 assembly due to partial loss-of-function in any of these factors might be expected to compromise TERC more severely than other sno/scaRNAs. Another way to view it is that more severe alterations or loss of function in factors that impact sno/scaRNA biogenesis more globally may not be compatible with early human development.

5.2 | Mutations impacting TERC secondary structure and Cajal body localization

TCAB1 (also known as WDR79/WRAP53) binds the Cajal body localization sequence (CAB box) in the terminal loop of scaRNAs including TERC[84,85] (Figure 1). TCAB1 incorporation into the dyskerin

holoenzyme is believed to occur after H/ACA-RNP assembly. TCAB1 serves to localize scaRNPs including telomerase to Cajal bodies instead of the nucleolus. Upon identification of TCAB1's function in telomere biology, candidate screening of a DC registry identified biallelic *TCAB1* mutations in two unrelated patients.[86] The mutations were found to compromise TCAB1 protein stability and nuclear localization, and in turn H/ACA-RNP and TERC trafficking to Cajal bodies. Although mislocalization of an otherwise intact telomerase RNP was shown to be a driver of impaired telomere maintenance in the setting of these mutations, subsequent studies showed that telomerase activity was also compromised by loss-of-function *TCAB1* mutations.[87] Specifically, TCAB1 was found to be required for proper folding of the CR4/CR5 domain of TERC, to enable association with TERT.[59] Importantly, unlike core H/ACA-RNP proteins, total TCAB1 loss is tolerated in human cells and results in impaired telomerase activity in the null state.[88] These data again indicate a particular sensitivity of TERC biogenesis and post-transcriptional trafficking to disruption of a factor that regulates multiple scaRNPs.

5.3 | Mutations impairing TERC 3′ end processing

Mechanisms of TERC transcriptional termination and 3′ end processing were unknown until recently. In 2015, whole exome sequencing of DC and HHS patients in the UK DC registry uncovered biallelic mutations in the *PARN* gene, which encodes a 3′ exoribonuclease.[89] At the same time, Garcia and colleagues found heterozygous *PARN* mutations in familial PF cohorts.[90] The majority of patients with *PARN* mutations in both groups had very short telomeres. These molecular and clinical findings firmly linked PARN to the spectrum of TBDs, with severity and phenotype correlating with gene dosage. However, the role of PARN in telomere biology was unclear. The canonical function of PARN was thought to be catalyzing the turnover of cytoplasmic mRNAs by degrading long poly(A) tails.[91] Mutations in *PARN* were thus proposed to cause telomere disease via effects on mRNA levels, particularly impacting telomere components and p53.[89] However, in *PARN*-mutant patient cells, decreased TERC RNA levels were also found,[89,92,93] the molecular basis of which was unclear given that TERC does not have a poly(A) tail. A few key additional observations led to insights on how *PARN* mutations might cause TERC deficiency. First, although early studies demonstrated a precise 3′ end for TERC, subsequent deep sequencing data indicated a larger diversity, including genomically extended and oligo-adenylated TERC ends.[94] Second, beyond a role in mRNA metabolism, PARN had been proposed to regulate ncRNA metabolism, particularly box H/ACA snoRNA 3′ end maturation and stabilization.[95] Given that TERC shared the same motif with box H/ACA snoRNAs, it was hypothesized that PARN might also regulate the productive maturation of TERC, which would explain the finding of diminished TERC levels and telomerase deficiency in patients with DC and IPF.[93] In cells derived from DC patients with biallelic *PARN* mutations, increased 3′ extended species of TERC were detected.[92,93] Deep sequencing revealed that these species were both genomically extended and oligo-adenylated, yielding short (~10 nt) tails on TERC, which would be expected to be degraded by the RNA exosome (Figure 2A). In keeping with this, TERC transcripts were found to be destabilized by PARN deficiency, leading to decreased telomerase activity and telomere length in patient cells, and their accumulation was reversible by restoring expression of PARN.[93] Other sno/scaRNAs were found to be altered in 3′ end processing,[92,93] but RNA sequencing performed on *PARN*-mutant patient cells did not indicate global effects on mRNAs.[93] These observations led to the conclusion that impaired TERC 3′ end maturation, and not mRNA turnover, is the major contributor to diseases caused by *PARN* mutations.[93] In support of this, later studies showed no genome-wide alterations in mRNA representation or poly(A) tail length when PARN was depleted in human cells.[96]

Simultaneous investigations of human TERC biogenesis mechanisms in cell lines corroborated and extended these findings. Transient PARN depletion in human cell lines results in accumulation of TERC 3′ extended forms.[93,97-99] The non-canonical polymerase PAPD5 is primarily responsible for the addition of non-templated adenosines to extended nascent TERC.[97-100] In yeast, the PAPD5 ortholog Trf4 is part of the TRAMP (Trf4, Air2, and Mtr4) complex, which serves a quality control function by oligo-adenylating misfolded RNAs and targeting them for degradation by the nuclear RNA exosome.[101] Although it is unclear whether human PAPD5 functions in a TRAMP-like complex, knockdown of PAPD5 decreases oligo-adenylation and increases mature TERC levels in normal cells.[99] Furthermore, PAPD5 inhibition by RNA interference in PARN-depleted cell lines or *PARN*-mutant patient cells reduces TERC oligo-adenylation and increases steady-state TERC levels, telomerase activity and telomere length.[97,98,100] A role for the RNA exosome downstream of PAPD5-mediated oligo-adenylation has been indicated by demonstration that knockdown of the core exosome components RRP6/EXOSC10 or RRP40/EXOSC3 increases mature TERC levels in PARN-deficient cells.[98,99] These findings collectively yield a model wherein steady state levels of TERC are controlled by competition between productive maturation of nascent TERC transcripts by PARN vs oligo-adenylation by PAPD5, which targets RNAs for degradation by the nuclear exosome[97-100] (Figure 2A).

Although these studies have illuminated biogenesis intermediates and critical final steps in TERC maturation, questions remain of precisely how and where TERC transcription terminates, and what factors govern the earliest steps in TERC maturation. Recent studies shed some light. First, 4-thiouridine pulse-chase labeling of nascent TERC transcripts demonstrates definitively that TERC species with short oligo-A tails are converted into mature TERC species, rather than solely representing intermediates for degradation.[102] Fusion of the TERC box H/ACA domain to U1 snRNA in an expression construct resulted in the accumulation of a U1-H/ACA hybrid transcript that was oligo-adenylated in a dyskerin- and PARN-sensitive manner. Thus, the TERC H/ACA domain is sufficient to dictate end-formation, as seen in an earlier study,[21] and confers regulation of nascent transcripts by dyskerin and PARN. Importantly, complete elimination of both PARN and PAPD5 resulted in normal levels of mature TERC, indicating that PARN/PAPD5-independent pathways for TERC post-transcriptional processing must exist.[102] The findings also reinforce and refine the model of competition between PARN and PAPD5 in TERC biogenesis,

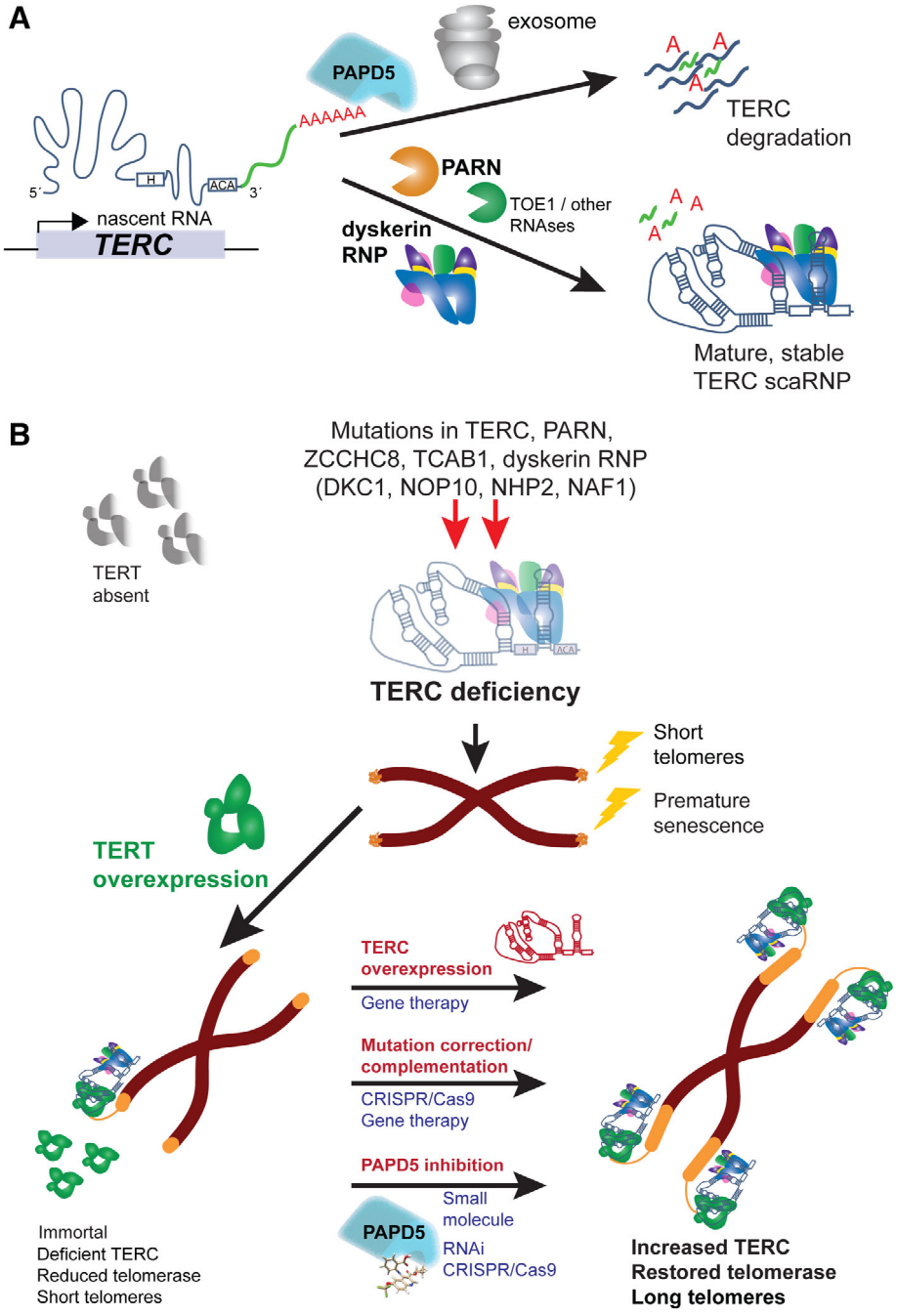

FIGURE 2 Model for telomerase RNA component (TERC) processing in health and dyskeratosis congenita/telomere biology disorders (DC/TBDs), and potential therapeutic strategies. A, TERC post-transcriptional regulation by RNA-binding proteins, polymerases, and nucleases. Nascent TERC transcripts contain genomically encoded 3′ extensions (green). The extensions can be substrates for adenylation by PAPD5, which stimulates destruction of TERC by the RNA exosome. Conversely, PARN and other exoribonucleases trim 3′ extensions to result in mature TERC. Association with the H/ACA ribonucleoprotein (RNP) is an early event and aids in TERC 3′ maturation/end definition, and scaRNP stability, trafficking, and function. Early processing events including transcriptional termination, processing of long transcripts, and NAF1 H/ACA-RNP exchange are not illustrated. B, TERC deficiency in DC/TBDs and therapeutic prospects. Hypomorphic mutations in TERC or other associated RNA processing and binding factors results in TERC deficiency. A patient somatic cell is depicted, in which TERT is absent, telomerase inactive, and telomeres critically short, resulting in senescence. Overexpression of TERT immortalizes cells carrying these mutations in vitro, but telomerase activity remains reduced and telomeres short because TERC is limiting. Strategies shown to restore TERC and thus telomerase and telomere elongation in patient cells in vitro are shown in red. Potential therapeutic modalities to translate each strategy are shown in blue

wherein PARN is specifically required to counteract rapid PAPD5-mediated destabilization of short, extended TERC transcripts.

With regard to the nature and fate of longer nascent TERC transcripts, knocking down the exosome components RRP40/EXOSC3 and RRP6/EXOSC10 results in the accumulation of nascent TERC transcripts extended ≥9 nts beyond the canonical end, as well as increasing mature forms.[103] At the same time, there is a reduction in short, extended TERC forms seen with PARN deficiency, suggesting that longer TERC transcripts processed by the RNA exosome ultimately lead to the formation of short ones that are then substrates for PARN.[103] Using in vitro transcribed TERC box H/ACA domain-containing RNA and nuclear extracts depleted of factors, it has been shown that processing long forms of TERC requires RRP6/EXOSC10. Surprisingly, dyskerin is also required for RRP-mediated conversion of long TERC forms into short PARN substrates. To explain this, extended TERC primary transcripts were shown to engage in tertiary interactions with nucleotides in the first hairpin structures and box H motifs of the box H/ACA domain. Transcripts folded in this manner are resistant to processing unless tertiary interactions are displaced by dyskerin binding. These results indicate a new role for dyskerin in TERC processing, beyond stabilization and trafficking. Whether this specific role is disrupted by human *DKC1* mutations remains to be determined. However, consistent with these results, knockdown of RRP40/EXOSC3 or PAPD5 was shown to increase TERC maturation

and telomere length in the context of a pathogenic *DKC1* mutation in human embryonic stem cells.[104]

Recent genetic findings in TBDs support a broader role of exosome components in processing nascent TERC RNA. In a family with PF, heterozygous mutations have been identified in *ZCCHC8*,[105] a component of the nuclear exosome targeting (NEXT) complex.[106] Patient cells carrying the mutation showed decreased ZCCHC8 protein but normal levels of two other NEXT components, RBM7 and SKIV2L2/MTR4. ZCCHC8 deficiency was accompanied by increased short and long forms of TERC, and~20% decrease in steady state levels TERC levels in patient fibroblasts. Notably, *ZCCHC8* null cancer cell lines could be generated and recapitulated a defect in TERC levels and telomerase activity, although long-term effects on telomere length were not described. Interestingly, homozygous frameshift *ZCCHC8* mutations (predicted to be null) have been reported in a patient with neurocognitive defects, but there is no information on telomere biology in this setting.[107] It is not clear how ZCCHC8 deficiency results mechanistically in net reduction of TERC levels or function. It is known that ZCCHC8 is required for targeting aberrant 3′ extended ncRNA transcripts to the nuclear exosome. To the extent that the exosome is involved in degradation of TERC after PAPD5-mediated oligo-adenylation of short transcripts, it might be counterintuitive that inhibiting trafficking to the exosome would result in a reduction in transcripts. However, it is possible that ZCCHC8/NEXT and the RNA exosome are also required for productive maturation of long TERC precursors by RRP6.[103] Whether there is a role for NEXT/RNA exosome in processing short TERC transcripts to their final form remains unknown.

5.4 | Other human disease genes potentially involved in TERC maturation

Biallelic germline mutations in *TOE1* (target of EGR1), encoding a CAF1 family 3′-exoribonuclease related to PARN, are associated with pontocerebellar hypoplasia (PCH) type VII.[108] TOE1-deficient patient cells harbor an increase in pre-snRNAs with non-genomically encoded adenosine residues, reminiscent of aberrant TERC species in PARN-deficient cells.[108] Interestingly, other forms of PCH are caused by germline mutations in exosome components, including RRP40/EXOSC3 and EXOSC8. Cerebellar hypoplasia is a feature of severe forms of TBDs such as HHS. These findings raise the question of whether clinical manifestations common to both PCH and TBDs can be explained by defective 3′ end processing of the same ncRNAs. Although TERC levels and telomere length have not been reported in PCH type VII patients, genome-wide ncRNA profiling indicates a potential role for TOE1 in TERC biogenesis.[96] TOE1 depletion has minimal effects on TERC steady state levels by itself, but RNA species with very short 3′ extensions are increased in general. Combined TOE1 and PARN knockdown results in additive effects in destabilizing TERC, as well as a global increase in RNA 3′ adenylation. Notably, inhibition of PAPD5 is sufficient to reverse the effects of both TOE1 and PARN depletion. In a detailed evaluation of the effects on telomere biology, TOE1 depletion in cell lines by CRISPR/Cas9 resulted in the accumulation of very short TERC adenylated species[109] without changes in overall TERC levels. However, with stable heterozygous *TOE1* deletion, telomerase activity was decreased and telomeres shortened over time. These studies show that TOE1 plays a role in TERC biogenesis nonredundant with that of PARN, likely removing the final few 3′ nucleotides and also contributing to TERC maturation in *PARN* null cells (Figure 2A). These results also lead to the speculation that impaired telomere maintenance contributes to disease manifestations in PCH VII patients, which remains to be studied.

5.5 | Therapeutic potential of modulating TERC processing

TERC deficiency limits telomere maintenance in cells from DC patients with mutations in *TERC*, *DKC1*, or *PARN*.[74,100,110,111] Ectopic *TERT* expression immortalizes cells carrying these lesions, but is insufficient to efficiently elongate telomeres (Figure 2B). Therefore, although stem cell self-renewal may be conferred by *TERT* expression, the replicative capacity of *TERT*-negative daughter cells is likely to remain low because of short telomere reserve. Overexpression of TERC in these settings restores telomerase activity and telomere elongation, as does *DKC1* gene correction,[112,113] suggesting potential treatment approaches via genome-editing or gene therapy (Figure 2B). However, DC and TBDs affect several organs, and genetic strategies to correct TERC deficiency in stem cells throughout the body are intractable at present.

The discovery that TERC is regulated by multiple components of the ncRNA post-transcriptional machinery has opened up a range of new targets through which TERC levels might be manipulated. Indeed, many of these are enzymes potentially amenable to small molecule inhibitors, which could provide systemic treatments. As described above, several studies have demonstrated that genetic inhibition of PAPD5 can restore TERC levels in PARN- or dyskerin-deficient states.[96,98-100,102,104,114] Stable long-term shRNA-mediated PAPD5 depletion is tolerated in *PARN*-mutant patient iPSCs and restores TERC levels, telomerase activity and telomere length[100] (Figure 2B). Along the same lines, long-term *PAPD5* knockdown in human embryonic stem cells engineered to express a pathogenic *DKC1* mutation (A353V) increases telomere length and improves in vitro hematopoietic differentiation capacity.[104] In terms of tolerability, *PAPD5* null human cell lines and pluripotent stem cells are able to be isolated and propagated indefinitely, and show decreased TERC oligo-adenylation and increased TERC levels.[102,114] These observations provide the basis for considering PAPD5 a "druggable" target to restore TERC and telomere length in certain forms of DC/TBDs[100] (Figure 2B).

Recently a high-throughput enzymatic screen identified novel and specific PAPD5 small molecule inhibitors that restored telomerase activity in DC patients' iPSCs.[114] One such PAPD5 inhibitor, a quinoline called BCH001, showed the capacity to increase TERC maturation and RNA levels and elongate telomeres in *PARN*-mutant patient stem cells (Figure 2B). Importantly, telomere elongation by BCH001 in patient cells was dependent on *TERT*, expressed either endogenously in iPSCs

or ectopically in fibroblasts. These results indicate that small molecule telomerase modulation could be achieved without immortalizing cells or circumventing the gatekeeper function of TERT, important safety considerations for systemic therapy. A second class of small molecule PAPD5 inhibitors, dihydroquinolizinones (DHQ), was identified in a hepatitis B surface antigen suppressor screen, and unexpectedly found to act via PAPD5 inhibition.[115,116] DHQ molecules increase TERC and telomere length in DC patient iPSCs in vitro.[114] In an in vivo mouse xenotransplant model using CRISPR/Cas9-engineered, PARN-deficient human hematopoietic stem and progenitor cells, oral administration of the DHQ molecule RG7834 restored TERC processing and telomere maintenance. Taken together, these results provide encouraging evidence that pharmacologic manipulation of the TERC biogenesis machinery can be used to modulate telomerase in stem cells throughout the body. Although data have thus far been provided for pathogenic *PARN* and *DKC1* mutations,[114] it is possible that other DC/TBD-associated mutations that affect TERC processing and accumulation (eg, *NOP10*, *NHP2*, *NAF1*, *TCAB1*, *ZCCHC8*, certain *TERC* alleles) may also be amenable to a PAPD5 inhibitor strategy. If successful, such an approach may provide a much-needed systemic therapy for patients with DC/TBDs and perhaps other degenerative disorders.

6 | PERSPECTIVES

Disease-causing mutations have revealed TERC biogenesis mechanisms and illuminated the sensitivity of human stem cells to TERC levels. These insights now allow one to consider how TERC manipulation might be achieved to treat DC/TBDs and other diseases. Fundamental questions remain. How does *TERC* transcription terminate? What is the precise location, trafficking, timing, and order of various stages of TERC processing? How do elements like chromatin, RNA modifications, and post-translation modifications impact TERC processing? Are there cell-type specific regulatory mechanisms that impact TERC levels? Is DC/TBD pathology in the setting of hypomorphic mutations in *DKC1*, *NOP10*, *NHP2*, *NAF1*, *PARN*, *TCAB1*, or *ZCCHC8* satisfactorily explained by effects on TERC alone? If not, can effects on other ncRNAs and their consequences be defined conclusively? Are the functions and specificities of TERC regulatory factors and pathways sufficiently conserved in animal models to test new therapeutics? Will reversing TERC deficiency pharmacologically be effective in treating or preventing DC/TBDs? As history has shown, staying close to the patients can be expected to yield answers to these and other important questions.

ACKNOWLEDGMENTS

This work was funded by NIH grant R01 DK107716, U.S. Department of Defense grant W81XWH-19-1-0572, Harrington Discovery Institute, and Harvard Stem Cell Institute.

CONFLICT OF INTEREST

The authors are named as inventors on patent applications related to manipulating TERC in telomere diseases.

AUTHOR CONTRIBUTIONS

Suneet Agarwal and Neha Nagpal wrote the manuscript.

DATA AVAILABILITY STATEMENT

Data sharing is not applicable to this article as no new data were created or analyzed in this study.

ORCID

Suneet Agarwal https://orcid.org/0000-0003-4910-3118

REFERENCES

1. Allsopp RC, Harley CB. Evidence for a critical telomere length in senescent human fibroblasts. *Exp Cell Res*. 1995;219:130-136.
2. Harley CB, Futcher AB, Greider CW. Telomeres shorten during ageing of human fibroblasts. *Nature*. 1990;345:458-460.
3. Greider CW. Telomerase RNA levels limit the telomere length equilibrium. *Cold Spring Harb Symp Quant Biol*. 2006;71:225-229.
4. Podlevsky JD, Chen JJ. Evolutionary perspectives of telomerase RNA structure and function. *RNA Biol*. 2016;13:720-732.
5. Webb CJ, Zakian VA. Telomerase RNA is more than a DNA template. *RNA Biol*. 2016;13:683-689.
6. Wu RA, Upton HE, Vogan JM, Collins K. Telomerase mechanism of telomere synthesis. *Annu Rev Biochem*. 2017;86:439-460.
7. Musgrove C, Jansson LI, Stone MD. New perspectives on telomerase RNA structure and function. *Wiley Interdiscip Rev RNA*. 2018;9:e1456.
8. Vasianovich Y, Wellinger RJ. Life and death of yeast telomerase RNA. *J Mol Biol*. 2017;429:3242-3254.
9. Greider CW, Blackburn EH. The telomere terminal transferase of Tetrahymena is a ribonucleoprotein enzyme with two kinds of primer specificity. *Cell*. 1987;51:887-898.
10. Greider CW, Blackburn EH. A telomeric sequence in the RNA of Tetrahymena telomerase required for telomere repeat synthesis. *Nature*. 1989;337:331-337.
11. Feng J, Funk WD, Wang SS, et al. The RNA component of human telomerase. *Science*. 1995;269:1236-1241.
12. Bodnar AG, Ouellette M, Frolkis M, et al. Extension of life-span by introduction of telomerase into normal human cells. *Science*. 1998;279:349-352.
13. Zaug AJ, Linger J, Cech TR. Method for determining RNA 3′ ends and application to human telomerase RNA. *Nucleic Acids Res*. 1996;24:532-533.
14. Mitchell JR, Cheng J, Collins K. A box H/ACA small nucleolar RNA-like domain at the human telomerase RNA 3′ end. *Mol Cell Biol*. 1999;19:567-576.
15. Ganot P, Caizergues-Ferrer M, Kiss T. The family of box ACA small nucleolar RNAs is defined by an evolutionarily conserved secondary structure and ubiquitous sequence elements essential for RNA accumulation. *Genes Dev*. 1997;11:941-956.
16. Kiss T, Fayet-Lebaron E, Jady BE. Box H/ACA small ribonucleoproteins. *Mol Cell*. 2010;37:597-606.
17. Podlevsky JD, Bley CJ, Omana RV, Qi X, Chen JJ. The telomerase database. *Nucleic Acids Res*. 2008;36:D339-D343.
18. Nguyen THD, Tam J, Wu RA, et al. Cryo-EM structure of substrate-bound human telomerase holoenzyme. *Nature*. 2018;557:190-195.
19. Blasco MA, Funk W, Villeponteau B, Greider CW. Functional characterization and developmental regulation of mouse telomerase RNA. *Science*. 1995;269:1267-1270.
20. Chen JL, Blasco MA, Greider CW. Secondary structure of vertebrate telomerase RNA. *Cell*. 2000;100:503-514.
21. Fu D, Collins K. Distinct biogenesis pathways for human telomerase RNA and H/ACA small nucleolar RNAs. *Mol Cell*. 2003;11:1361-1372.

22. Jady BE, Bertrand E, Kiss T. Human telomerase RNA and box H/ACA scaRNAs share a common Cajal body-specific localization signal. *J Cell Biol*. 2004;164:647-652.
23. Kirwan M, Dokal I. Dyskeratosis congenita: a genetic disorder of many faces. *Clin Genet*. 2008;73:103-112.
24. Dokal I. Dyskeratosis congenita in all its forms. *Br J Haematol*. 2000; 110:768-779.
25. Knight SW, Vulliamy T, Forni GL, Oscier D, Mason PJ, Dokal I. Fine mapping of the dyskeratosis congenita locus in Xq28. *J Med Genet*. 1996;33:993-995.
26. Heiss NS, Knight SW, Vulliamy TJ, et al. X-linked dyskeratosis congenita is caused by mutations in a highly conserved gene with putative nucleolar functions. *Nat Genet*. 1998;19:32-38.
27. Jiang W, Middleton K, Yoon HJ, Fouquet C, Carbon J. An essential yeast protein, CBF5p, binds in vitro to centromeres and microtubules. *Mol Cell Biol*. 1993;13:4884-4893.
28. Meier UT, Blobel G. NAP57, a mammalian nucleolar protein with a putative homolog in yeast and bacteria. *J Cell Biol*. 1994;127:1505-1514.
29. Mitchell JR, Wood E, Collins K. A telomerase component is defective in the human disease dyskeratosis congenita. *Nature*. 1999;402: 551-555.
30. Vulliamy T, Marrone A, Goldman F, et al. The RNA component of telomerase is mutated in autosomal dominant dyskeratosis congenita. *Nature*. 2001;413:432-435.
31. Armanios M, Blackburn EH. The telomere syndromes. *Nat Rev Genet*. 2012;13:693-704.
32. Calado RT, Young NS. Telomere diseases. *N Engl J Med*. 2009;361: 2353-2365.
33. Knight SW, Heiss NS, Vulliamy TJ, et al. Unexplained aplastic anaemia, immunodeficiency, and cerebellar hypoplasia (Hoyeraal-Hreidarsson syndrome) due to mutations in the dyskeratosis congenita gene, DKC1. *Br J Haematol*. 1999;107:335-339.
34. Glousker G, Touzot F, Revy P, Tzfati Y, Savage SA. Unraveling the pathogenesis of Hoyeraal-Hreidarsson syndrome, a complex telomere biology disorder. *Br J Haematol*. 2015;170:457-471.
35. Du HY, Pumbo E, Ivanovich J, et al. TERC and TERT gene mutations in patients with bone marrow failure and the significance of telomere length measurements. *Blood*. 2009;113:309-316.
36. Fogarty PF, Yamaguchi H, Wiestner A, et al. Late presentation of dyskeratosis congenita as apparently acquired aplastic anaemia due to mutations in telomerase RNA. *Lancet*. 2003;362:1628-1630.
37. Keith WN, Vulliamy T, Zhao J, et al. A mutation in a functional Sp1 binding site of the telomerase RNA gene (hTERC) promoter in a patient with paroxysmal nocturnal haemoglobinuria. *BMC Blood Disord*. 2004;4:3.
38. Kirwan M, Vulliamy T, Marrone A, et al. Defining the pathogenic role of telomerase mutations in myelodysplastic syndrome and acute myeloid leukemia. *Hum Mutat*. 2009;30:1567-1573.
39. Ly H, Calado RT, Allard P, et al. Functional characterization of telomerase RNA variants found in patients with hematologic disorders. *Blood*. 2005;105:2332-2339.
40. Marrone A, Sokhal P, Walne A, et al. Functional characterization of novel telomerase RNA (TERC) mutations in patients with diverse clinical and pathological presentations. *Haematologica*. 2007;92:1013-1020.
41. Marrone A, Stevens D, Vulliamy T, Dokal I, Mason PJ. Heterozygous telomerase RNA mutations found in dyskeratosis congenita and aplastic anemia reduce telomerase activity via haploinsufficiency. *Blood*. 2004;104:3936-3942.
42. Ortmann CA, Niemeyer CM, Wawer A, Ebell W, Baumann I, Kratz CP. TERC mutations in children with refractory cytopenia. *Haematologica*. 2006;91:707-708.
43. Vulliamy T, Marrone A, Szydlo R, Walne A, Mason PJ, Dokal I. Disease anticipation is associated with progressive telomere shortening in families with dyskeratosis congenita due to mutations in TERC. *Nat Genet*. 2004;36:447-449.
44. Yamaguchi H, Baerlocher GM, Lansdorp PM, et al. Mutations of the human telomerase RNA gene (TERC) in aplastic anemia and myelodysplastic syndrome. *Blood*. 2003;102:916-918.
45. Armanios MY, Chen JJ, Cogan JD, et al. Telomerase mutations in families with idiopathic pulmonary fibrosis. *N Engl J Med*. 2007;356: 1317-1326.
46. Calado RT, Brudno J, Mehta P, et al. Constitutional telomerase mutations are genetic risk factors for cirrhosis. *Hepatology*. 2011;53: 1600-1607.
47. Tsakiri KD, Cronkhite JT, Kuan PJ, et al. Adult-onset pulmonary fibrosis caused by mutations in telomerase. *Proc Natl Acad Sci USA*. 2007;104:7552-7557.
48. Alter BP, Giri N, Savage SA, Rosenberg PS. Cancer in dyskeratosis congenita. *Blood*. 2009;113:6549-6557.
49. Diaz de Leon A, Cronkhite JT, Katzenstein AL, et al. Telomere lengths, pulmonary fibrosis and telomerase (TERT) mutations. *PLoS One*. 2010;5:e10680.
50. Armanios M, Chen JL, Chang YP, et al. Haploinsufficiency of telomerase reverse transcriptase leads to anticipation in autosomal dominant dyskeratosis congenita. *Proc Natl Acad Sci USA*. 2005;102: 15960-15964.
51. Jongmans MC, Verwiel ET, Heijdra Y, et al. Revertant somatic mosaicism by mitotic recombination in dyskeratosis congenita. *Am J Hum Genet*. 2012;90:426-433.
52. Collopy LC, Walne AJ, Cardoso S, et al. Triallelic and epigenetic-like inheritance in human disorders of telomerase. *Blood*. 2015;126: 176-184.
53. Alder JK, Hanumanthu VS, Strong MA, et al. Diagnostic utility of telomere length testing in a hospital-based setting. *Proc Natl Acad Sci USA*. 2018;115:E2358-E2365.
54. Aalbers AM, Kajigaya S, van den Heuvel-Eibrink MM, van der Velden VH, Calado RT, Young NS. Human telomere disease due to disruption of the CCAAT box of the TERC promoter. *Blood*. 2012; 119:3060-3063.
55. Robart AR, Collins K. Investigation of human telomerase holoenzyme assembly, activity, and processivity using disease-linked subunit variants. *J Biol Chem*. 2010;285:4375-4386.
56. Agarwal S, Loh YH, McLoughlin EM, et al. Telomere elongation in induced pluripotent stem cells from dyskeratosis congenita patients. *Nature*. 2010;464:292-296.
57. Mitchell JR, Collins K. Human telomerase activation requires two independent interactions between telomerase RNA and telomerase reverse transcriptase. *Mol Cell*. 2000;6:361-371.
58. Boyraz B, Bellomo CM, Fleming MD, Cutler CS, Agarwal S. A novel TERC CR4/CR5 domain mutation causes telomere disease via decreased TERT binding. *Blood*. 2016;128:2089-2092.
59. Chen L, Roake CM, Freund A, et al. An activity switch in human telomerase based on RNA conformation and shaped by TCAB1. *Cell*. 2018;174:218-30.e13.
60. Bertuch AA. The molecular genetics of the telomere biology disorders. *RNA Biol*. 2016;13:696-706.
61. Niewisch MR, Savage SA. An update on the biology and management of dyskeratosis congenita and related telomere biology disorders. *Expert Rev Hematol*. 2019;12:1037-1052.
62. Kiss T, Fayet E, Jady BE, Richard P, Weber M. Biogenesis and intranuclear trafficking of human box C/D and H/ACA RNPs. *Cold Spring Harb Symp Quant Biol*. 2006;71:407-417.
63. Stanley SE, Gable DL, Wagner CL, et al. Loss-of-function mutations in the RNA biogenesis factor NAF1 predispose to pulmonary fibrosis-emphysema. *Sci Transl Med*. 2016;8:351ra107.
64. Vulliamy T, Beswick R, Kirwan M, et al. Mutations in the telomerase component NHP2 cause the premature ageing syndrome dyskeratosis congenita. *Proc Natl Acad Sci USA*. 2008;105:8073-8078.
65. Walne AJ, Vulliamy T, Marrone A, et al. Genetic heterogeneity in autosomal recessive dyskeratosis congenita with one subtype due

to mutations in the telomerase-associated protein NOP10. *Hum Mol Genet*. 2007;16:1619-1629.
66. Lafontaine DL, Bousquet-Antonelli C, Henry Y, Caizergues-Ferrer M, Tollervey D. The box H + ACA snoRNAs carry Cbf5p, the putative rRNA pseudouridine synthase. *Genes Dev*. 1998;12:527-537.
67. Zebarjadian Y, King T, Fournier MJ, Clarke L, Carbon J. Point mutations in yeast CBF5 can abolish in vivo pseudouridylation of rRNA. *Mol Cell Biol*. 1999;19:7461-7472.
68. Meier UT. The many facets of H/ACA ribonucleoproteins. *Chromosoma*. 2005;114:1-14.
69. Terns M, Terns R. Noncoding RNAs of the H/ACA family. *Cold Spring Harb Symp Quant Biol*. 2006;71:395-405.
70. Darzacq X, Jady BE, Verheggen C, Kiss AM, Bertrand E, Kiss T. Cajal body-specific small nuclear RNAs: a novel class of 2′-O-methylation and pseudouridylation guide RNAs. *EMBO J*. 2002;21:2746-2756.
71. Kiss AM, Jady BE, Darzacq X, Verheggen C, Bertrand E, Kiss TA. Cajal body-specific pseudouridylation guide RNA is composed of two box H/ACA snoRNA-like domains. *Nucleic Acids Res*. 2002;30:4643-4649.
72. Richard P, Darzacq X, Bertrand E, Jady BE, Verheggen C, Kiss T. A common sequence motif determines the Cajal body-specific localization of box H/ACA scaRNAs. *EMBO J*. 2003;22:4283-4293.
73. Kim NK, Theimer CA, Mitchell JR, Collins K, Feigon J. Effect of pseudouridylation on the structure and activity of the catalytically essential P6.1 hairpin in human telomerase RNA. *Nucleic Acids Res*. 2010;38:6746-6756.
74. Wong JM, Collins K. Telomerase RNA level limits telomere maintenance in X-linked dyskeratosis congenita. *Genes Dev*. 2006;20:2848-2858.
75. Batista LF, Pech MF, Zhong FL, et al. Telomere shortening and loss of self-renewal in dyskeratosis congenita induced pluripotent stem cells. *Nature*. 2011;474:399-402.
76. Gu BW, Apicella M, Mills J, et al. Impaired telomere maintenance and decreased canonical WNT signaling but normal ribosome biogenesis in induced pluripotent stem cells from X-linked dyskeratosis congenita patients. *PLoS One*. 2015;10:e0127414.
77. Thumati NR, Zeng XL, Au HH, Jang CJ, Jan E, Wong JM. Severity of X-linked dyskeratosis congenita (DKCX) cellular defects is not directly related to dyskerin (DKC1) activity in ribosomal RNA biogenesis or mRNA translation. *Hum Mutat*. 2013;34:1698-1707.
78. Bellodi C, McMahon M, Contreras A, et al. H/ACA small RNA dysfunctions in disease reveal key roles for noncoding RNA modifications in hematopoietic stem cell differentiation. *Cell Rep*. 2013;3:1493-1502.
79. Penzo M, Rocchi L, Brugiere S, et al. Human ribosomes from cells with reduced dyskerin levels are intrinsically altered in translation. *FASEB J*. 2015;29:3472-3482.
80. Schwartz S, Bernstein DA, Mumbach MR, et al. Transcriptome-wide mapping reveals widespread dynamic-regulated pseudouridylation of ncRNA and mRNA. *Cell*. 2014;159:148-162.
81. Yoon A, Peng G, Brandenburger Y, et al. Impaired control of IRES-mediated translation in X-linked dyskeratosis congenita. *Science*. 2006;312:902-906.
82. Balogh E, Chandler JC, Varga M, et al. Pseudouridylation defect due to DKC1 and NOP10 mutations causes nephrotic syndrome with cataracts, hearing impairment, and enterocolitis. *Proc Natl Acad Sci USA*. 2020;117:15137-15147.
83. Egan ED, Collins K. An enhanced H/ACA RNP assembly mechanism for human telomerase RNA. *Mol Cell Biol*. 2012;32:2428-2439.
84. Venteicher AS, Abreu EB, Meng Z, et al. A human telomerase holoenzyme protein required for Cajal body localization and telomere synthesis. *Science*. 2009;323:644-648.
85. Tycowski KT, Shu MD, Kukoyi A, Steitz JA. A conserved WD40 protein binds the Cajal body localization signal of scaRNP particles. *Mol Cell*. 2009;34:47-57.
86. Zhong F, Savage SA, Shkreli M, et al. Disruption of telomerase trafficking by TCAB1 mutation causes dyskeratosis congenita. *Genes Dev*. 2011;25:11-16.
87. Freund A, Zhong FL, Venteicher AS, et al. Proteostatic control of telomerase function through TRiC-mediated folding of TCAB1. *Cell*. 2014;159:1389-1403.
88. Vogan JM, Zhang X, Youmans DT, et al. Minimized human telomerase maintains telomeres and resolves endogenous roles of H/ACA proteins, TCAB1, and Cajal bodies. *Elife*. 2016;5.1-21.
89. Tummala H, Walne A, Collopy L, et al. Poly(A)-specific ribonuclease deficiency impacts telomere biology and causes dyskeratosis congenita. *J Clin Invest*. 2015;125:2151-2160.
90. Stuart BD, Choi J, Zaidi S, et al. Exome sequencing links mutations in PARN and RTEL1 with familial pulmonary fibrosis and telomere shortening. *Nat Genet*. 2015;47:512-517.
91. Virtanen A, Henriksson N, Nilsson P, Nissbeck M. Poly(A)-specific ribonuclease (PARN): an allosterically regulated, processive and mRNA cap-interacting deadenylase. *Crit Rev Biochem Mol Biol*. 2013;48:192-209.
92. Dhanraj S, Gunja SM, Deveau AP, et al. Bone marrow failure and developmental delay caused by mutations in poly(A)-specific ribonuclease (PARN). *J Med Genet*. 2015;52:738-748.
93. Moon DH, Segal M, Boyraz B, et al. Poly(A)-specific ribonuclease (PARN) mediates 3′-end maturation of the telomerase RNA component. *Nat Genet*. 2015;47:1482-1488.
94. Goldfarb KC, Cech TR. 3′ terminal diversity of MRP RNA and other human noncoding RNAs revealed by deep sequencing. *BMC Mol Biol*. 2013;14:23.
95. Berndt H, Harnisch C, Rammelt C, et al. Maturation of mammalian H/ACA box snoRNAs: PAPD5-dependent adenylation and PARN-dependent trimming. *RNA*. 2012;18:958-972.
96. Son A, Park JE, Kim VN. PARN and TOE1 constitute a 3′ end maturation module for nuclear non-coding RNAs. *Cell Rep*. 2018;23:888-898.
97. Nguyen D, Grenier St-Sauveur V, Bergeron D, Dupuis-Sandoval F, Scott MS, Bachand F. A polyadenylation-dependent 3′ end maturation pathway is required for the synthesis of the human telomerase RNA. *Cell Rep*. 2015;13:2244-2257.
98. Shukla S, Schmidt JC, Goldfarb KC, Cech TR, Parker R. Inhibition of telomerase RNA decay rescues telomerase deficiency caused by dyskerin or PARN defects. *Nat Struct Mol Biol*. 2016;23:286-292.
99. Tseng CK, Wang HF, Burns AM, Schroeder MR, Gaspari M, Baumann P. Human telomerase RNA processing and quality control. *Cell Rep*. 2015;13:2232-2243.
100. Boyraz B, Moon DH, Segal M, et al. Post-transcriptional manipulation of TERC reverses molecular hallmarks of telomere disease. *J Clin Invest*. 2016;126:3377-3382.
101. Vanacova S, Wolf J, Martin G, et al. A new yeast poly(A) polymerase complex involved in RNA quality control. *PLoS Biol*. 2005;3:e189.
102. Roake CM, Chen L, Chakravarthy AL, Ferrell JE Jr, Raffa GD, Artandi SE. Disruption of telomerase RNA maturation kinetics precipitates disease. *Mol Cell*. 2019;74:688-700. e3.
103. Tseng CK, Wang HF, Schroeder MR, Baumann P. The H/ACA complex disrupts triplex in hTR precursor to permit processing by RRP6 and PARN. *Nat Commun*. 2018;9:5430.
104. Fok WC, Shukla S, Vessoni AT, et al. Posttranscriptional modulation of TERC by PAPD5 inhibition rescues hematopoietic development in dyskeratosis congenita. *Blood*. 2019;133:1308-1312.
105. Gable DL, Gaysinskaya V, Atik CC, et al. ZCCHC8, the nuclear exosome targeting component, is mutated in familial pulmonary fibrosis and is required for telomerase RNA maturation. *Genes Dev*. 2019;33:1381-1396.
106. Lubas M, Christensen MS, Kristiansen MS, et al. Interaction profiling identifies the human nuclear exosome targeting complex. *Mol Cell*. 2011;43:624-637.

107. Najmabadi H, Hu H, Garshasbi M, et al. Deep sequencing reveals 50 novel genes for recessive cognitive disorders. *Nature*. 2011;478:57-63.
108. Lardelli RM, Schaffer AE, Eggens VR, et al. Biallelic mutations in the 3′ exonuclease TOE1 cause pontocerebellar hypoplasia and uncover a role in snRNA processing. *Nat Genet*. 2017;49:457-464.
109. Deng T, Huang Y, Weng K, et al. TOE1 acts as a 3′ exonuclease for telomerase RNA and regulates telomere maintenance. *Nucleic Acids Res*. 2019;47:391-405.
110. Kirwan M, Beswick R, Vulliamy T, et al. Exogenous TERC alone can enhance proliferative potential, telomerase activity and telomere length in lymphocytes from dyskeratosis congenita patients. *Br J Haematol*. 2009;144:771-781.
111. Westin ER, Chavez E, Lee KM, et al. Telomere restoration and extension of proliferative lifespan in dyskeratosis congenita fibroblasts. *Aging Cell*. 2007;6:383-394.
112. Paulsen BS, Mandal PK, Frock RL, et al. Ectopic expression of RAD52 and dn53BP1 improves homology-directed repair during CRISPR/Cas9-mediated genome editing. *Nat Biomed Eng*. 2017;1:878-888.
113. Woo DH, Chen Q, Yang TL, et al. Enhancing a Wnt-telomere feedback loop restores intestinal stem cell function in a human organotypic model of dyskeratosis congenita. *Cell Stem Cell*. 2016;19:397-405.
114. Nagpal N, Wang J, Zeng J, et al. Small-molecule PAPD5 inhibitors restore telomerase activity in patient stem cells. *Cell Stem Cell*. 2020;26:896-909.
115. Mueller H, Lopez A, Tropberger P, et al. PAPD5/7 are host factors that are required for hepatitis B virus RNA stabilization. *Hepatology*. 2019;69:1398-1411.
116. Mueller H, Wildum S, Luangsay S, et al. A novel orally available small molecule that inhibits hepatitis B virus expression. *J Hepatol*. 2018;68:412-420.

How to cite this article: Nagpal N, Agarwal S. Telomerase RNA processing: Implications for human health and disease. *Stem Cells*. 2020;1–12. https://doi.org/10.1002/stem.3270